

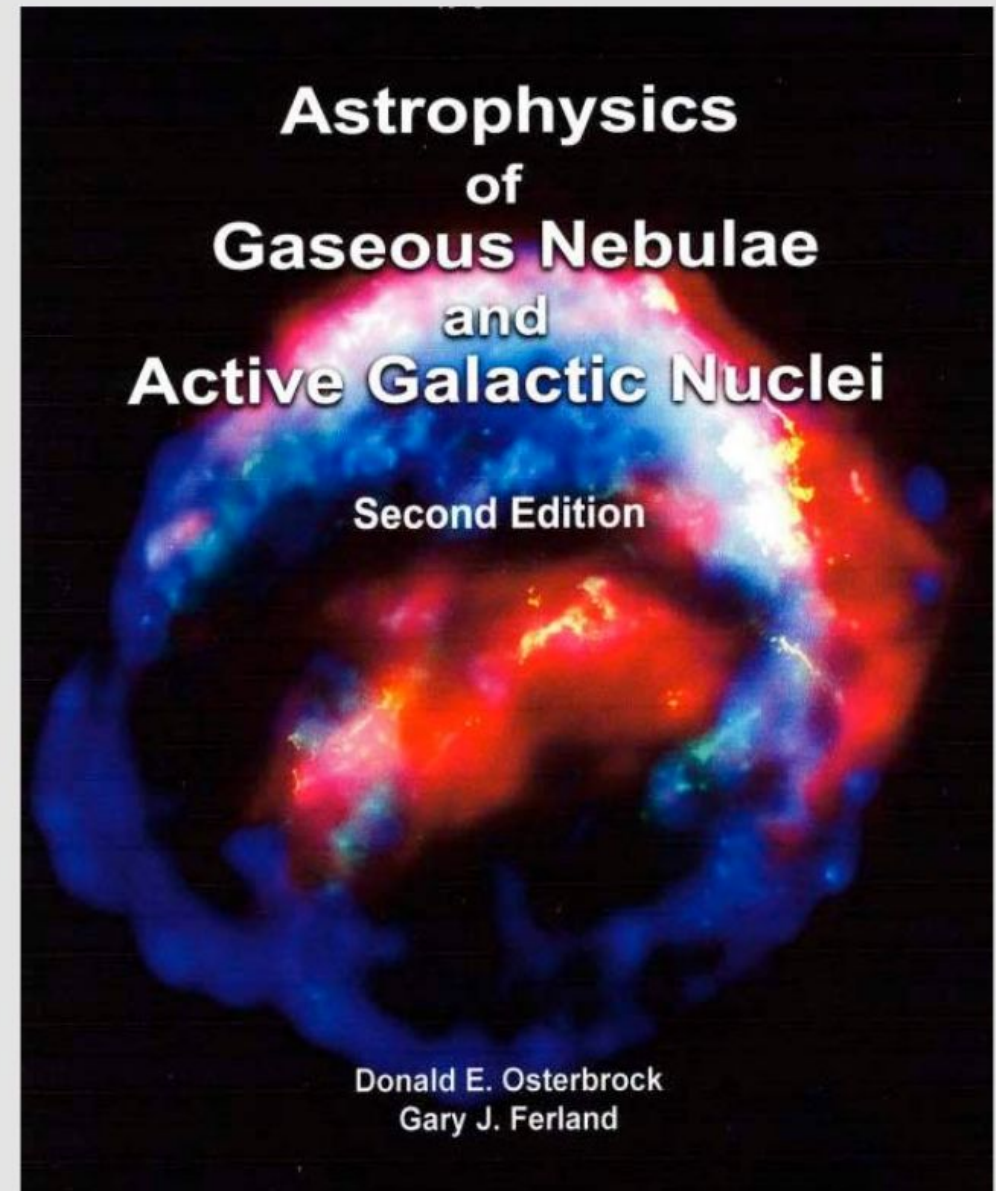
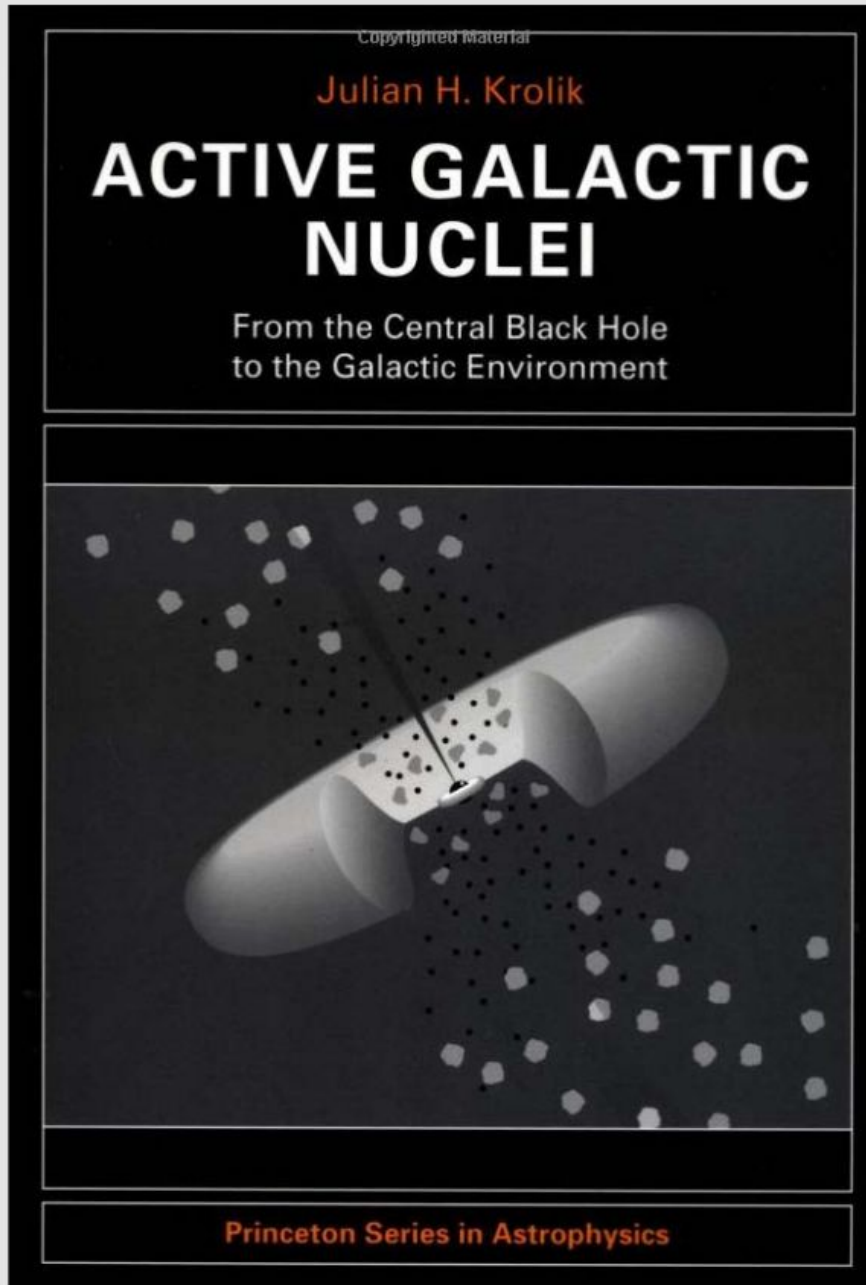
Active Galactic Nuclei



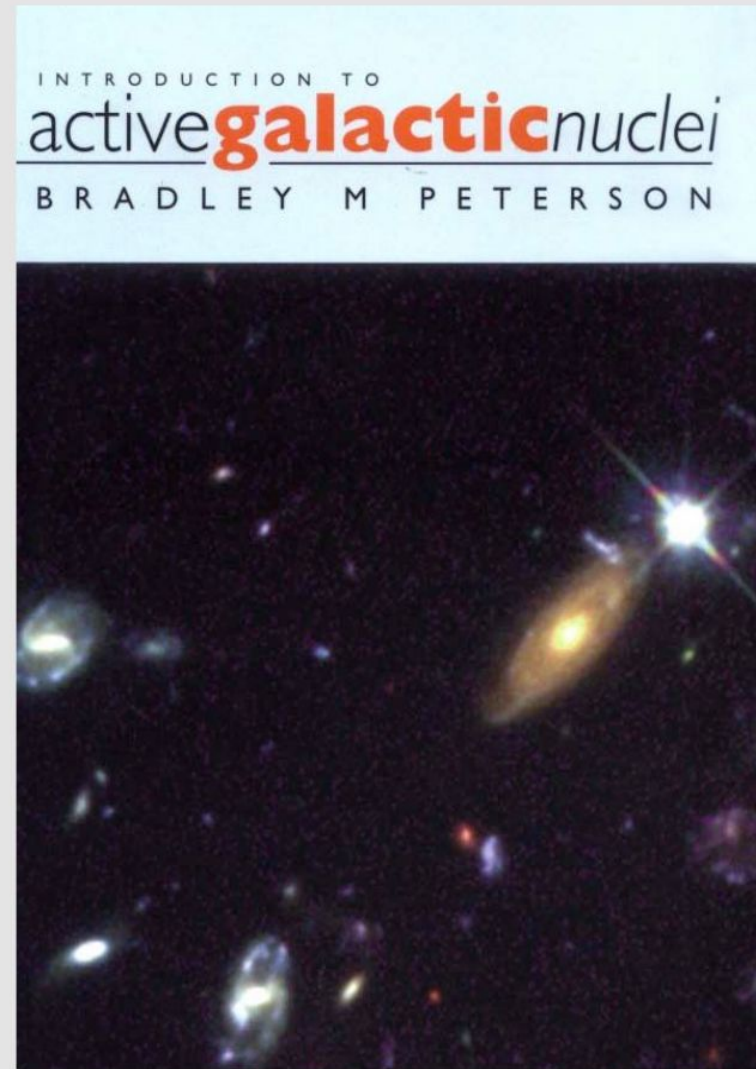
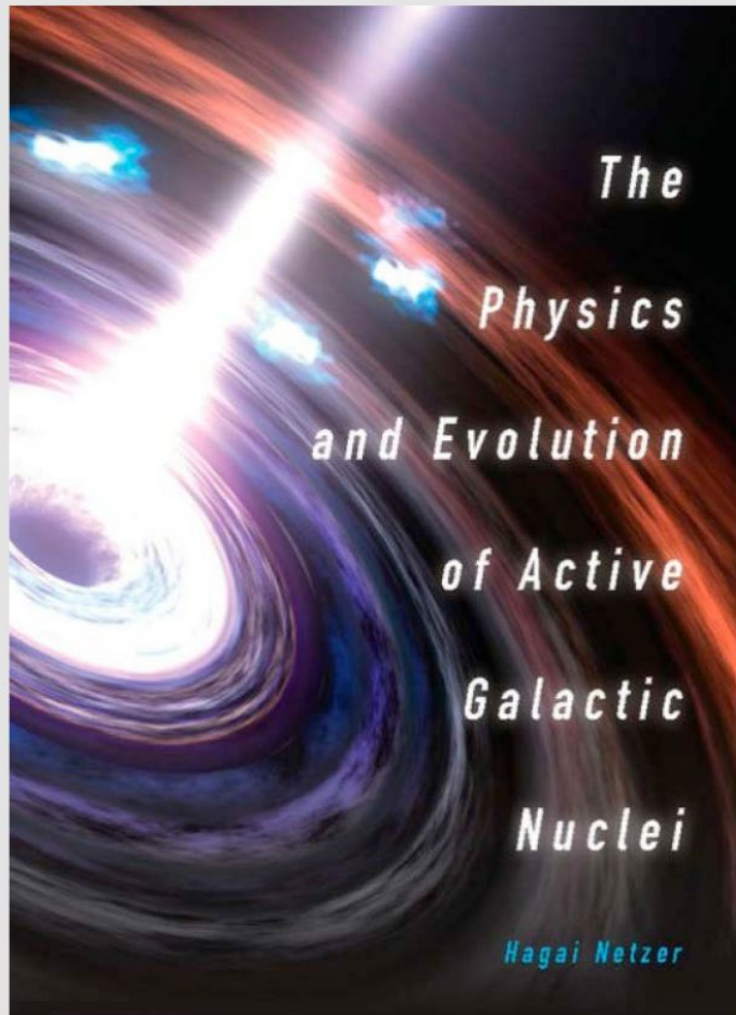
Outline

- Early history
- AGN basics
- Finding AGNs
- AGN terminology
- AGN unification
- Dissecting AGNs
- Focused lecture: Proving the Evidence of a SuperMassive BH

Some references



Some references

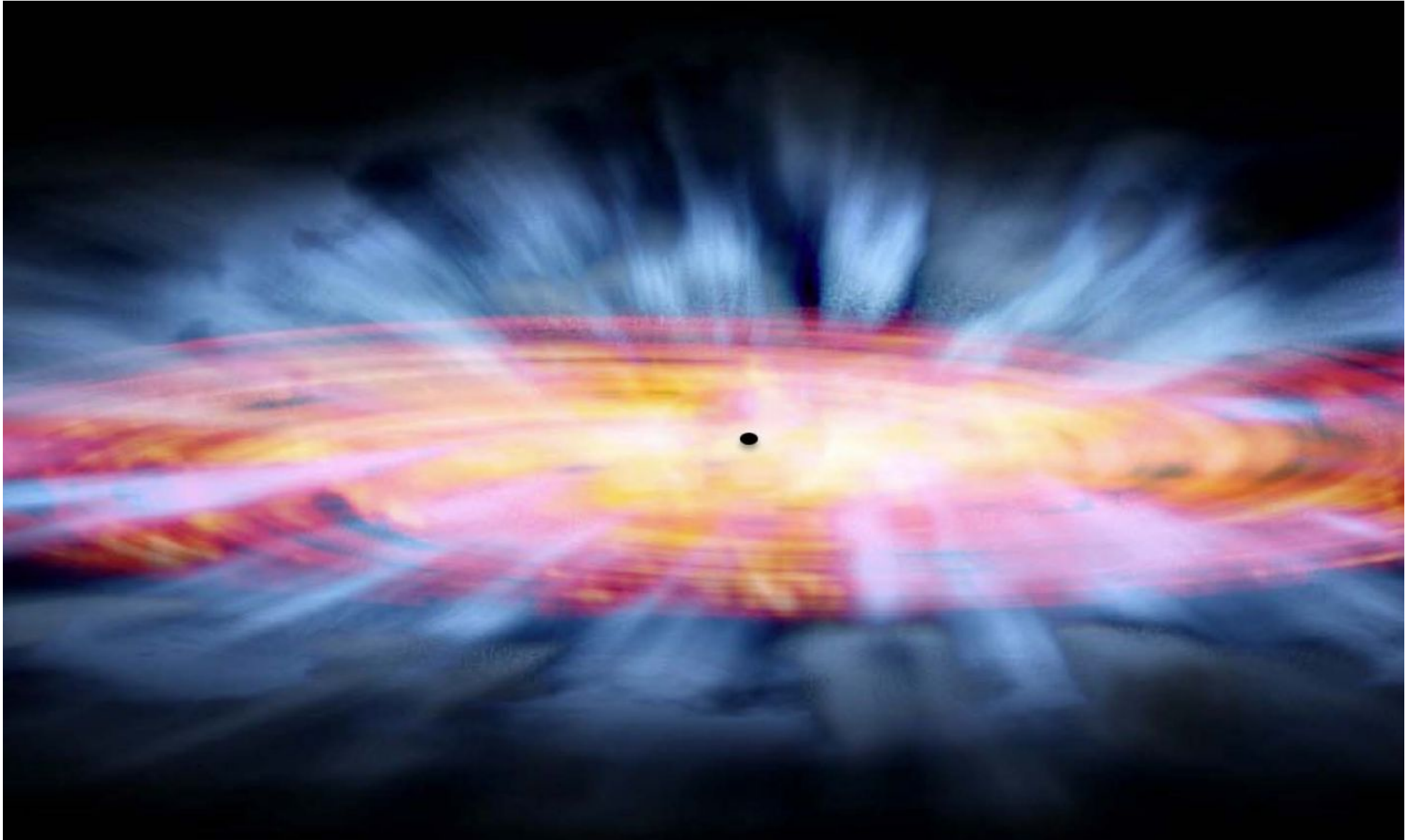


- Plus tons of online resources:
 - Monaco

Outline

- Early history
- AGN basics
- Finding AGNs
- AGN terminology
- AGN unification
- Dissecting AGNs
- Focused lecture: Proving the Evidence of a SuperMassive BH

Early History of AGNs



Early History

- 1908 – Edward Fath notices strong emission lines from H, O, Ne in the nuclear spectrum of NGC 1068. This was way before:
 - 1915 – General Relativity
 - 1916 – Schwarzschild solution found, but not fully understood
 - Early 20s realizing that galaxies were extragalactic objects!!
- 1917 – Vesto Slipher obtains a higher quality spectrum of NGC 1068 and notes its emission lines are unusually broad
- 1918 – Herber Curtis notes in M87 a “curious straight ray ... connected with the nucleus by a thin line of matter”
- 1924-1929 – General realization that galaxies are extragalactic – led by Edwin Hubble
- 1926 – Edwin Hubble notices the nuclear emission-line spectra of NGC 1068, NGC 4051, NGC 4151

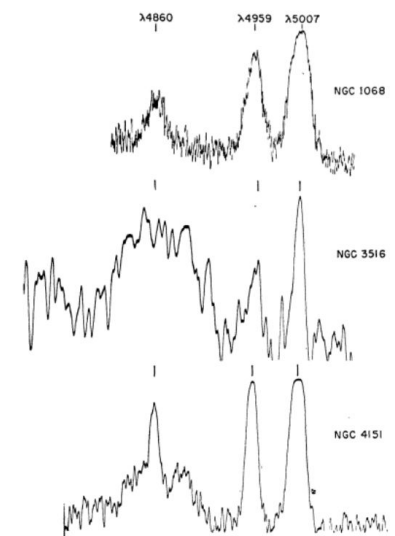
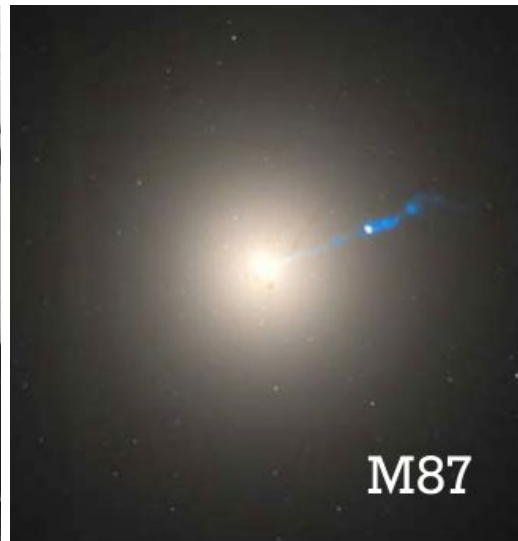
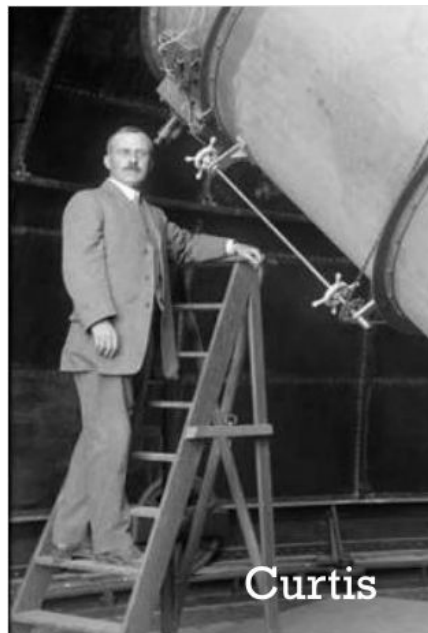
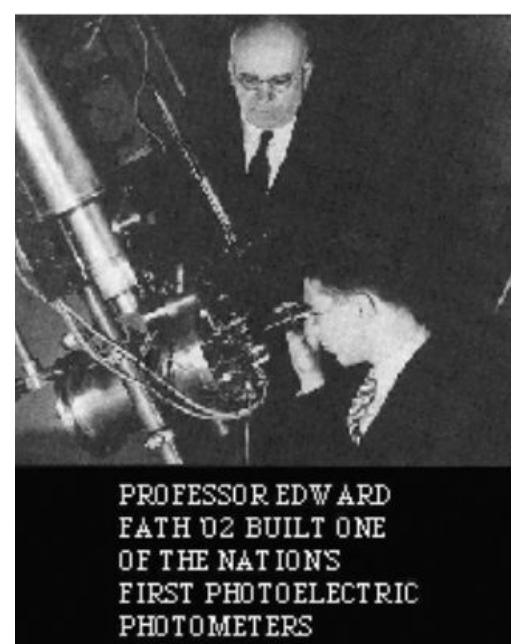
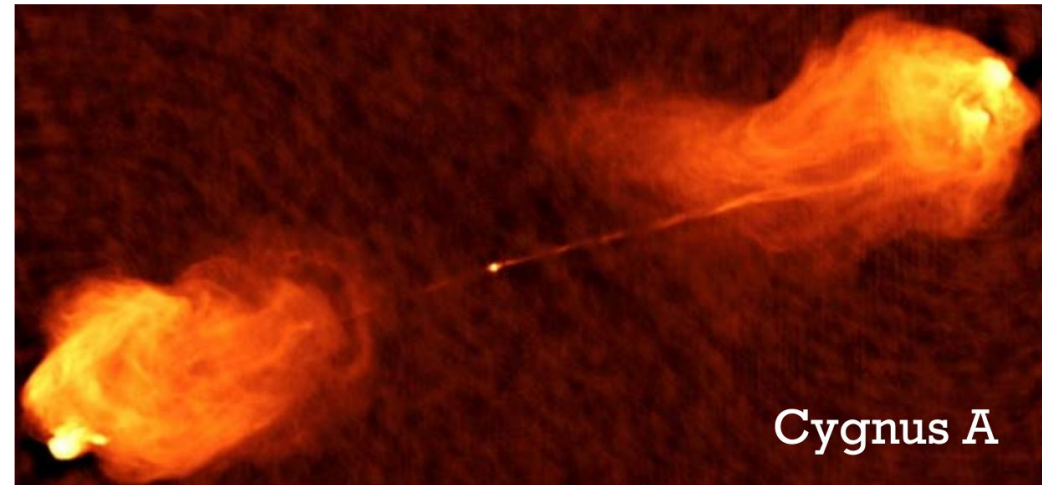
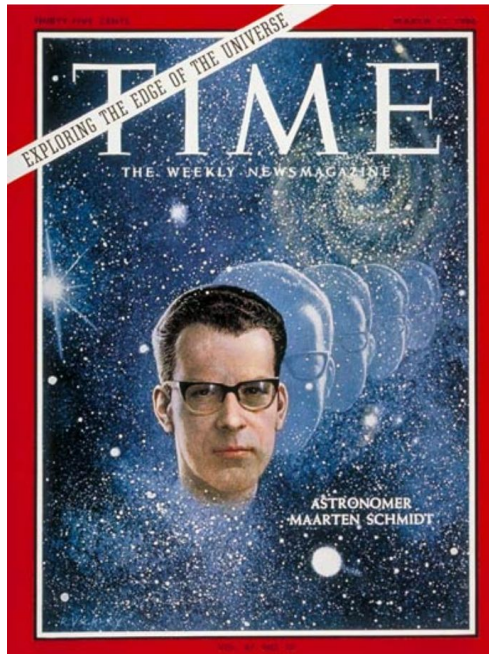


FIG. 1.—Microphotometer tracings of the emission lines $\lambda\lambda$ 4860 ($H\beta$), 4959 and 5007 ($O III$) in the nebulae NGC 1068, 3516, and 4151.

Early History

- 1939 – Grote Reber discovers the radio source Cygnus A
- 1943 – Carl Seyfert shows that a fraction of galaxies have strong, broad emission lines and that these galaxies are especially luminous – now known as “Seyfert galaxies”
- 1954 – Walter Baade and Rudolph Minkowski find the counterpart to Cygnus A at $z = 0.057$
- 1963 – Maarten Schmidt discovers 3C273 to have $z = 0.158$
- 1964 – Zeldovich & Novikov and Salpeter speculate about black holes powering quasars
- 1967 – The term “black hole” comes into general use
- 1968 – Donald Lynden Bell notes that many galactic nuclei may contain “collapsed old quasars”
- After – AGNs become a topic of widespread study



Outline

- Early history
- **AGN basics**
- Finding AGNs
- AGN terminology
- AGN unification
- Dissecting AGNs
- Focused lecture: Proving the Evidence of a SuperMassive BH

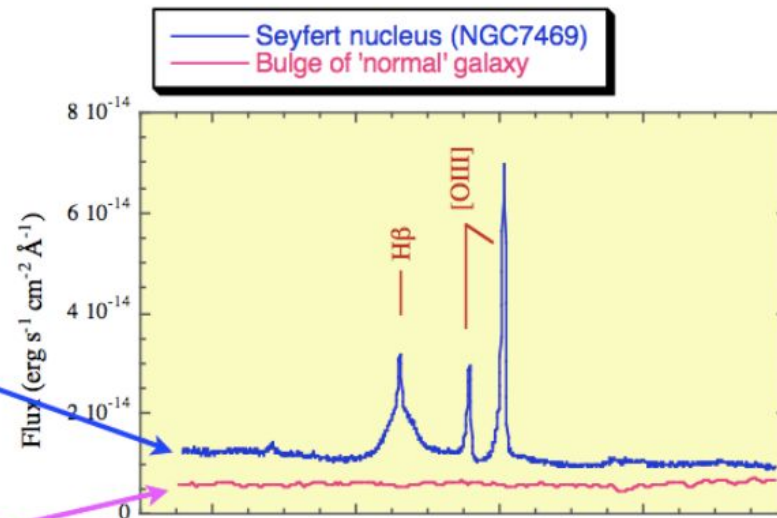
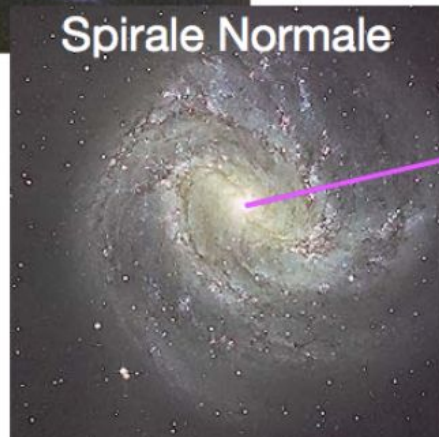
.AGN basics: What are Active Galaxies?



- In the local universe...
 - 10^{-6} of massive galaxies contain luminous quasars
 - $\sim 5\%$ are moderately luminous (Seyfert galaxies)
 - $\sim 30\%$ show signs of low-level nuclear activity

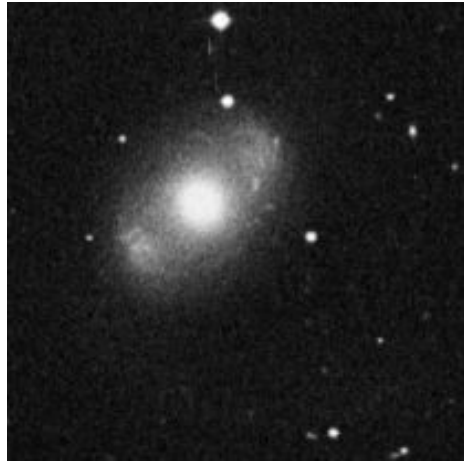
Seyfert Galaxies

- Carl Seyfert (40s)
- Peculiar spiral galaxies with strong emission lines in the nuclei

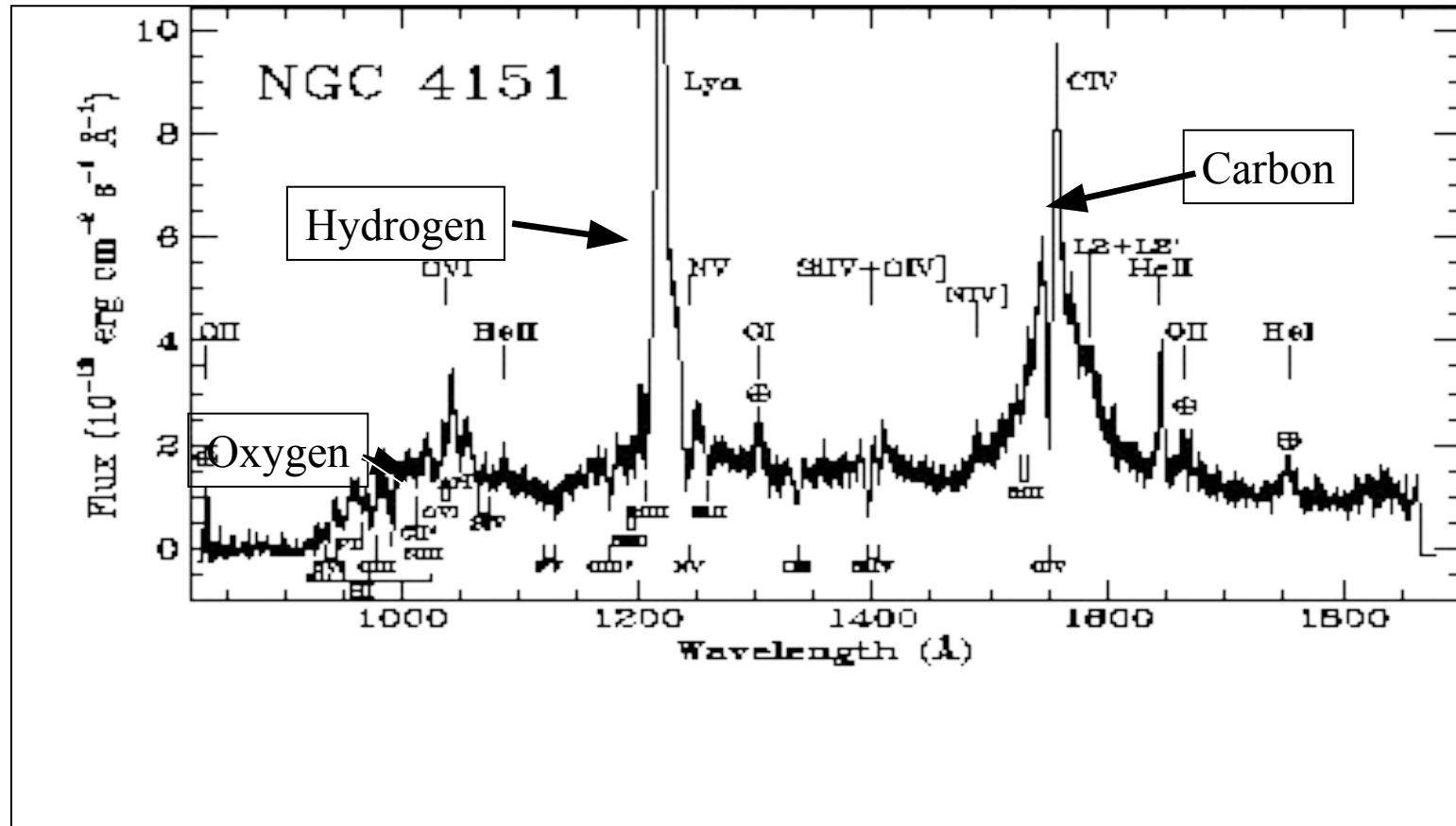


- Emission lines indicates an ionization level of the gas larger than HII regions and
- Emission lines can have FWHM > 1000 km/s (normal galaxies ~ few 100s km/s)

Ultraviolet Spectrum of Seyfert Galaxies

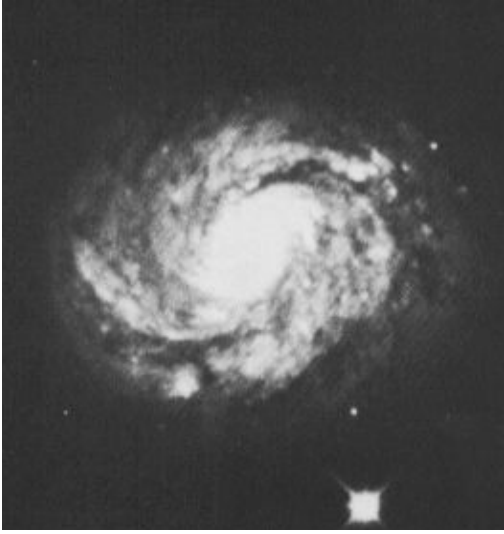


NGC 4151:
Digital Sky Survey



UV spectrum of the Seyfert galaxy NGC 4151
observed with Hopkins UV Telescope

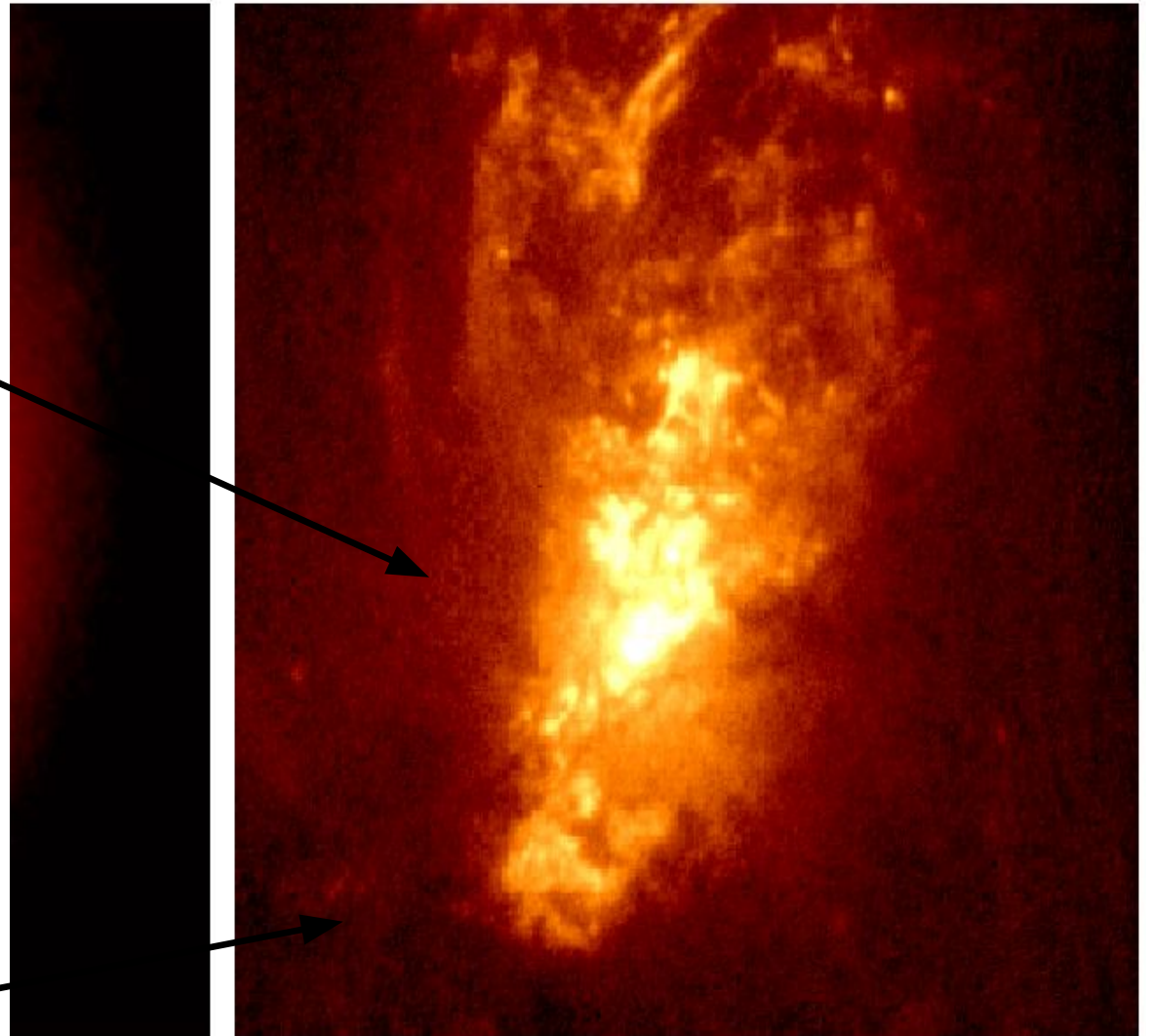
NGC 1068: An Obscured Seyfert



This bright cloud has a direct view of the intense nucleus

Radiation and (possibly) a wind escapes through a cone-shaped funnel

Nucleus is hidden in here

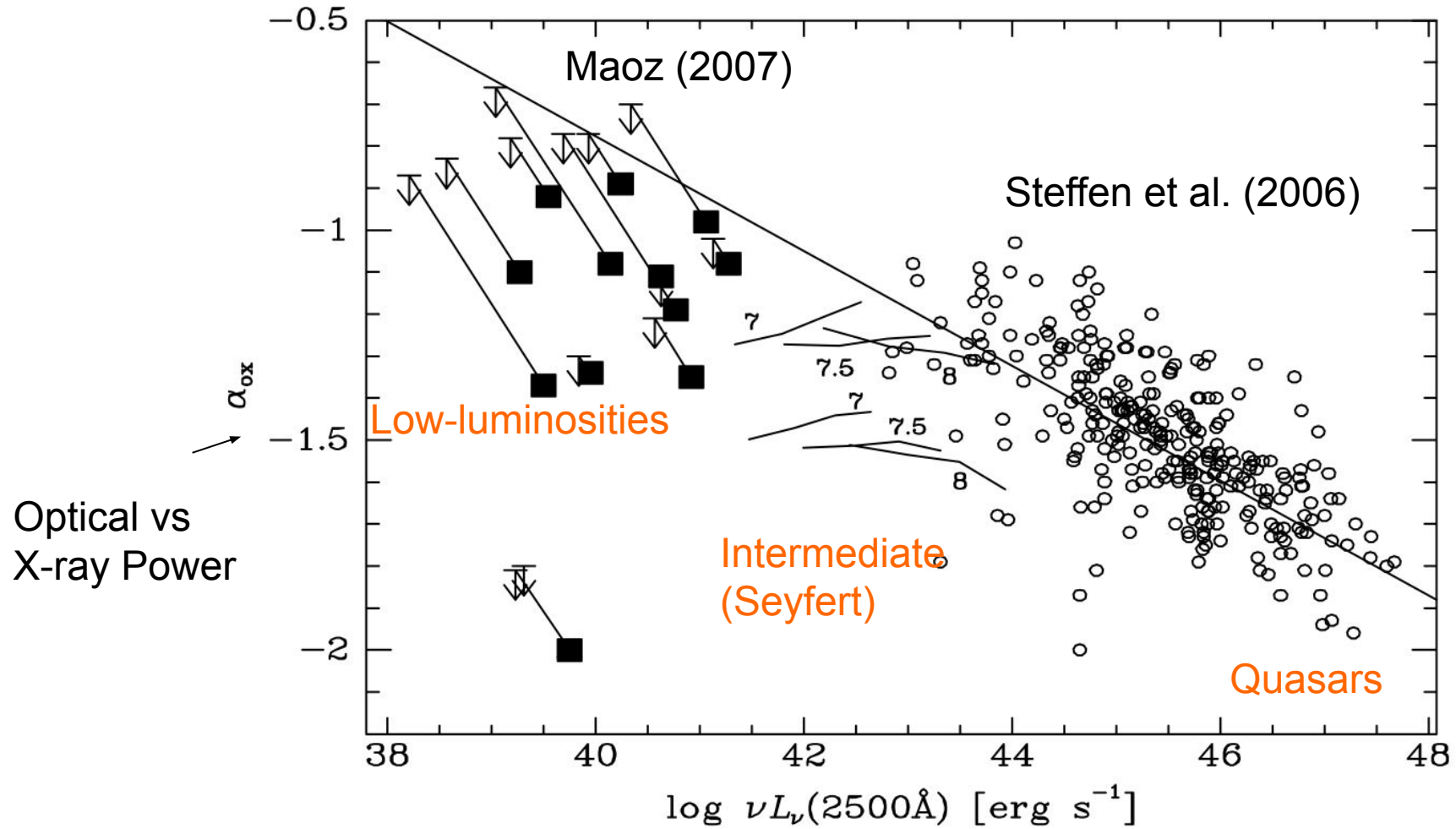


Basic Observed Properties of AGNs

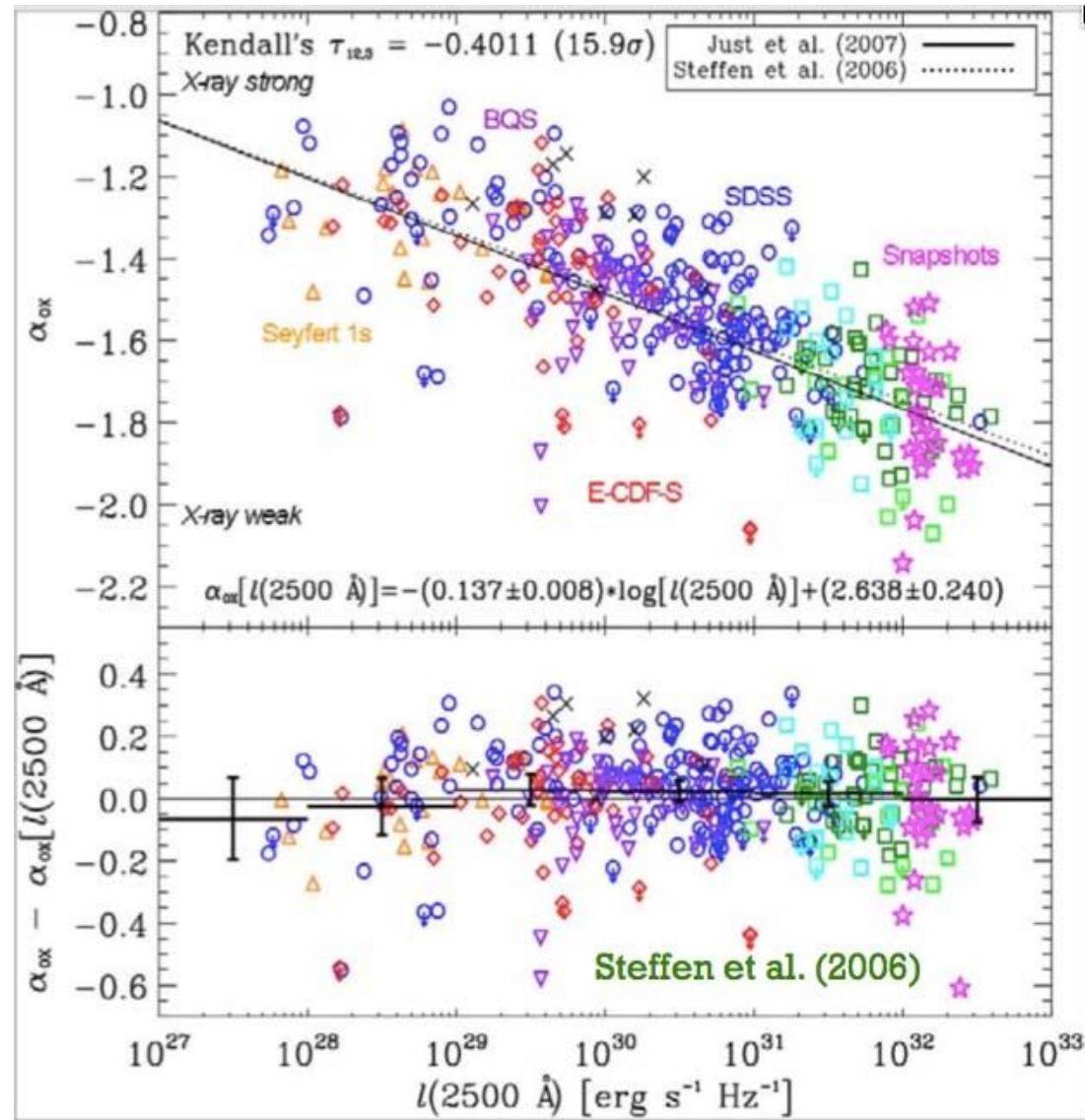
Five main observed properties

- Broad range of luminosities, reaching very large values.
- Strong and broad optical/UV emission lines.
- Emission over a very broad band (very unlikely from stars).
- Variability.
- Particle jets.

Broad Range of Luminosities



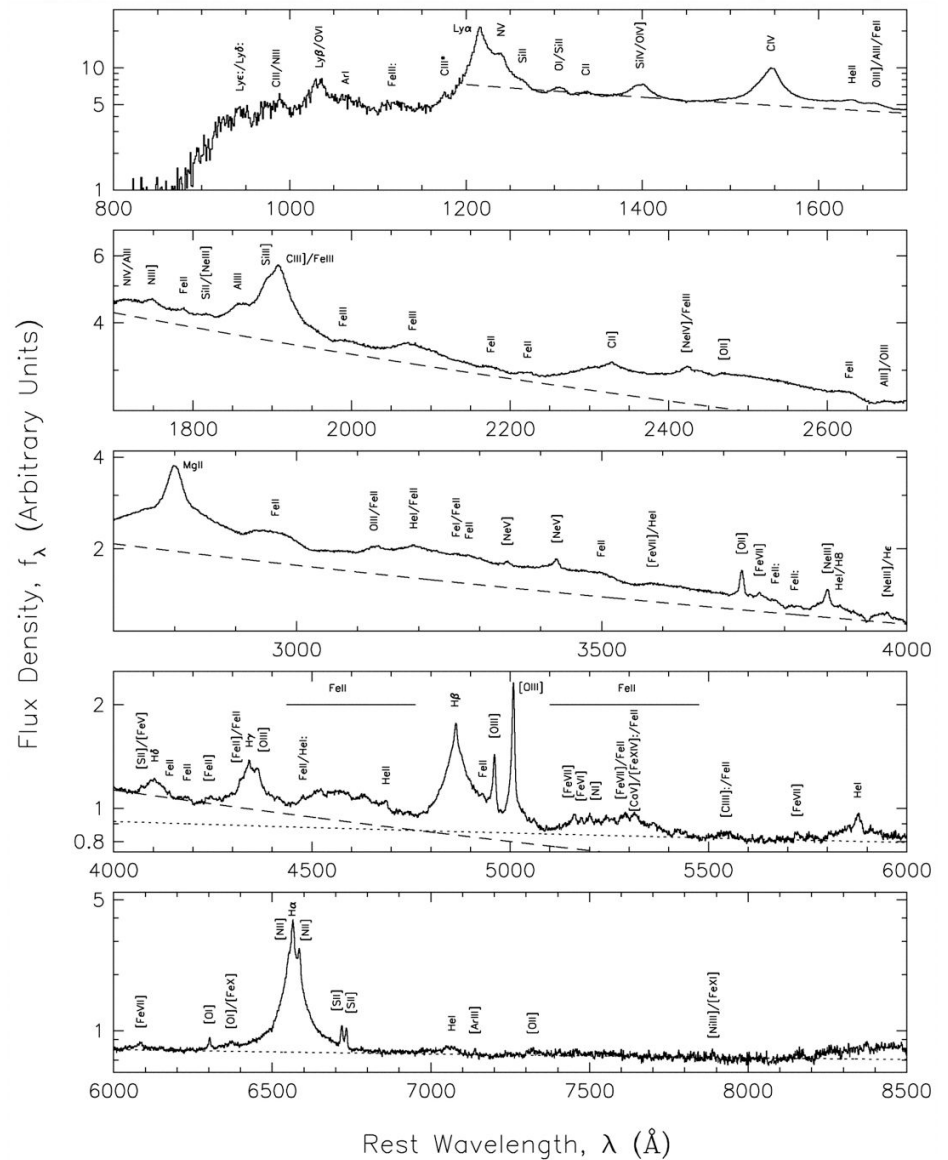
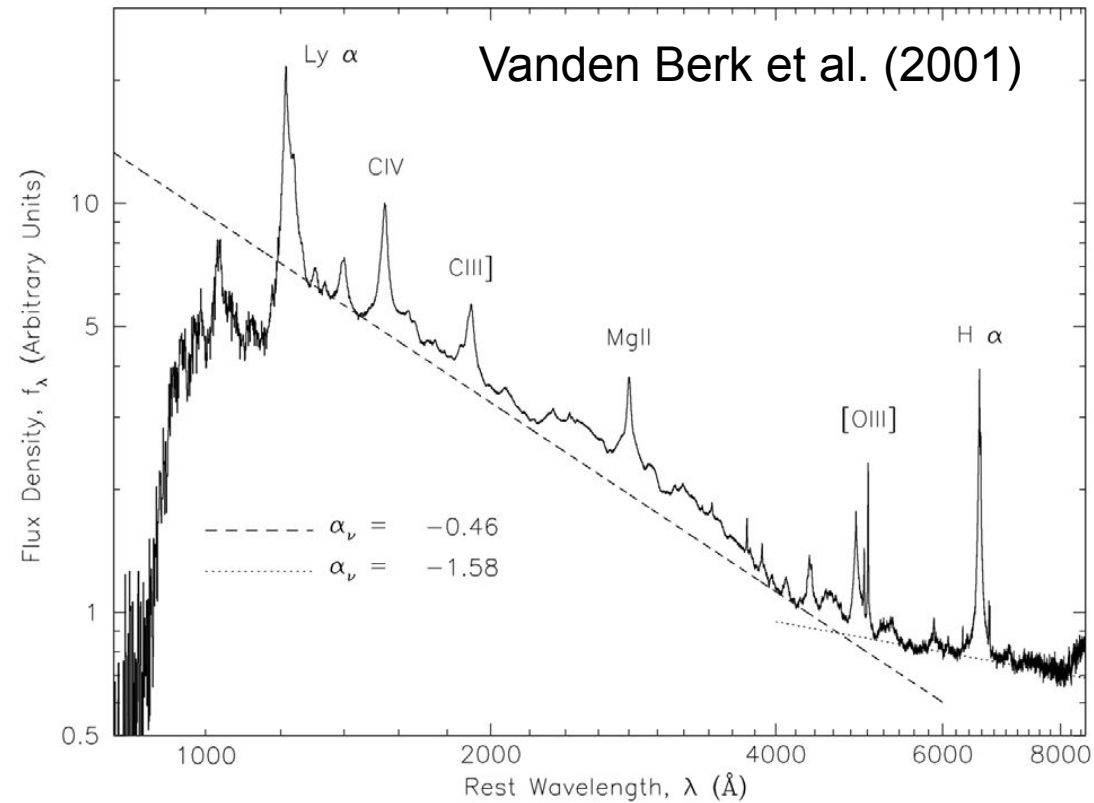
Broad Range of Luminosities



Broad Range of Luminosities

- Span 9+ orders of magnitude in luminosity.
- There is no strict lower limit on luminosity; e.g., even the black hole at the center of our Galaxy shows some intermittent activity at very low levels (comparable with 10^{33} in the previous units).
- At very low luminosities, the distinction between active and normal galaxies is largely semantic. There is no clear bimodal separation of properties, for example.
- There is a maximum observed luminosity, and we believe that we have found examples of the most luminous AGNs that exist (i.e., the most luminous quasars).
- They outshine their own galaxy by factors of 100-1000s.. Can easily be detected to high-z

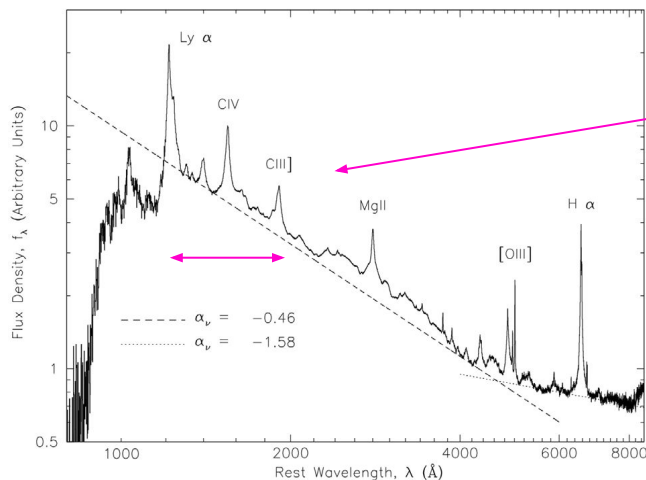
Strong and broad optical/UV emission lines.



- Stacked Spectra from SDSS (“average spectra”)
- Dashed approx continuum
- Strong and broad optical/UV emission lines
- Almost like a forest of ELs

Strong and broad optical/UV emission lines.

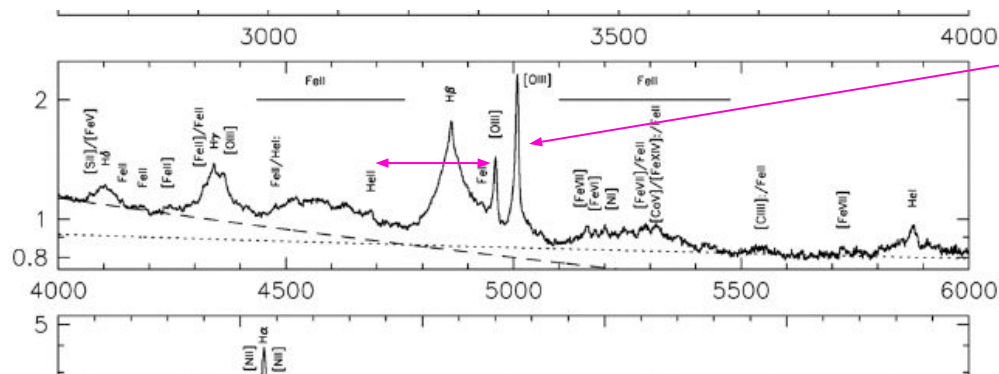
- **What is telling us?**
- Indicates the presence of ionized nebular gas.
- Gas is photo-ionized by the bright central source.
- Line widths indicate high-speed motions with a wide range of velocities, up to $\sim 25000 \text{ km s}^{-1}$!!



Not thermal motion, but doppler \rightarrow bulk motions

Strong and broad optical/UV emission lines.

- **What is telling us?**
- Indicates the presence of ionized nebular gas.
- Gas is photo-ionized by the bright central source.
- Line widths indicate high-speed motions with a wide range of velocities, up to $\sim 25000 \text{ km s}^{-1}$!!



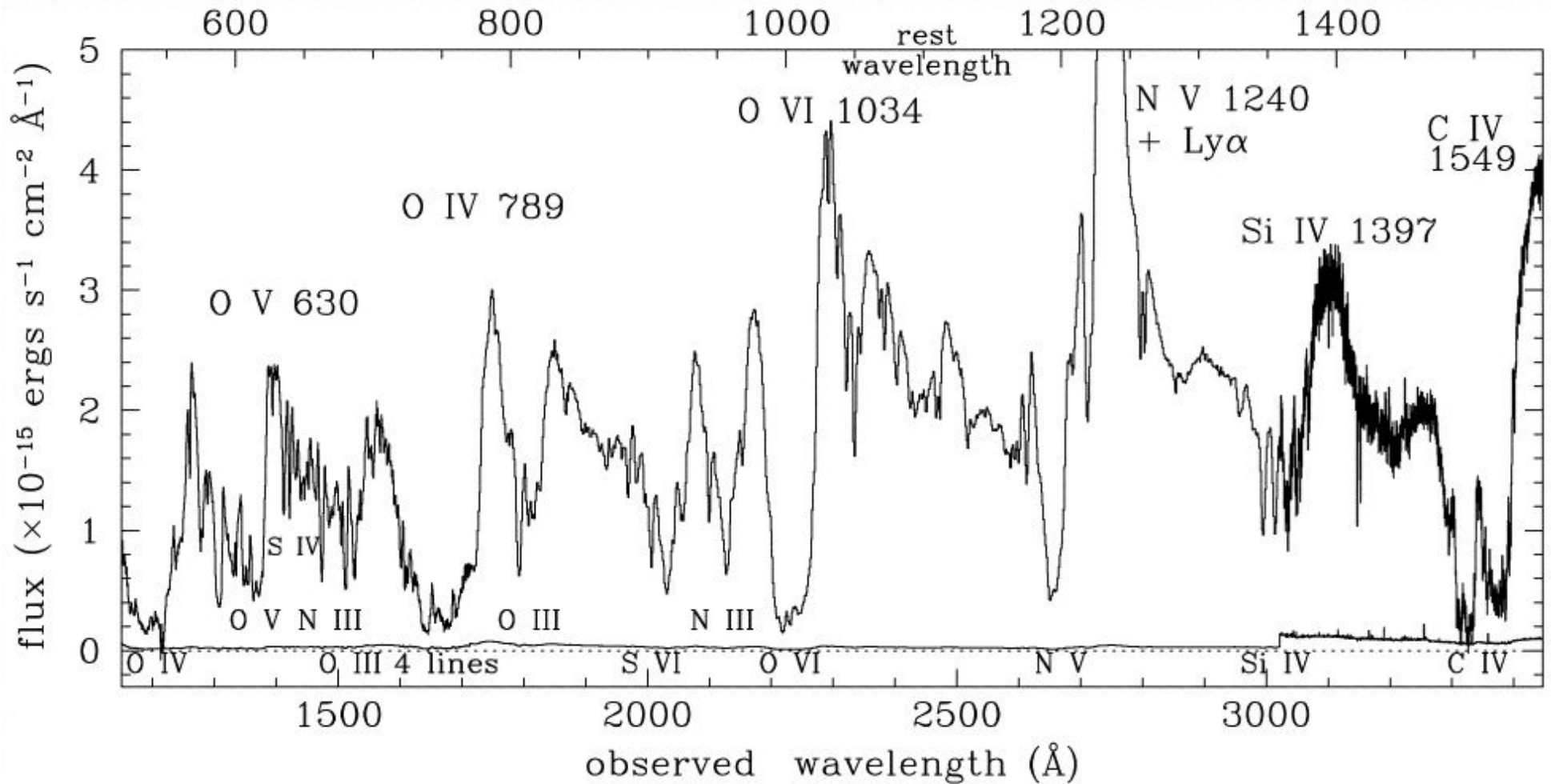
Some lines are narrower [O III] vs H β

- Broad-line and Narrow-line regions of AGNs

Strong and broad optical/UV emission lines.

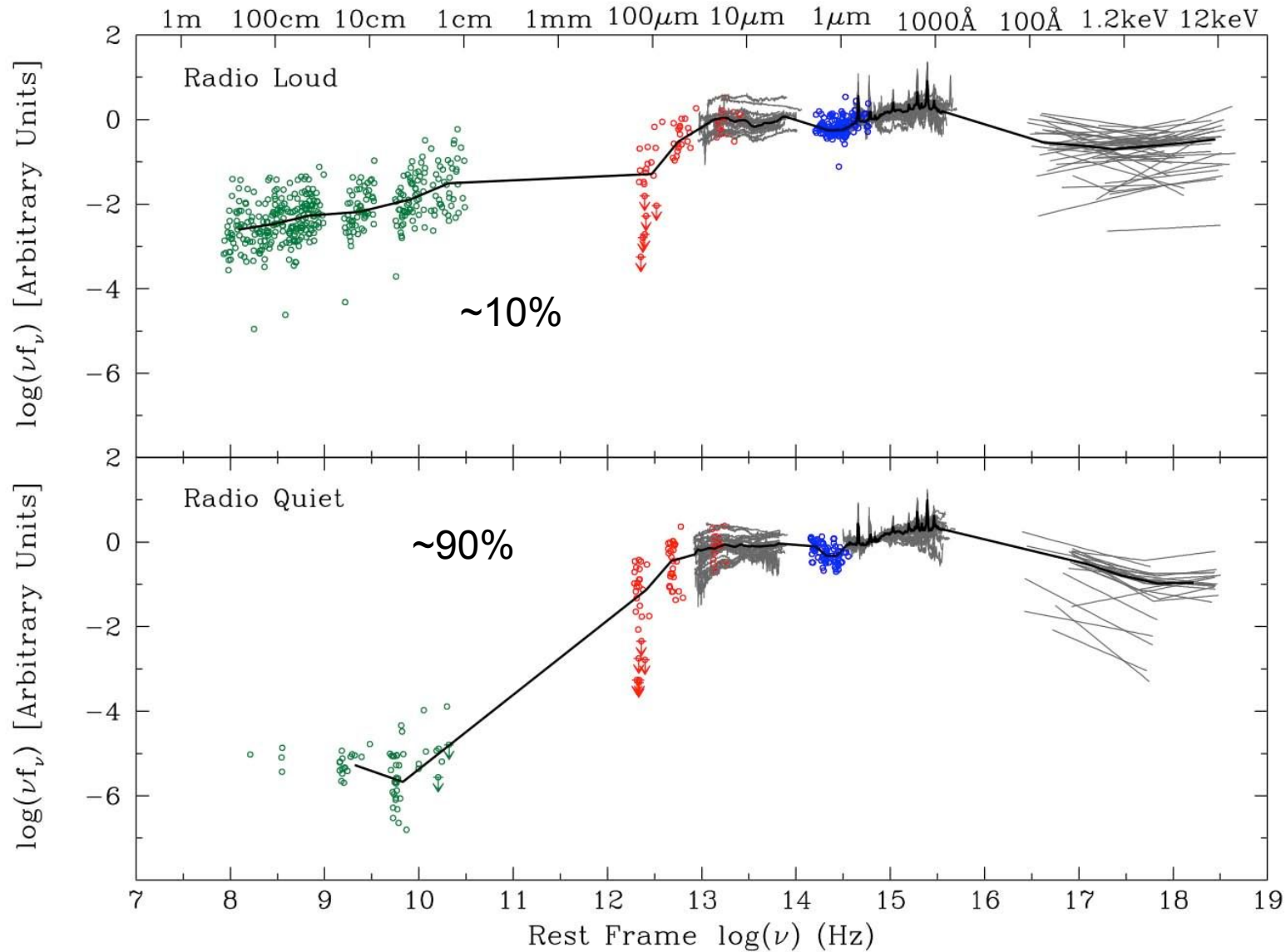
- What is it telling us?
- Indicates the presence of ionized nebular gas.
- Gas is photo-ionized by the bright central source.
- Line widths indicate high-speed motions with a wide range of velocities, up to $\sim 25000 \text{ km s}^{-1}$!!
- Abundances about solar or slightly super-solar (very difficult measurements).
- (Sometimes) AGNs present blue-shifted absorption lines

Blueshifted absorption



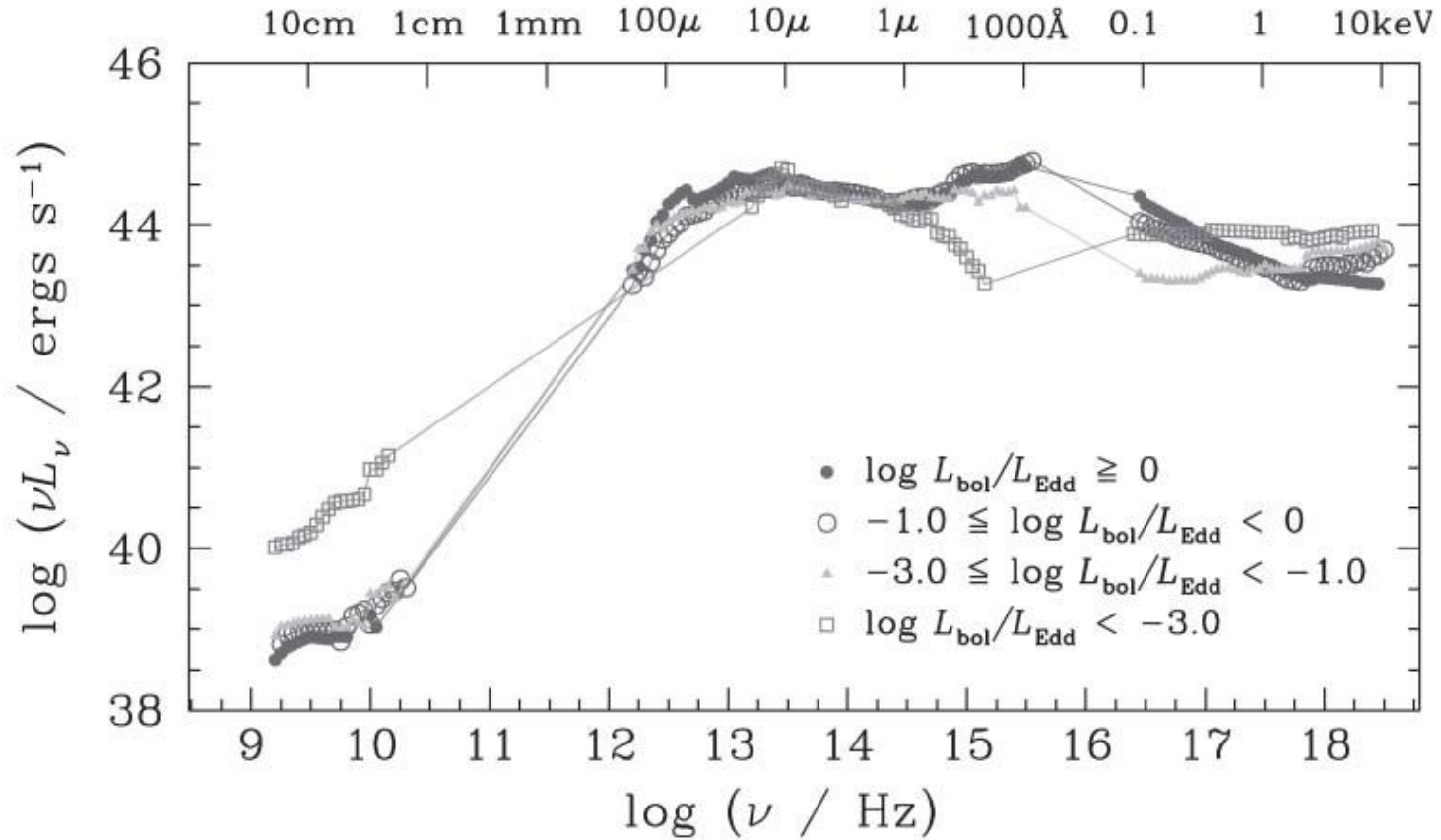
- Can be very broad (large velocities-thousands km/s)
- Indicate the presence of absorbing gas along the LOS

Emission over a very broad band



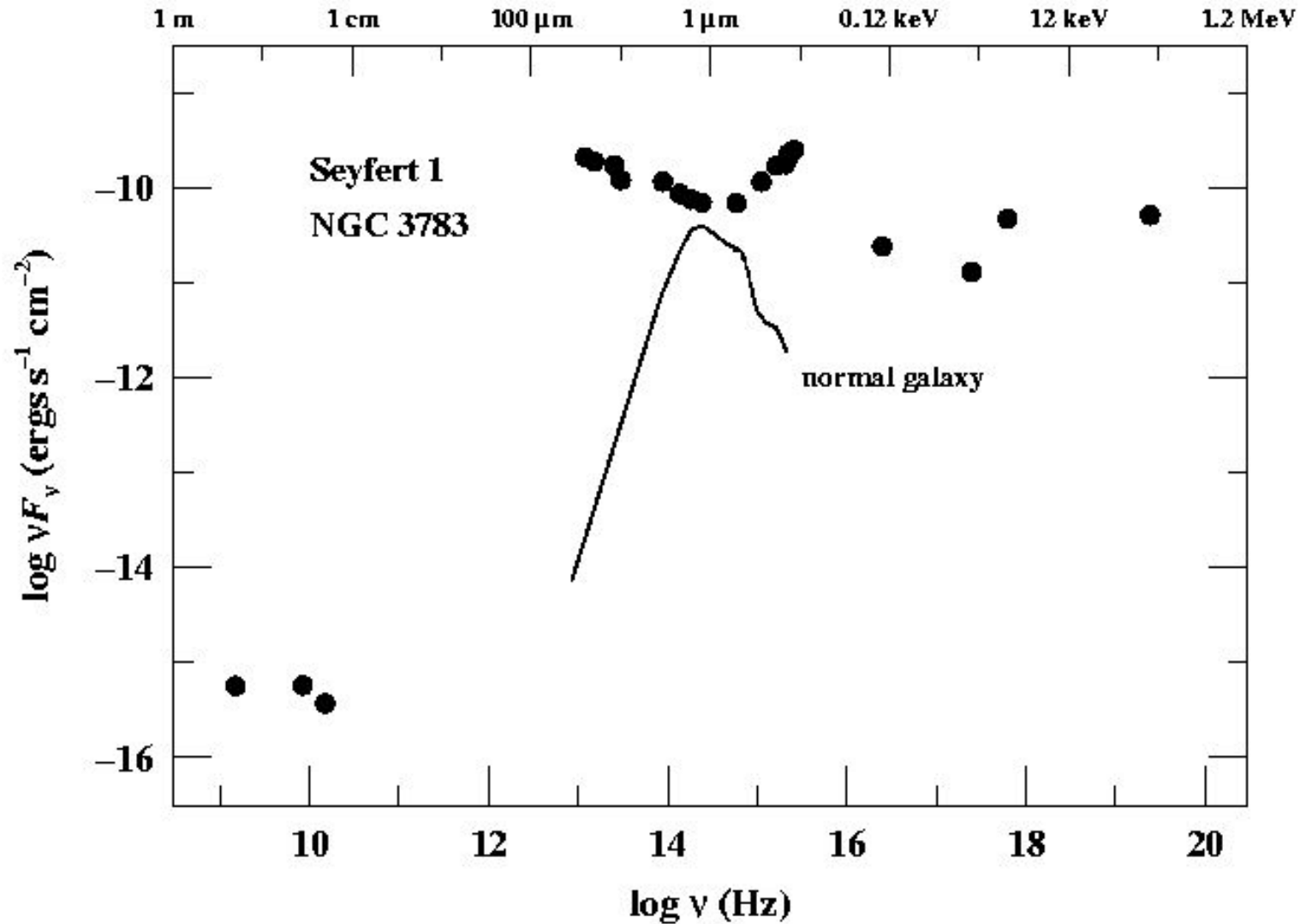
Typically much flatter spectrum w.r.t. e.g. stellar emission

Emission over a very broad band



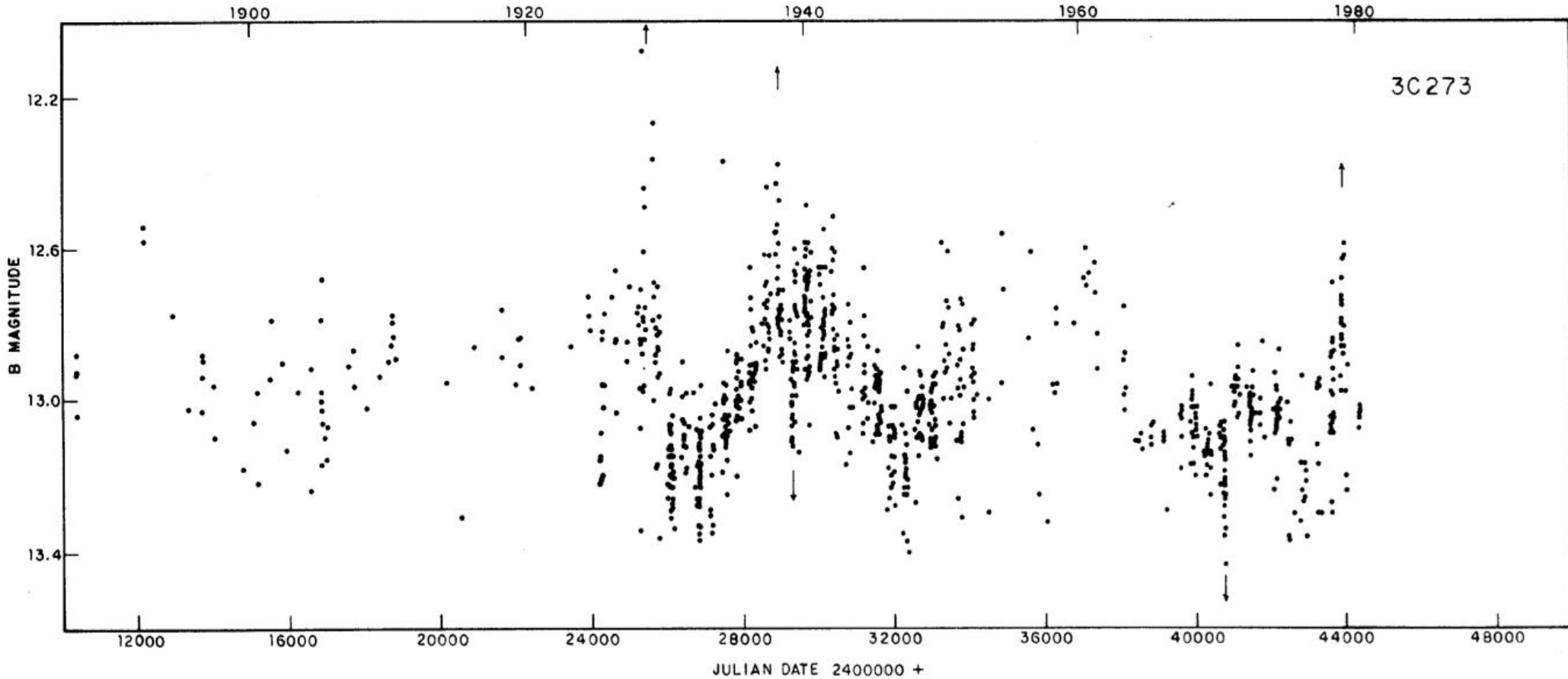
Ho et al. 2008

Emission over a very broad band



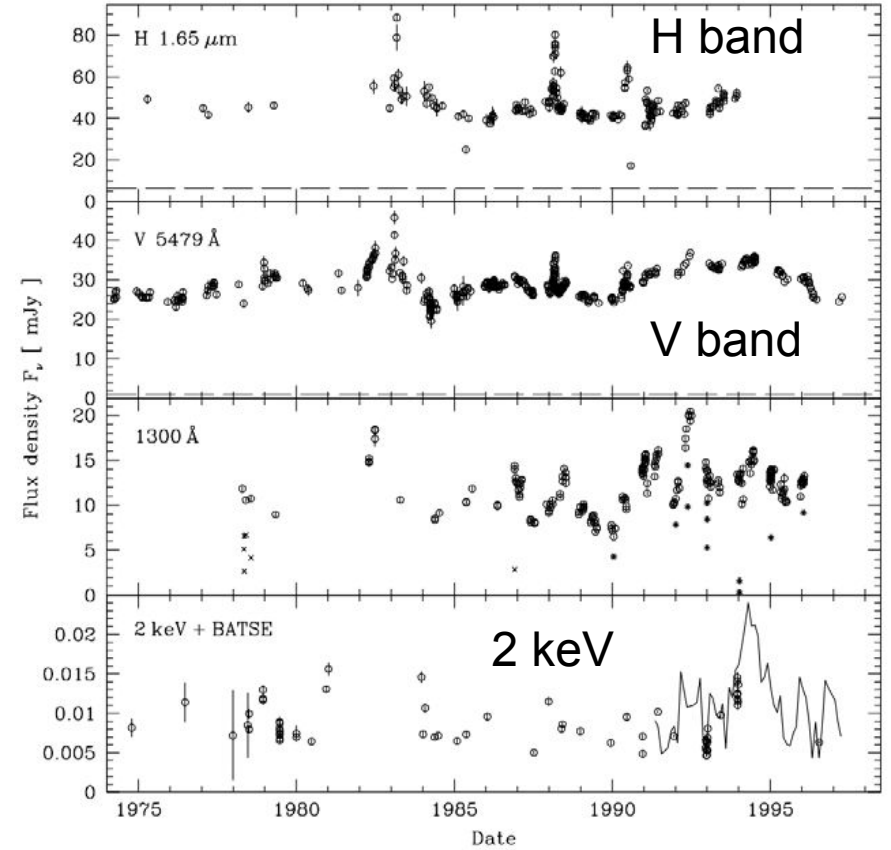
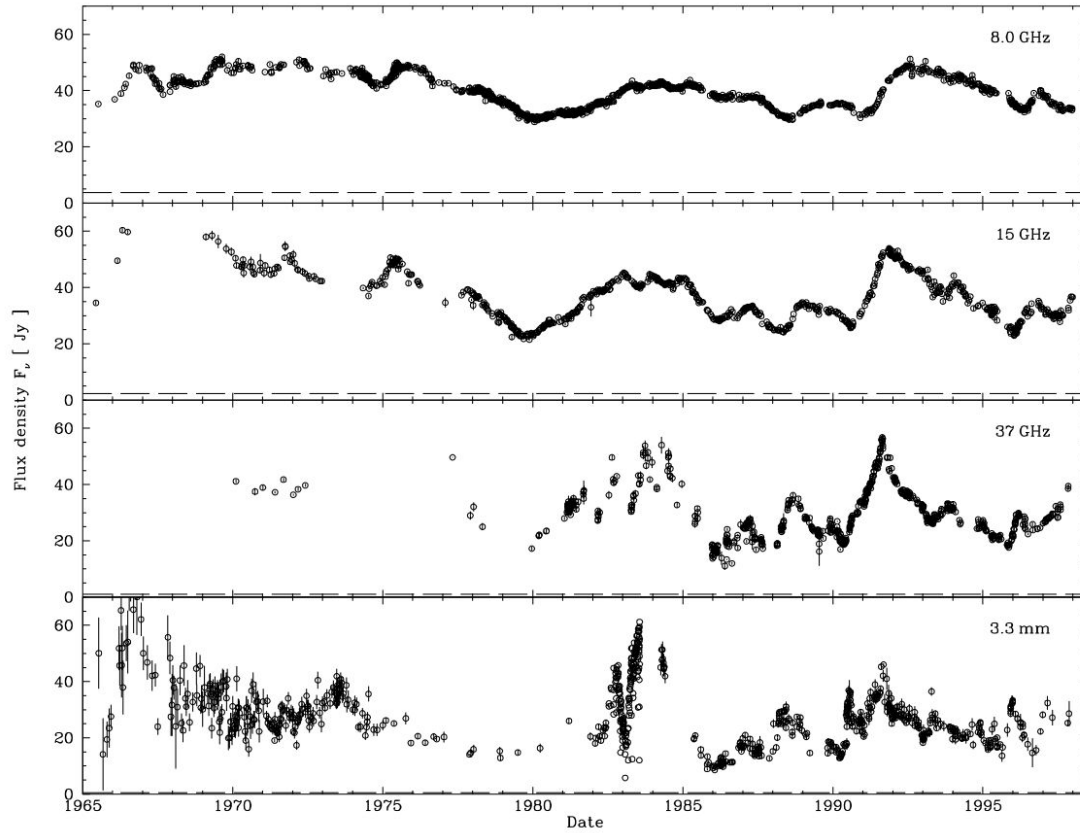
Typically much flatter spectrum w.r.t. e.g. stellar emission

Variability of AGNs

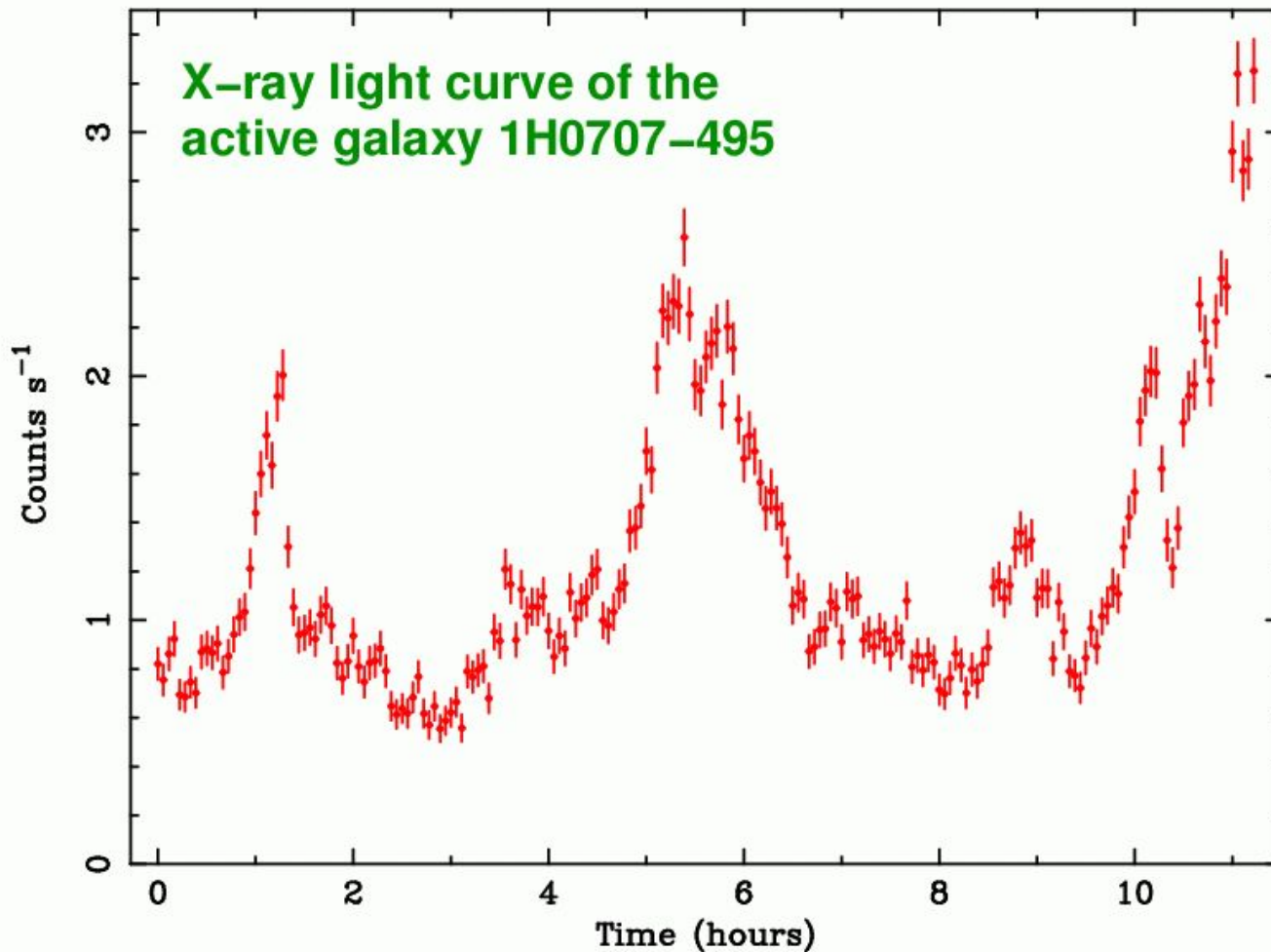


- 100 years of 3C 273
- The variability is generally chaotic without a clear period or quasi-period.

Variability of AGNs

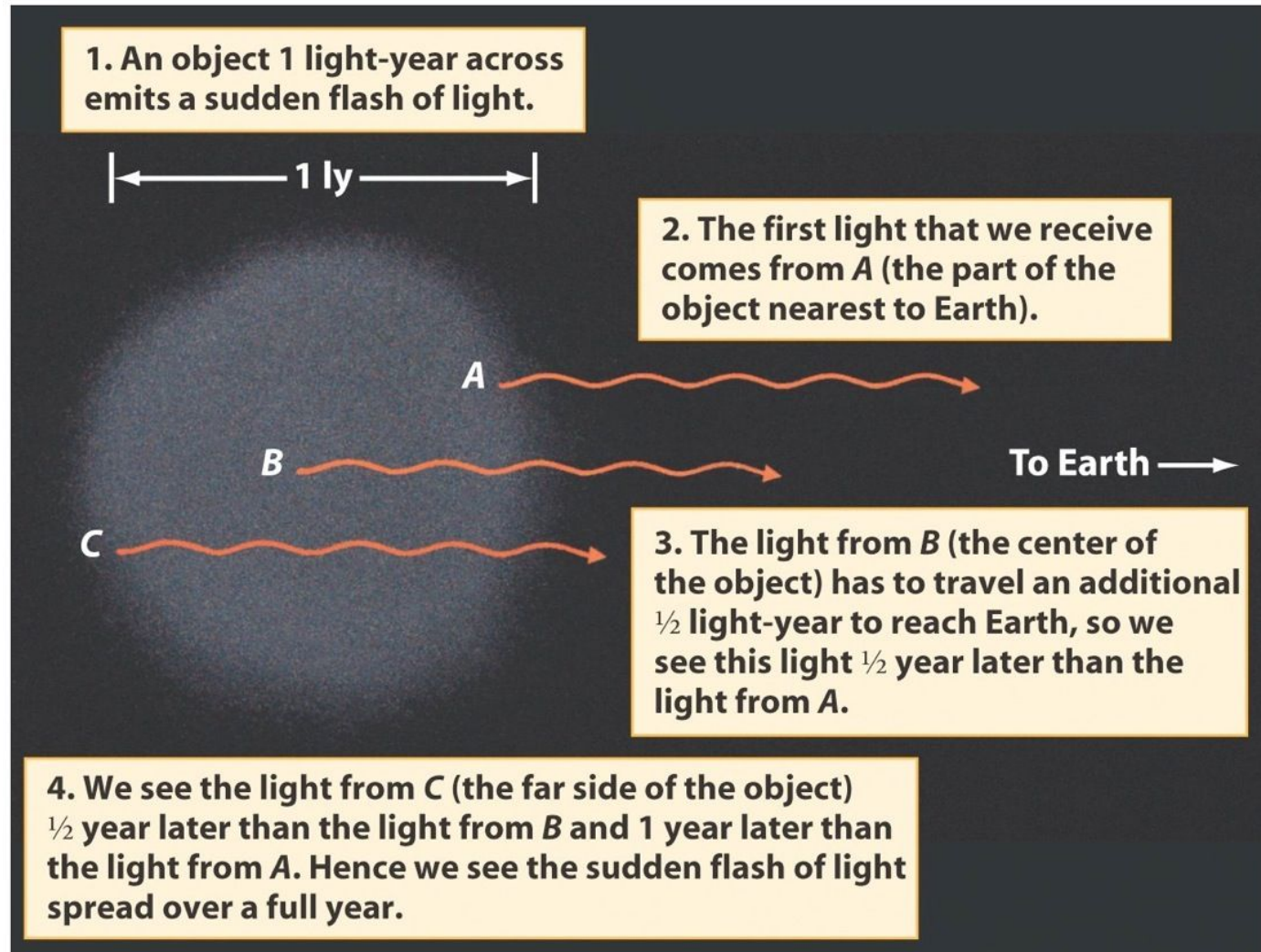


Variability of AGNs



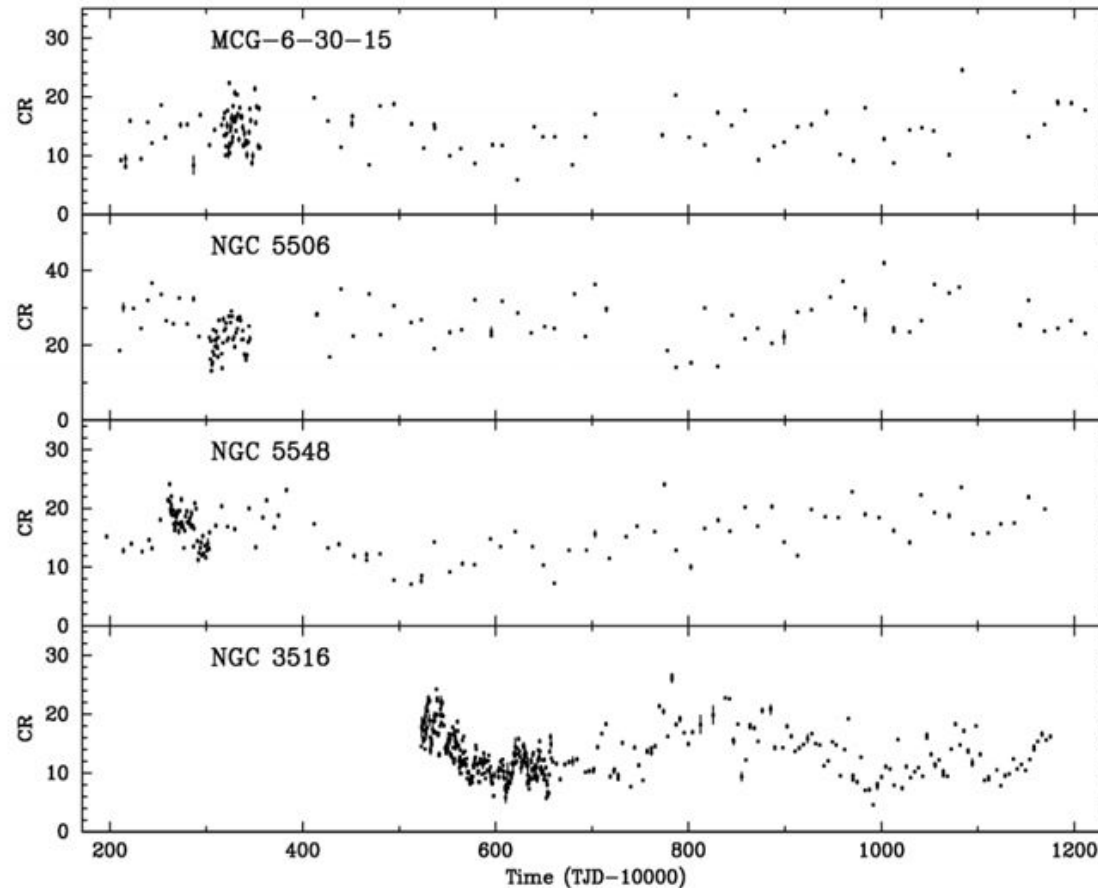
- Variability increases (larger amplitude and more rapid) as one moves to higher frequencies.
- Rapid X-ray Variability on Timescales Down to Minutes!!
- X-ray variability often implies an emission-region size of light hours or less.

Variability of AGNs



- Rapid X-ray Variability on Timescales Down to Minutes!!
- X-ray variability often implies an emission-region size of light hours or less.

Variability of AGNs



Long-Term 2-10
keV Monitoring
of Five Seyfert
Galaxies

- Variability increases (larger amplitude and more rapid) as one moves to higher frequencies.
- Rapid X-ray Variability on Timescales Down to Minutes!!
- X-ray variability often implies an emission-region size of light hours or less.

Emission-Line Variability

C IV Variability in NGC 5548

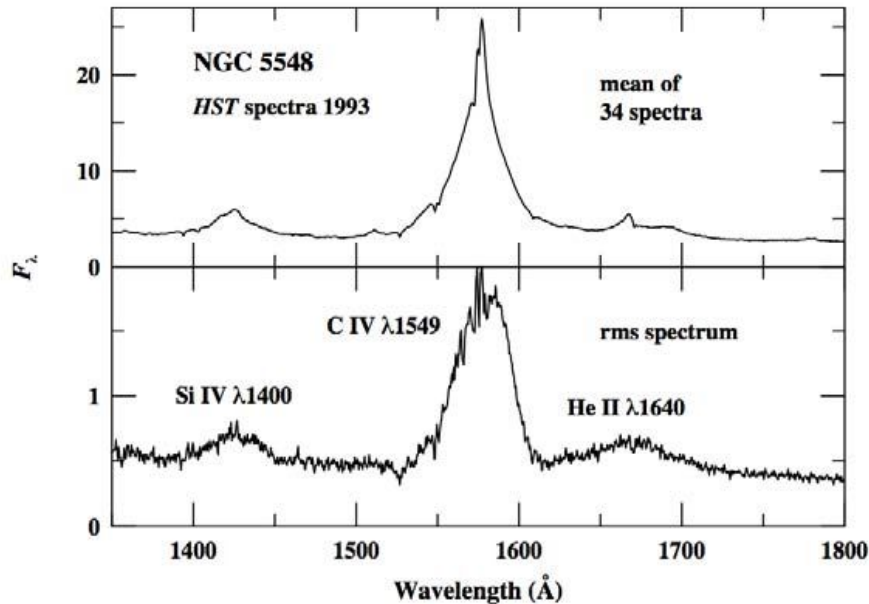


Figure 4. The top panel shows the mean spectrum computed from 34 HST spectra of the variable Seyfert 1 galaxy NGC 5548⁴⁰. The lower panel shows the rms spectrum based on variations around this mean. The rms spectrum thus isolates the variable components of the spectrum. Fluxes are in units of $10^{-15} \text{ ergs s}^{-1} \text{ cm}^{-2} \text{ \AA}^{-1}$.

H β Variability of Markarian 335

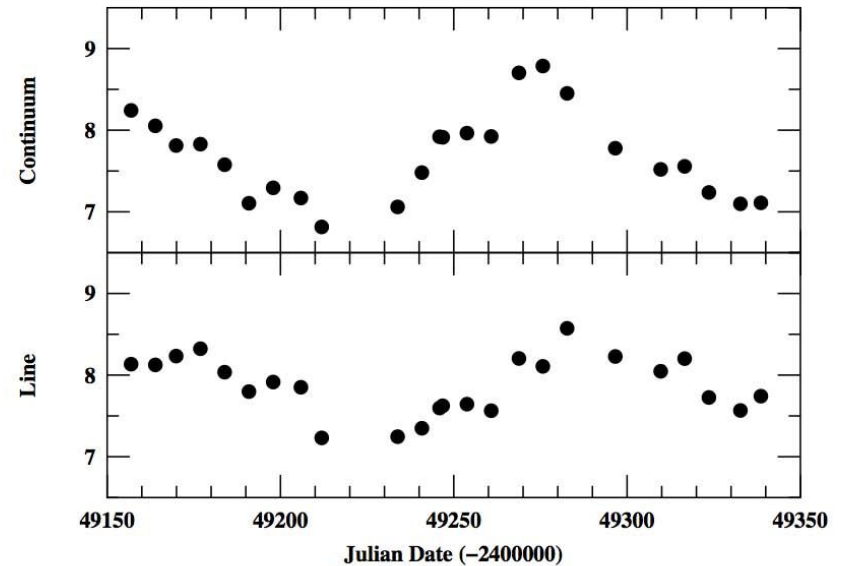
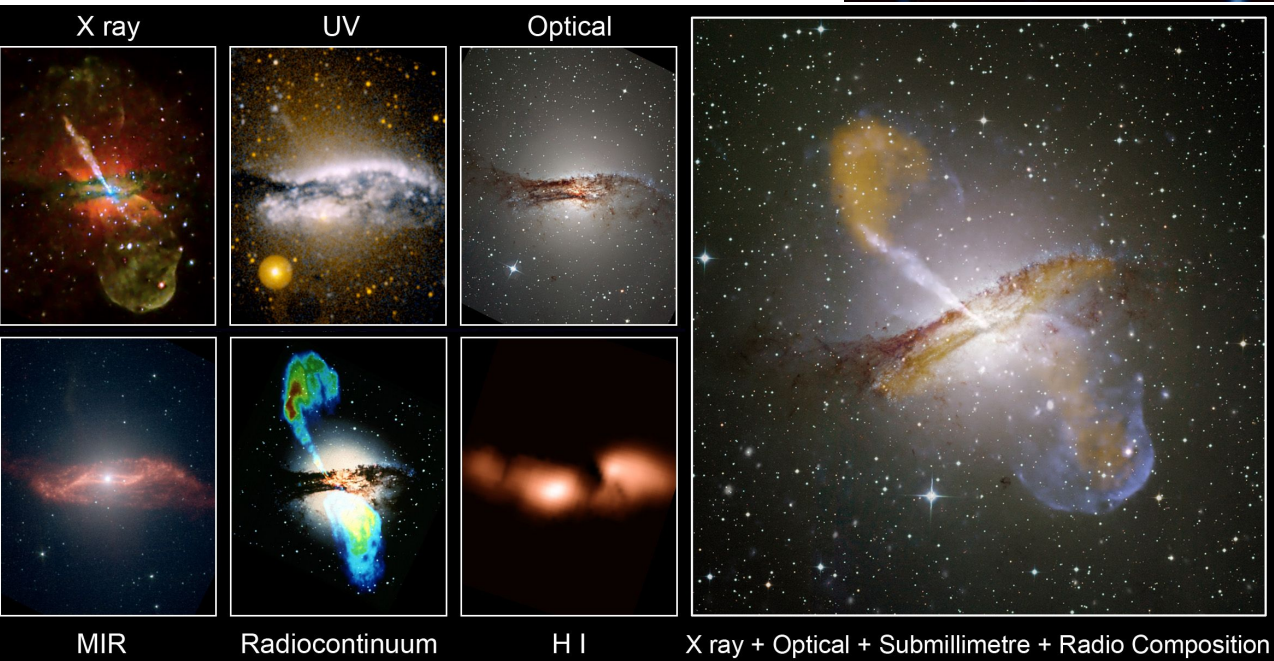
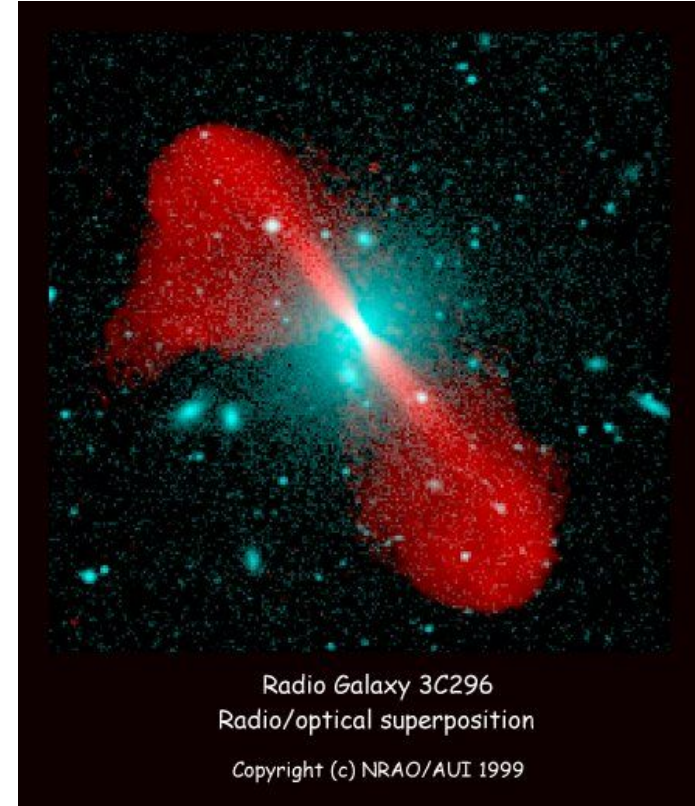
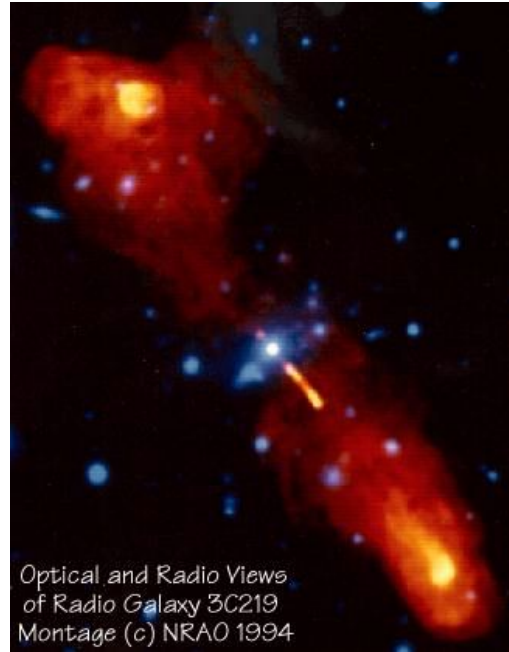
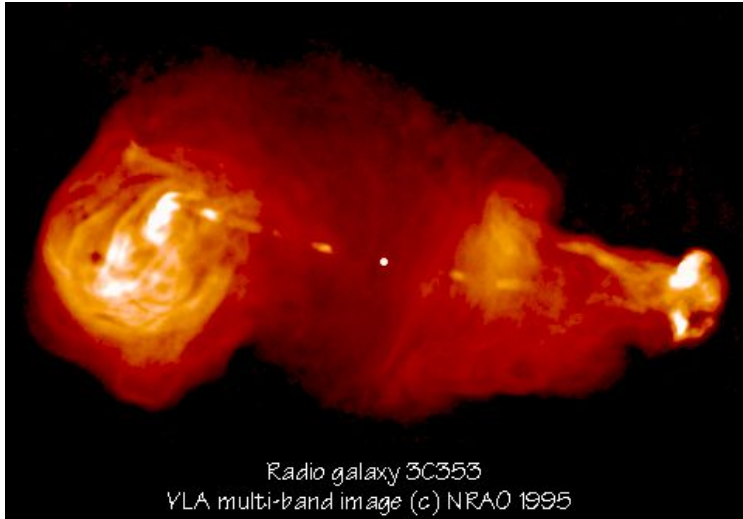


Figure 23. The H β emission-line and optical continuum fluxes for Mrk 335, as shown in Fig. 22, are plotted as a function of time. It is clear from the figure that the continuum and emission-line fluxes are well-correlated, and that the correlation can be improved by a linear shift in time of one time series relative to the other. The optimum linear correlation occurs by shifting the emission-line light curve backwards by 15.6 days.

- The broad emission lines also vary, generally following the continuum with a lag.
- Leads to the idea of that there's a physical time delay \rightarrow different regions between continuum and EL regions (reverberation mapping)

Particle Jets



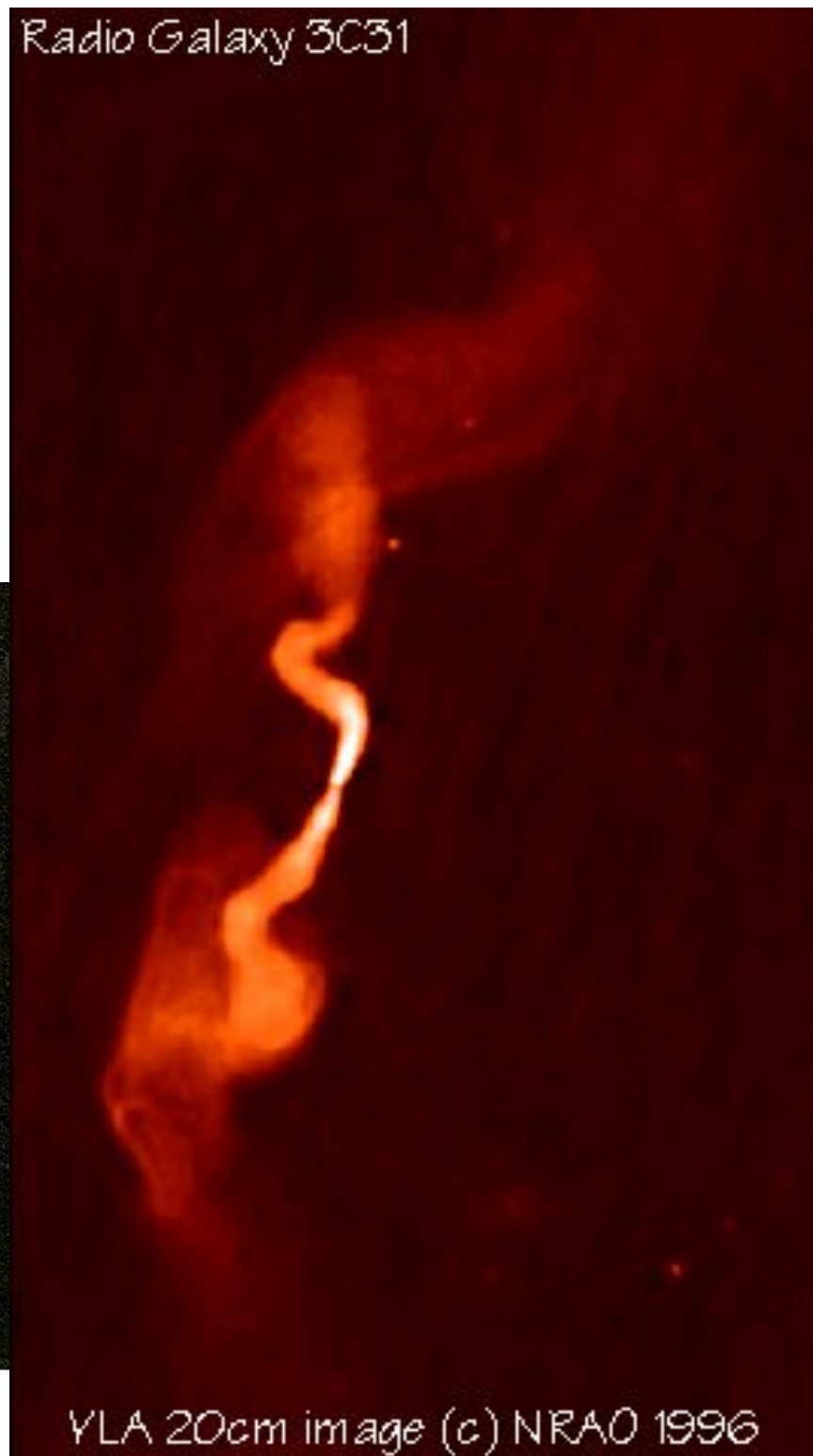
Centaurus A

- A significant minority of AGNs (about 10%) emit powerful particle jets.
- These produce strong radio emission via synchrotron – such AGNs are “radio loud”.

- **How do we know the jets**
- **are streams of gas?**

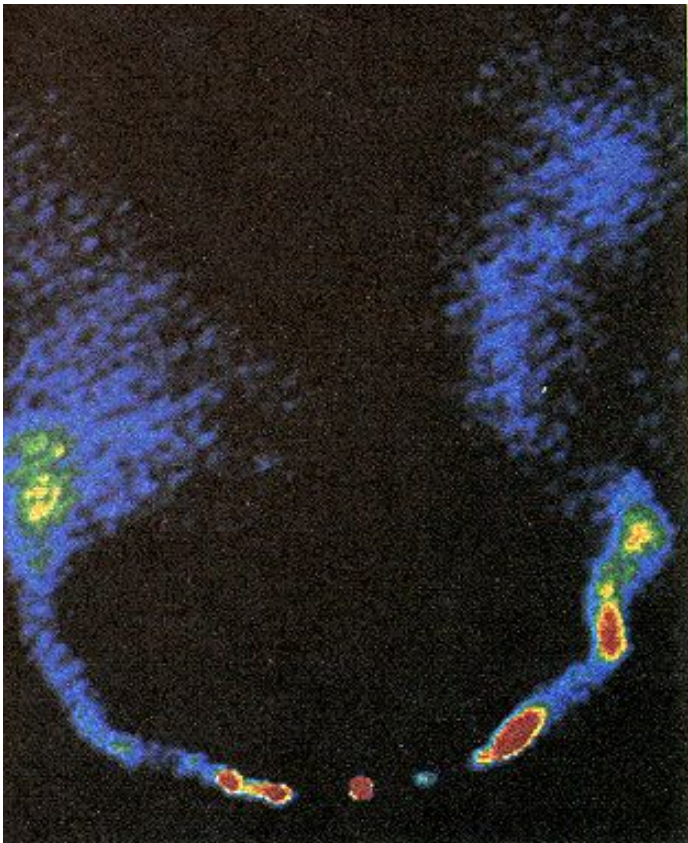
- They produce of kind of “skywriting” when interacting with background

Radio Galaxy 3C31

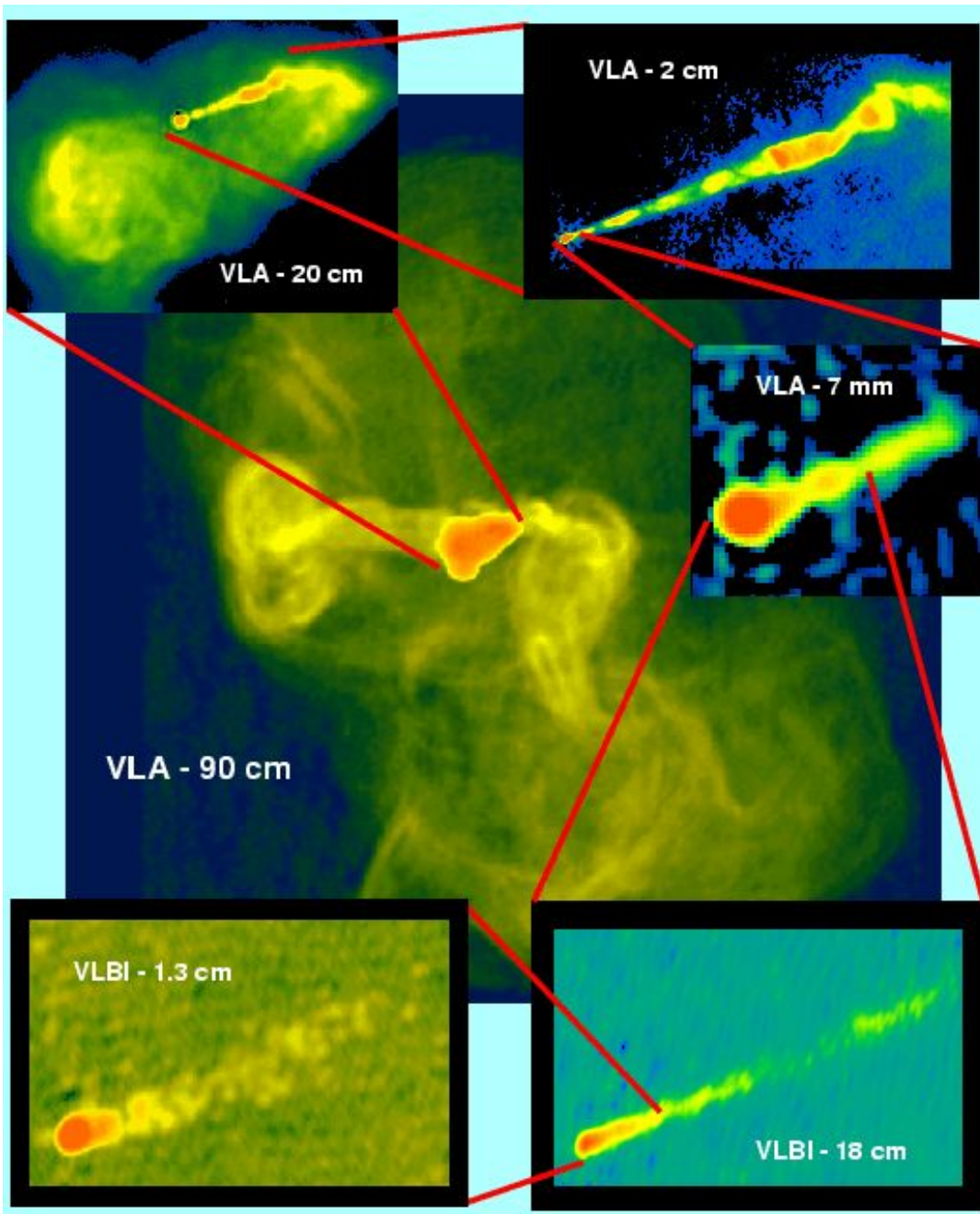


VLA 20cm image (c) NRAO 1996

NGC 1265
a “radio trail”

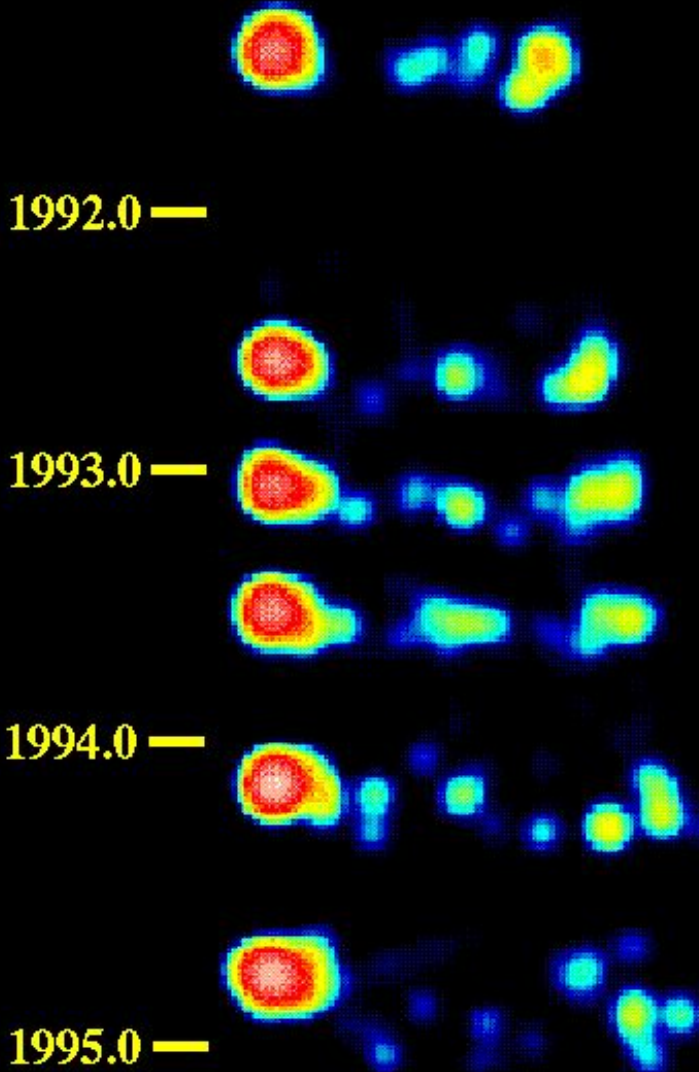


Particle Jets



- Zooming in on the jet of M87.
- Note the pointing stability over a very long timescale.
- Implies some “gyroscope” keeping the pointing fixed.
- Can trace the jet down to the vicinity of the SMBH.

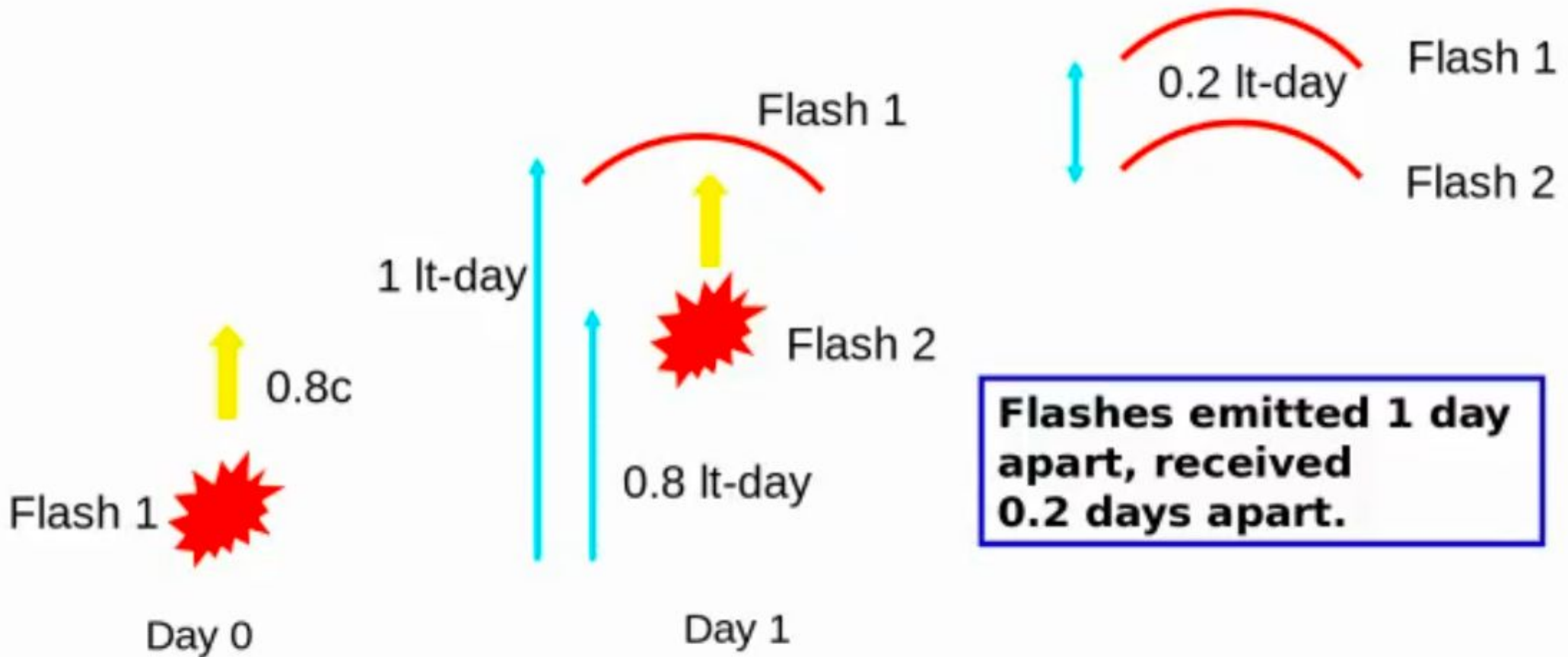
3C 279 Superluminal Motion



5 milliarcseconds

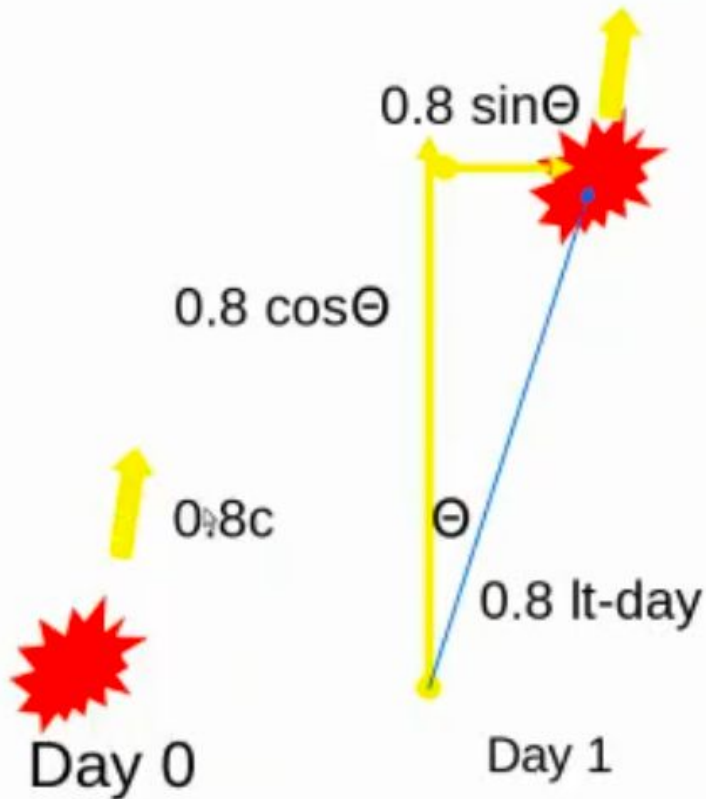
Super-Luminal Motions

- Suppose source emits flashes 1 day apart, while moving toward you at $0.8c$



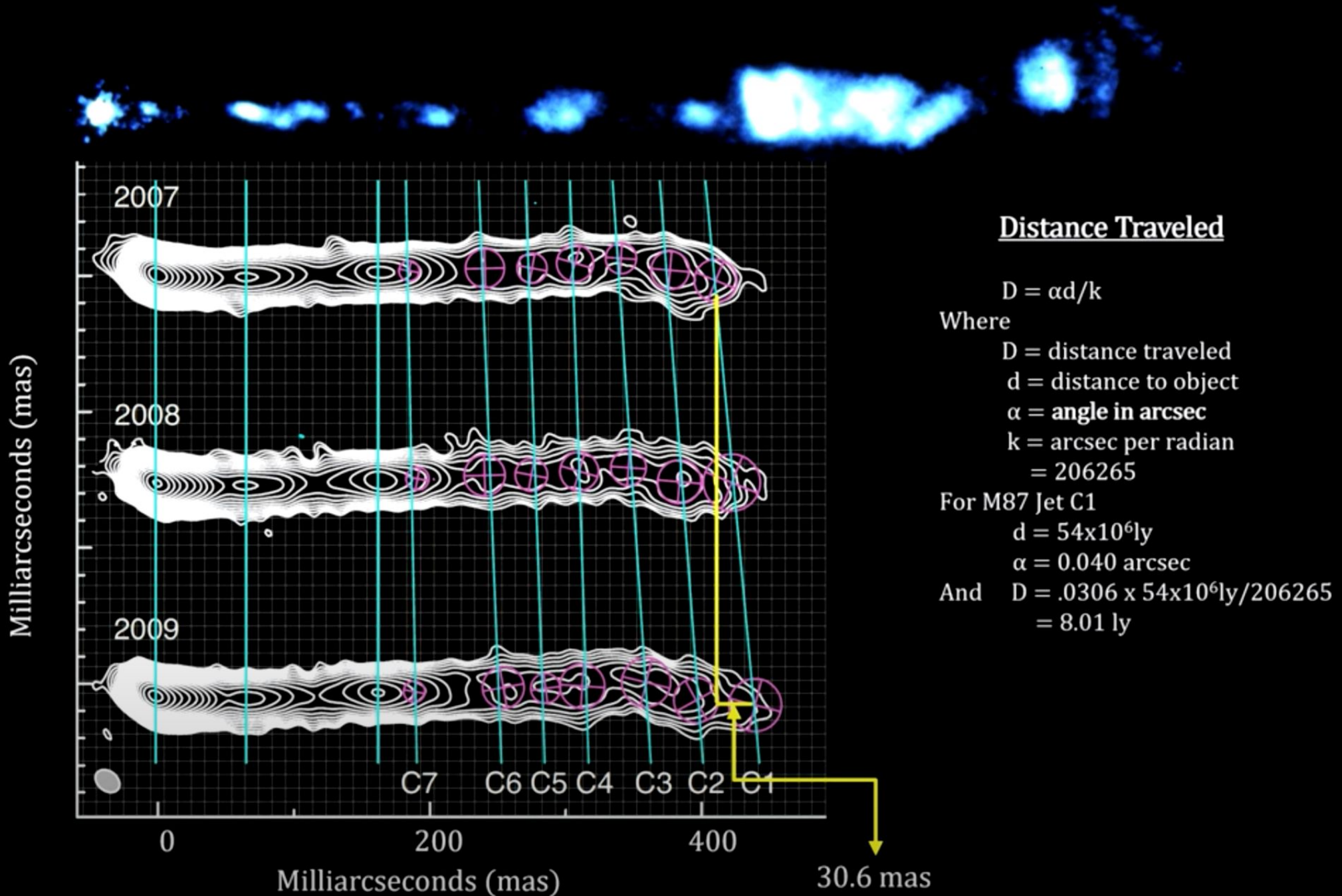
Super-Luminal Motions

- Consider continuously glowing blob, moving *almost* directly toward you at $0.8c$



Actual dist. traveled: 0.8 lt-day
Apparent travel time: $(1 - 0.8 \cos\theta) \text{ day}$
Sideways dist: $0.8 \sin\theta$
Apparent sideways speed:
 $0.8 \sin\theta / (1 - 0.8 \cos\theta) c$

Super-Luminal Motions on M87



Super-Luminal Motions

Let

$$\delta t = (t_2 - t_1)$$

$$D = v \delta t$$

θ = the viewing angle

$$D' = v \delta t \sin \theta$$

D_L = the long distance to the object at point B

φ = the milliarcsec movement angle

$$t_1' = t_1 + (D_L + D \cos \theta) / c$$

$$t_2' = t_2 + D_L / c$$

$$\delta t' = (t_2' - t_1')$$

Then

$$\delta t' = \delta t (1 - (v/c) \cos \theta)$$

$$\delta t = \delta t' / (1 - (v/c) \cos \theta)$$

$$v = D / \delta t$$

$$v' = D' / \delta t'$$

$$v' = v \sin \theta / (1 - (v/c) \cos \theta)$$

$$v = v' / (\sin \theta + (v/c) \cos \theta)$$

We observe

$$\theta = 14^\circ$$

$$\varphi = 30.6 \text{ mas}$$

$$\delta t' = 2 \text{ yr}$$

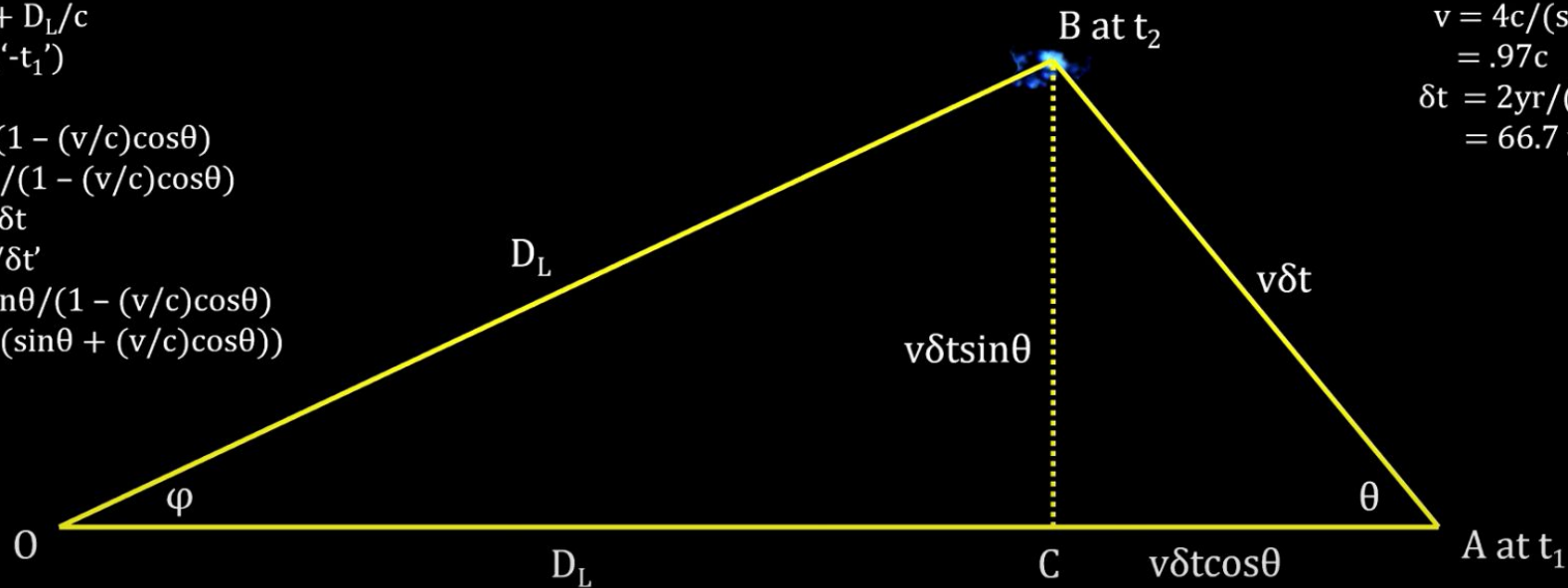
We calculate

$$D' = 8.01 \text{ ly}$$

$$v' = 4c$$

$$v = 4c / (\sin 14^\circ + (4c/c) \cos 14^\circ) = .97c$$

$$\delta t = 2 \text{ yr} / (1 - (4c/c) \cos 14^\circ) = 66.7 \text{ yr}$$



Radiative Mechanism needs to explain:

- Broad range of luminosities, reaching very large values.
- Strong and broad optical/UV emission lines.
- Emission over a very broad band.
- Variability.
- Relativistic Particle jets.

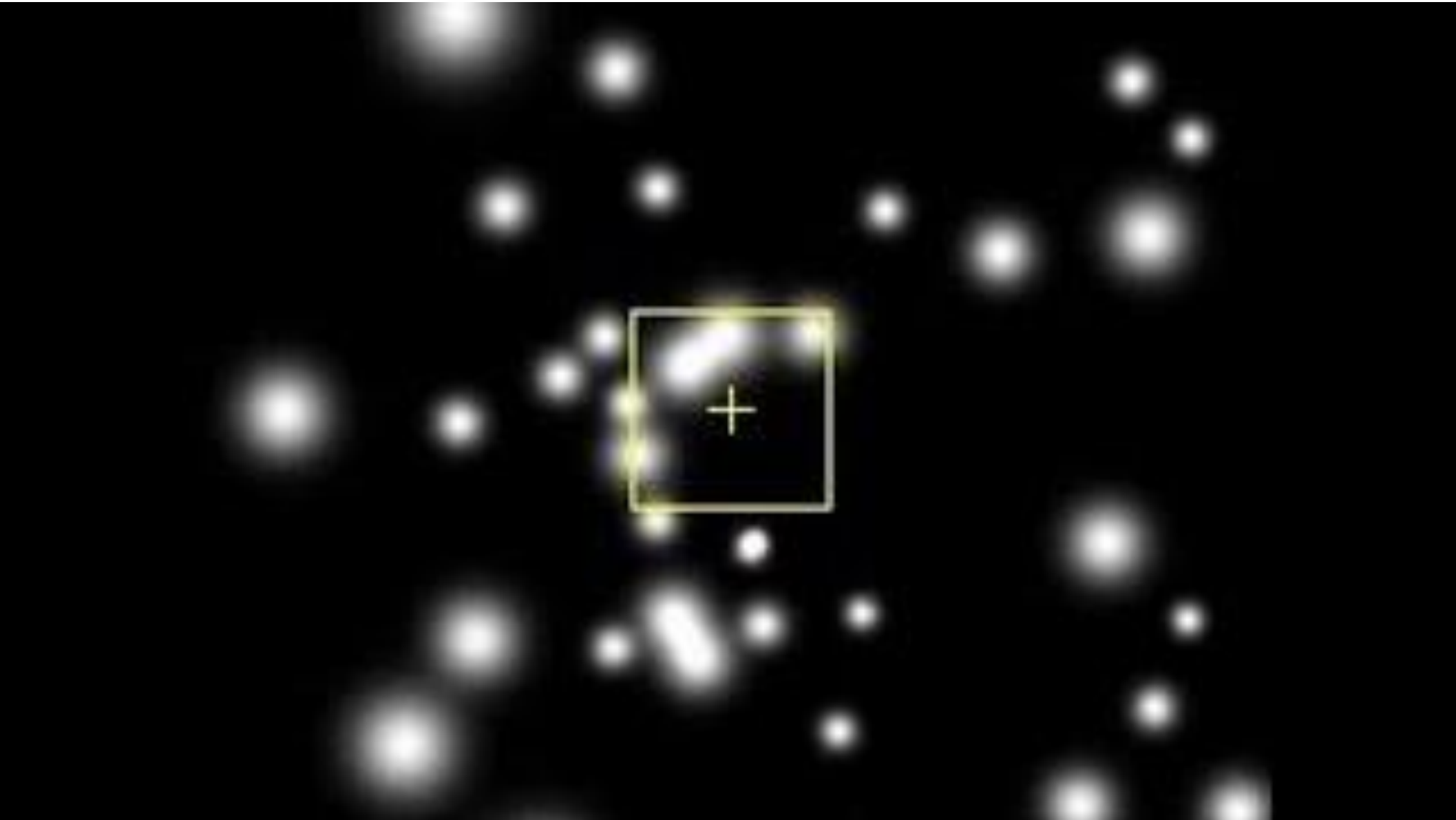
Radiative Mechanism needs to explain:

- Broad range of luminosities, reaching very large values.
- Strong and broad optical/UV emission lines.
- Emission over a very broad band.
- Variability.
- Relativistic Particle jets.



Black Hole + Accretion Disk Model

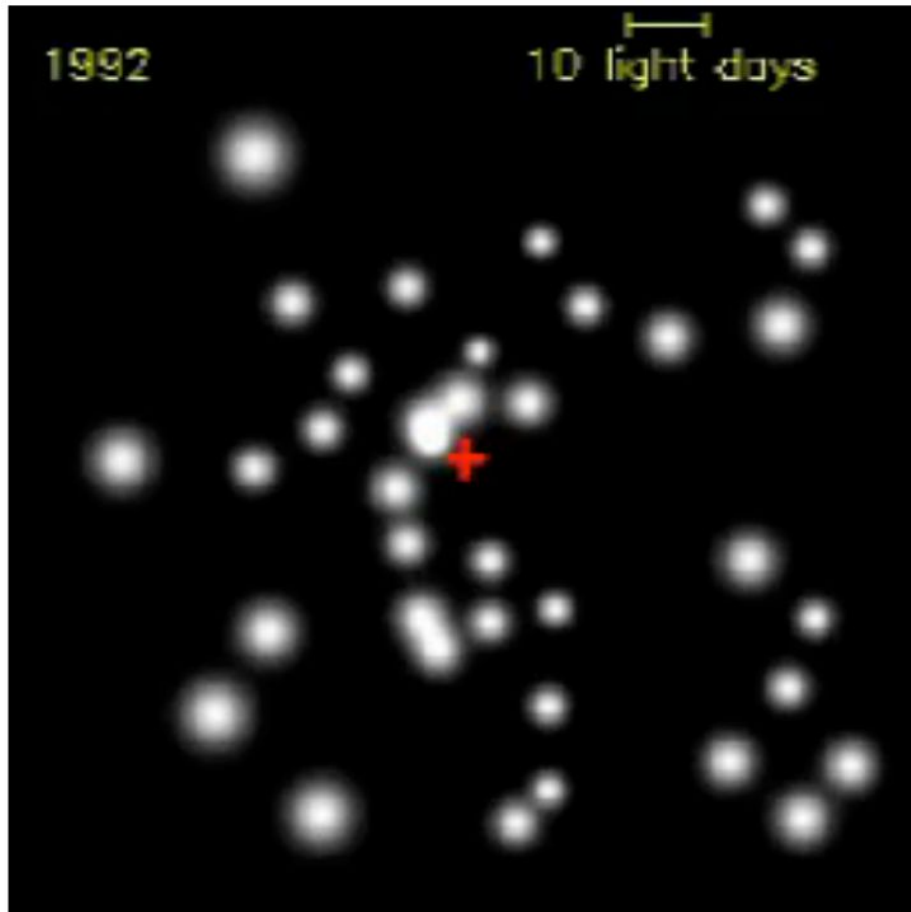
Sagittarius - A



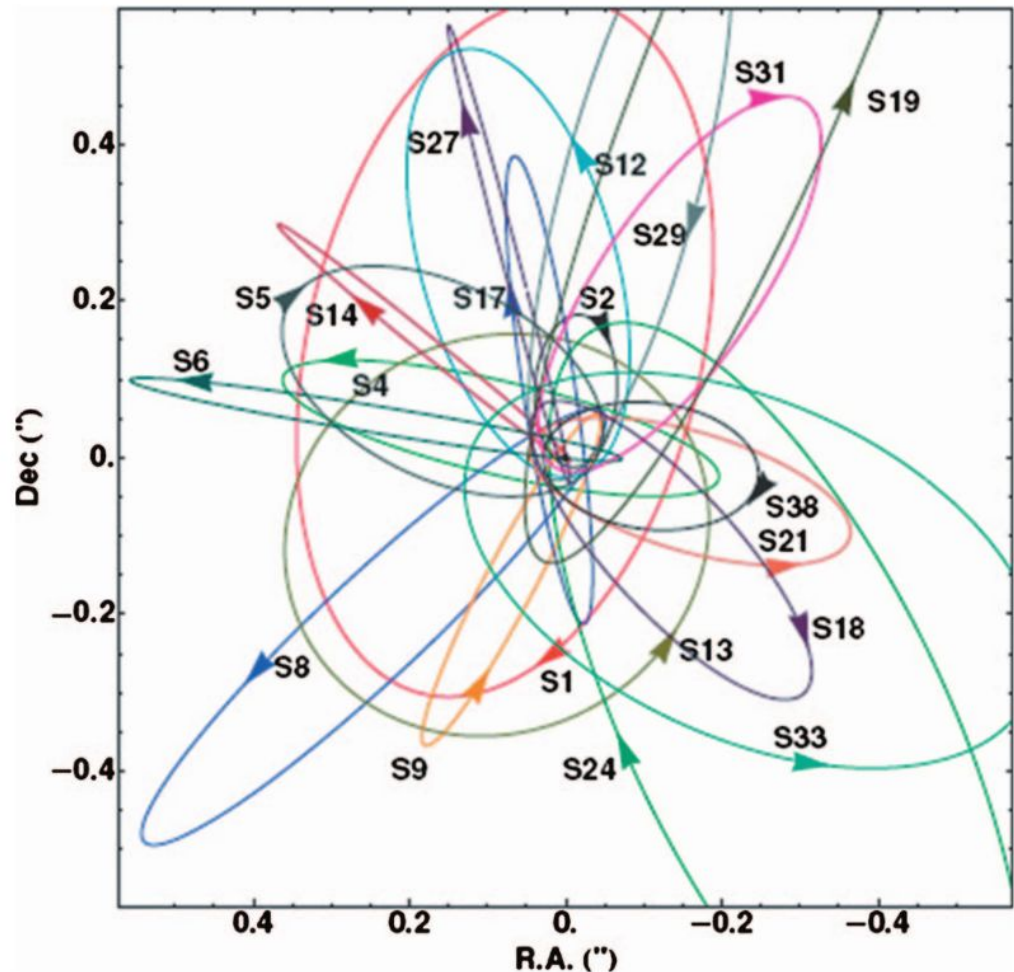
- Dynamical mass of Sagittarius - A \rightarrow few 10^6 Msun within ~ 10 s AU

Star proper motions and orbits

Breakthrough from the detection of accelerations

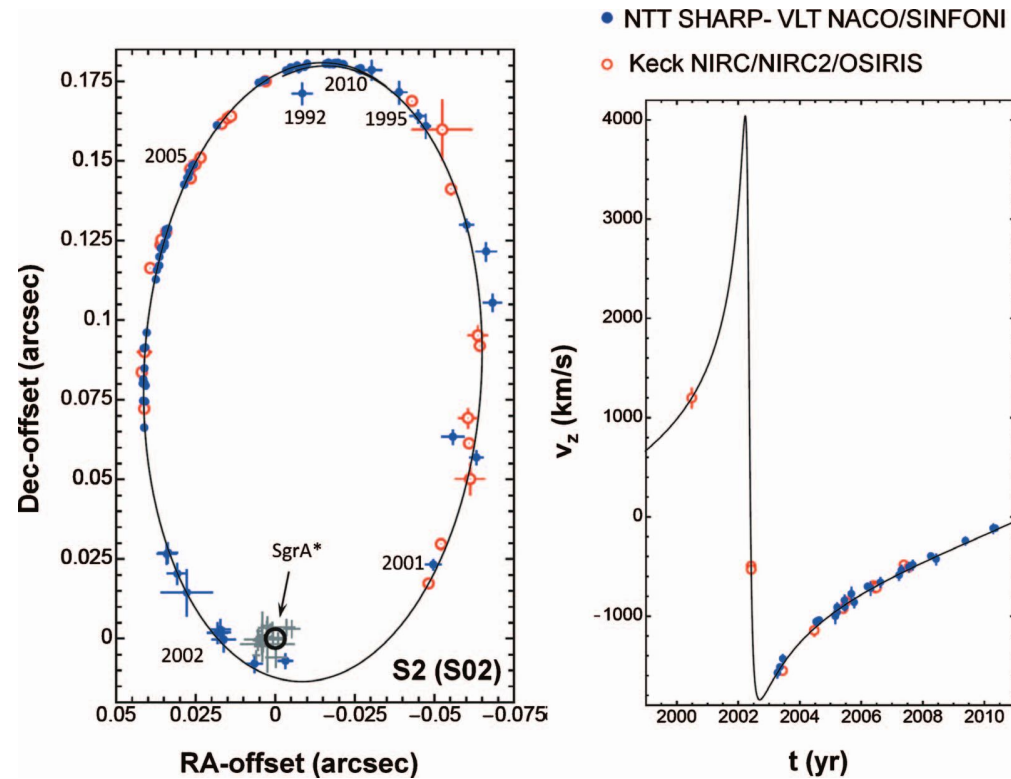


Proper motions



Gillessen+2009

Dynamical Masses: S2 star



Using Kepler's Third Law ...

Fitting orbit and radial velocities:

Period ~ 15.8 y

Eccentricity ~ 0.87

Semi-major axis ~ 1025 AU

Pericenter ~ 125 AU

$$M_{\text{BH}} \sim 4.3 \times 10^6 M_{\odot}$$

Gillessen +2009

Orbit is not closed for possible proper motion of the BH. Grey crosses are IR flares

Marconi

$$\left(\frac{2\pi}{P}\right)^2 = \frac{GM}{a^3}$$

$$M = M_{\odot} \left(\frac{a}{1 \text{ AU}}\right)^3 \left(\frac{P}{1 \text{ yr}}\right)^{-2}$$

$$M = 4.3 \times 10^6 M_{\odot} \left(\frac{a}{1025 \text{ AU}}\right)^3 \left(\frac{P}{15.8 \text{ yr}}\right)^{-2}$$

Other Methods

Which are the scales probed in terms of the Schwarzschild radius, i.e. the BH typical size?

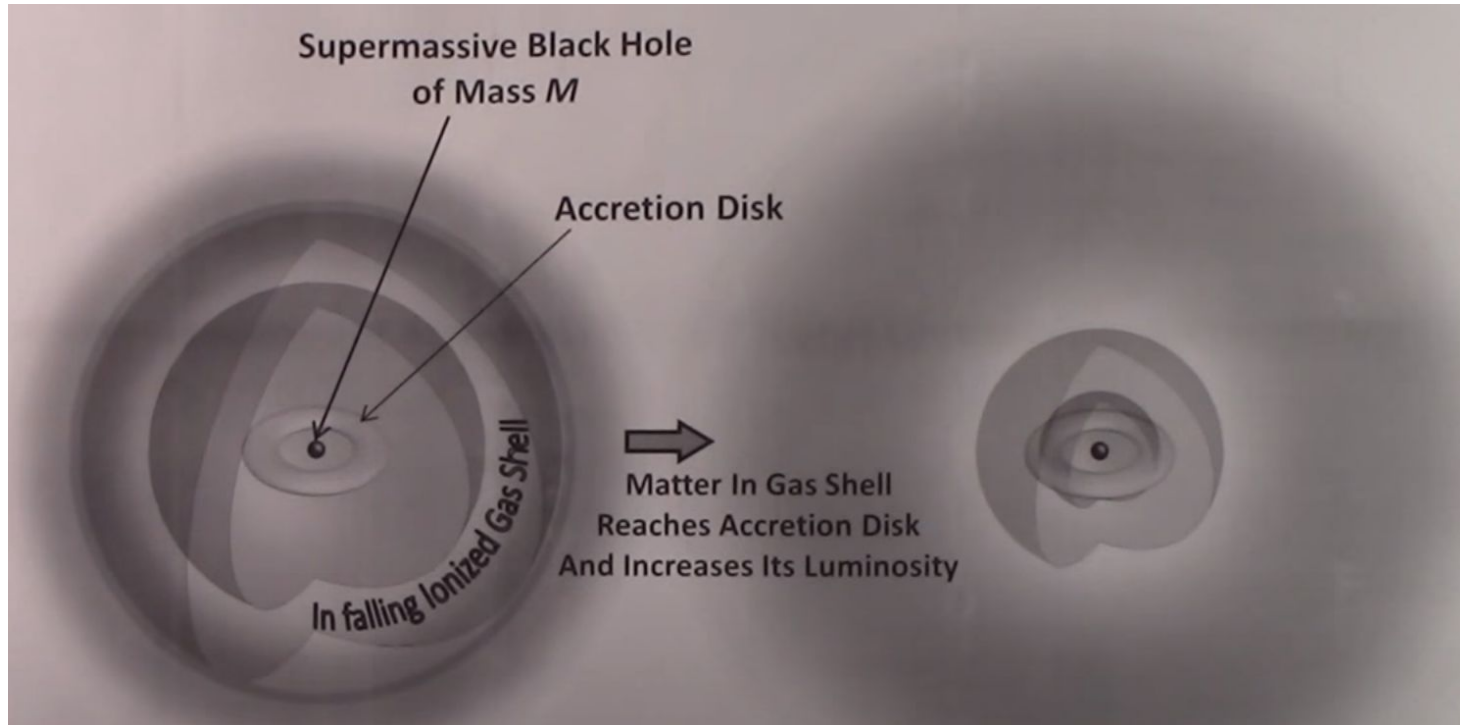
$$\theta_S = \frac{R_S}{D} = 2 \frac{GM_{\text{BH}}}{c^2 D} \simeq 10^{-7} \text{ arcsec} \left(\frac{M_{\text{BH}}}{10^8 M_{\odot}} \right) \left(\frac{D}{20 \text{ Mpc}} \right)$$

TABLE I
Probing the centers of galaxies.

Method & Telescope	Scale (R_S)	No. of SBH Detections	M_{\bullet} Range (M_{\odot})	Typical Densities ($M_{\odot} \text{ pc}^{-3}$)
Fe $K\alpha$ line (XEUS, ConX)	3–10	0	N/A	N/A
Reverberation mapping (Ground based optical)	600	36	10^6 – 4×10^8	$\gtrsim 10^{10}$
Stellar proper motion (Keck, NTT, VLT)	1000	1	4×10^6	4×10^{16}
H ₂ O megamasers (VLBI)	10^4	1	4×10^7	4×10^9
Gas dynamics (optical) (Mostly <i>HST</i>)	10^6	11	7×10^7 – 4×10^9	$\sim 10^5$
Stellar dynamics (Mostly <i>HST</i>)	10^6	17	10^7 – 3×10^9	$\sim 10^5$

The columns give all methods which can (or, in the case of the Fe $K\alpha$ line emission, might) be used

Eddington Limit

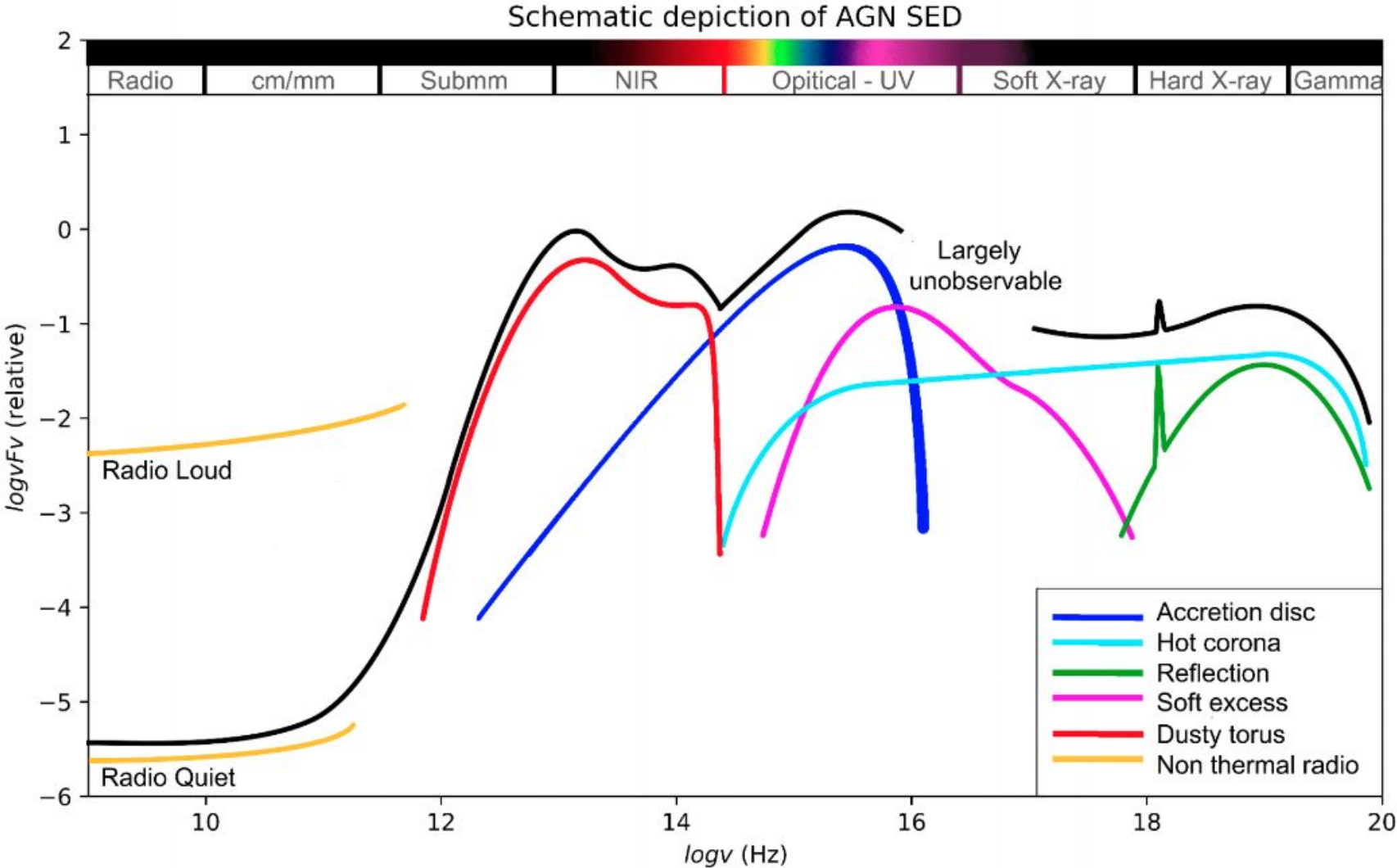


- Accretion produces radiation: radiation makes pressure – can this inhibit further accretion?
- Radiation pressure acts on electrons; but electrons and ions (protons) cannot separate because of Coulomb force.

$$F_{rad} = \frac{L\sigma_T}{4\pi cr^2} = F_{grav} = \frac{GM(m_p + m_e)}{r^2} \quad \rightarrow \quad L \leq L_{Edd} = \frac{4\pi GMm_p c}{\sigma_T}$$

$(m_p \gg m_e)$

Black Hole + Accretion Disk Model



Origin of the X-ray Emission

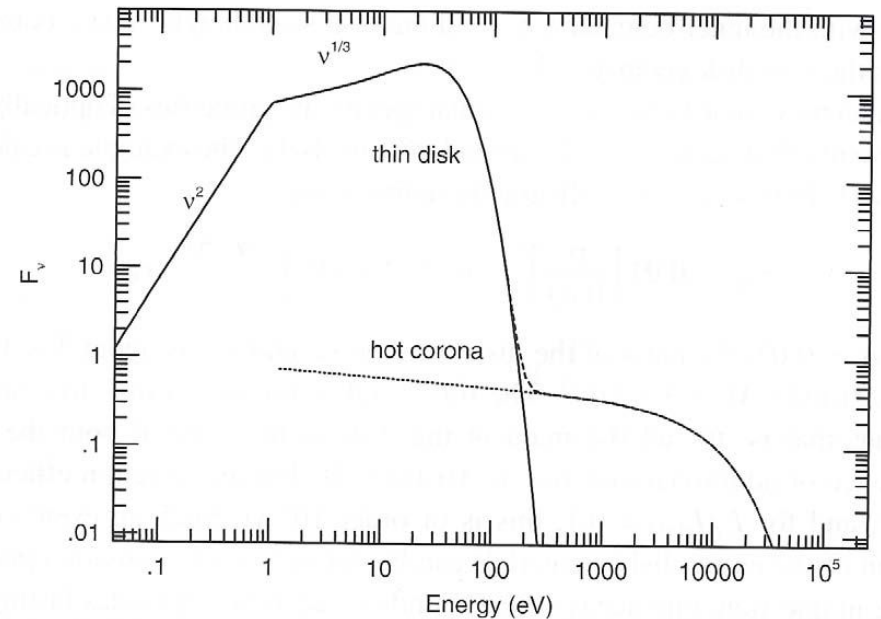
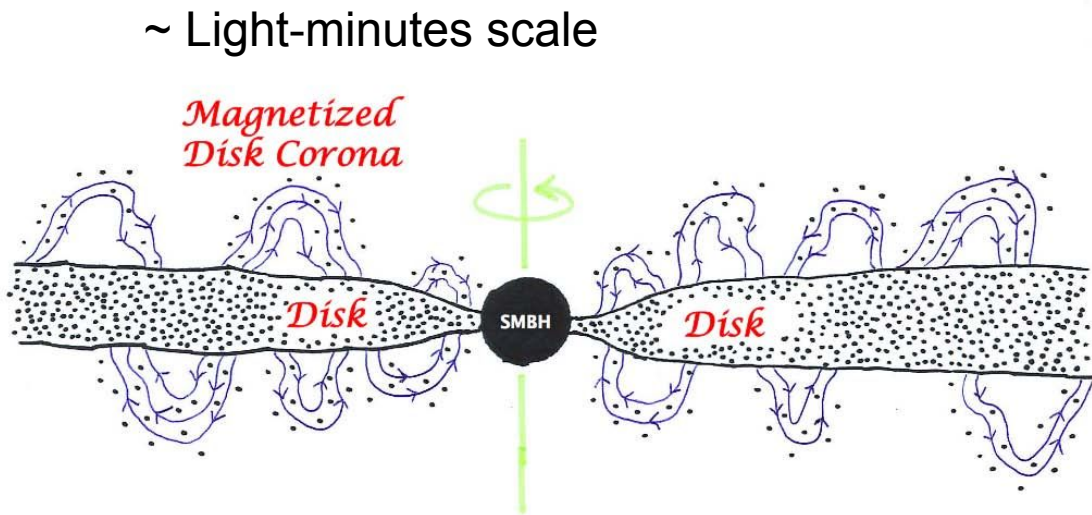
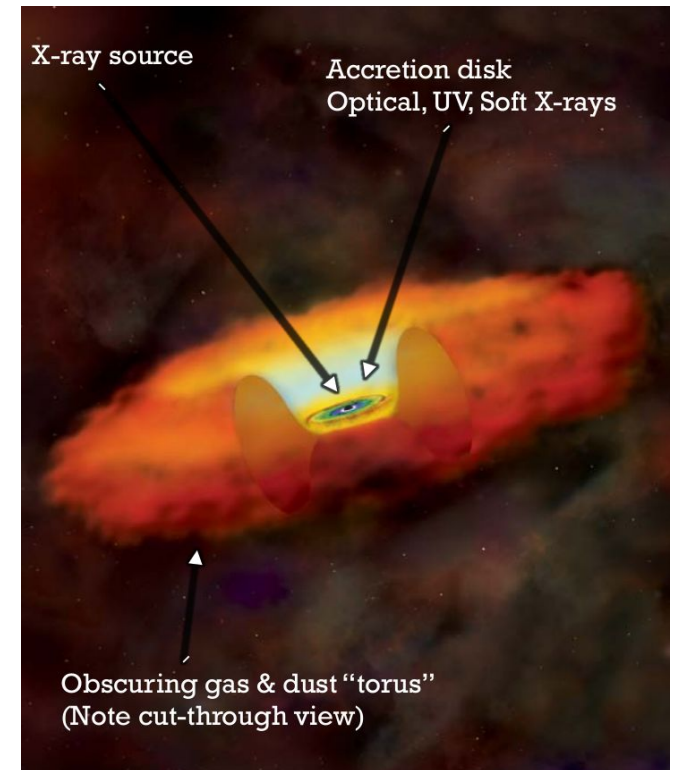
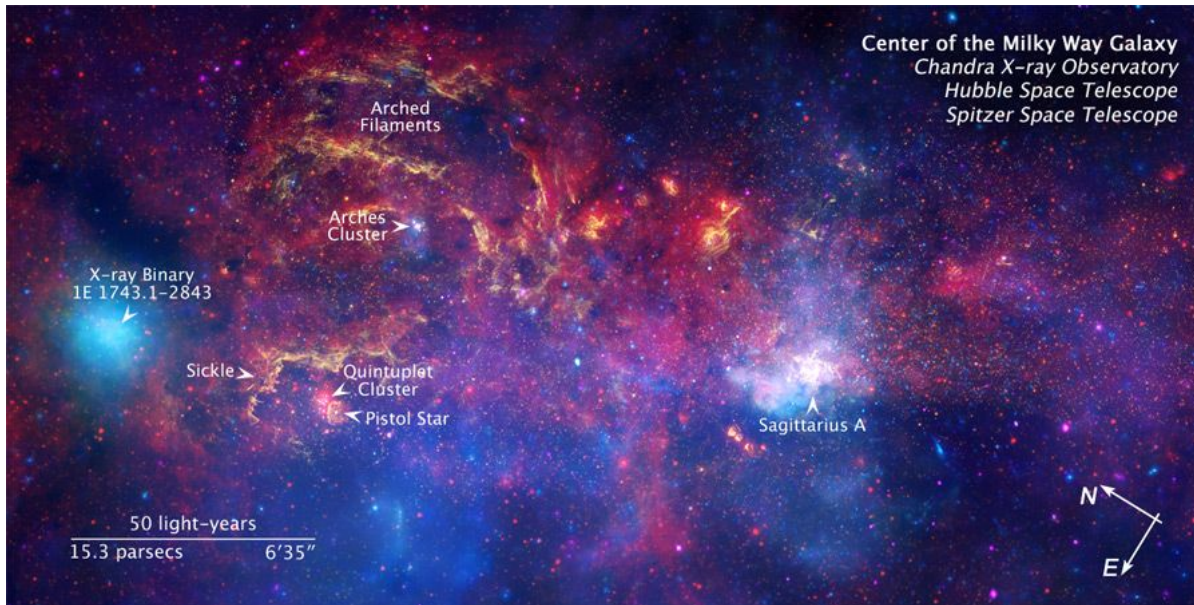


Figure 4.3. A schematic of a combined disk–corona spectrum. The maximum temperature of the geometrically thin, optically thick accretion disk is $T_{\text{max}} = 10^5$ K, and its outer boundary temperature is determined by the conditions at the self-gravity radius. The disk is surrounded by an optically thin corona with $T_{\text{cor}} = 10^8$ K.

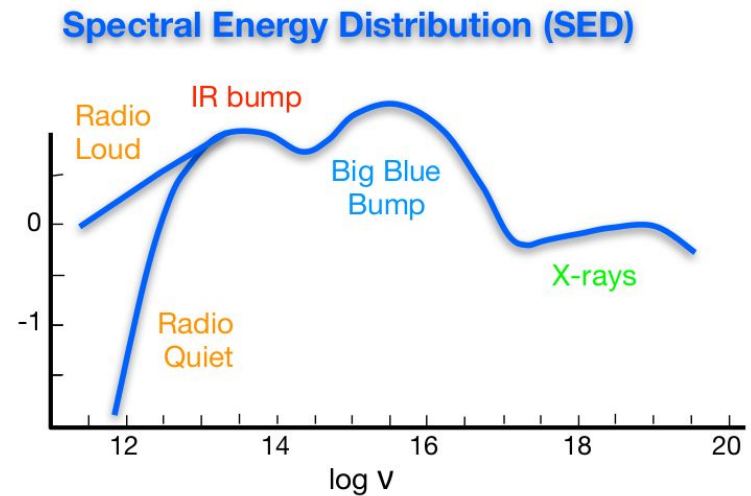
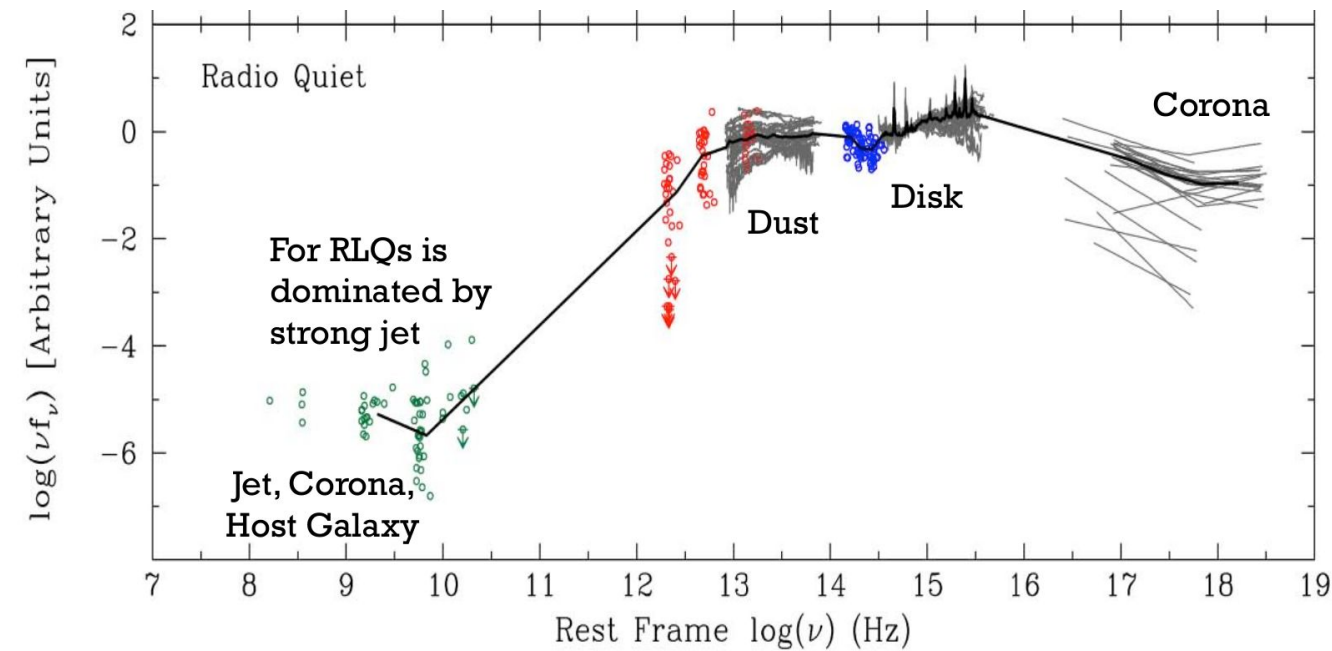
- X-rays are not naturally produced by AGN disks; the disk is too cool.
- Need to add an accretion disk “corona” with a temperature of ~ 150 keV.
- This makes X-rays by Compton scattering.
- Perhaps low-energy X-rays from disk component (soft X-ray excess)

Obscuration and Radiation Reprocessing



- Many active galaxies have obscuring/reprocessing material, often envisioned to be in the form of a "torus".
- This material likely produces much of the infrared emission as reprocessed "waste heat" from dust.

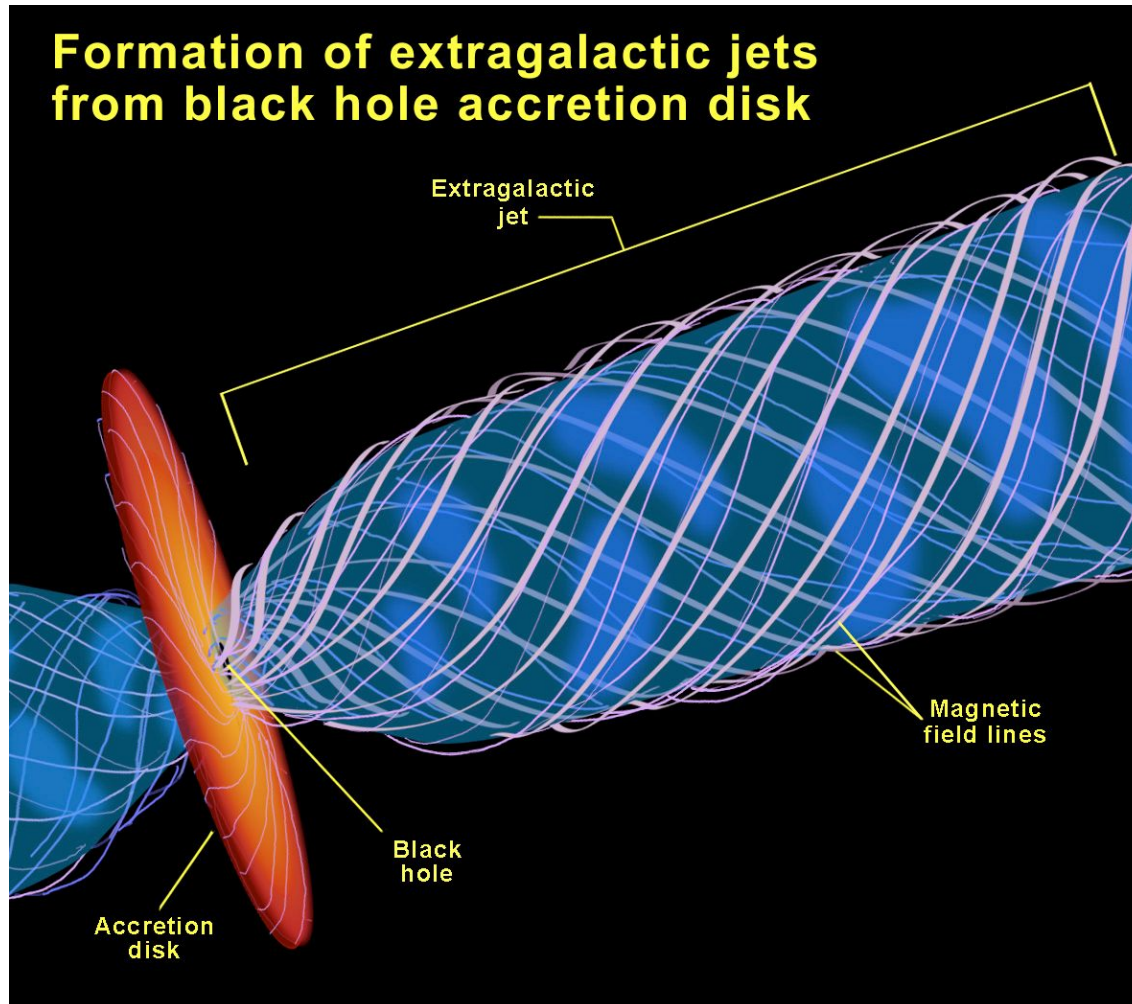
Explaining Emission Over a Very Broad Band



Explaining Variability

- The accretion disk is expected to have about the correct size to explain the observed variability timescales.
- It naturally explains the change in variability as a function of frequency.
- At a fundamental level, the physical origin of the variations is **STILL POORLY UNDERSTOOD!!**
- MHD simulations of accretion disks indicate several possible causes of variability: local random variations in dissipation, non-axisymmetric structures, global precession of tilted flows, etc.
- A deeper understanding will require proper simulation of both dynamics and thermodynamics.
- Also can have variable accretion rates, variable obscuration, microlensing.

Explaining Particle Jets



BH Accretion is a natural good candidate:

- Relativistic Motions
- Magnetic Fields (also responsible for the X-ray Corona emission)
- Stable “gyroscopes”

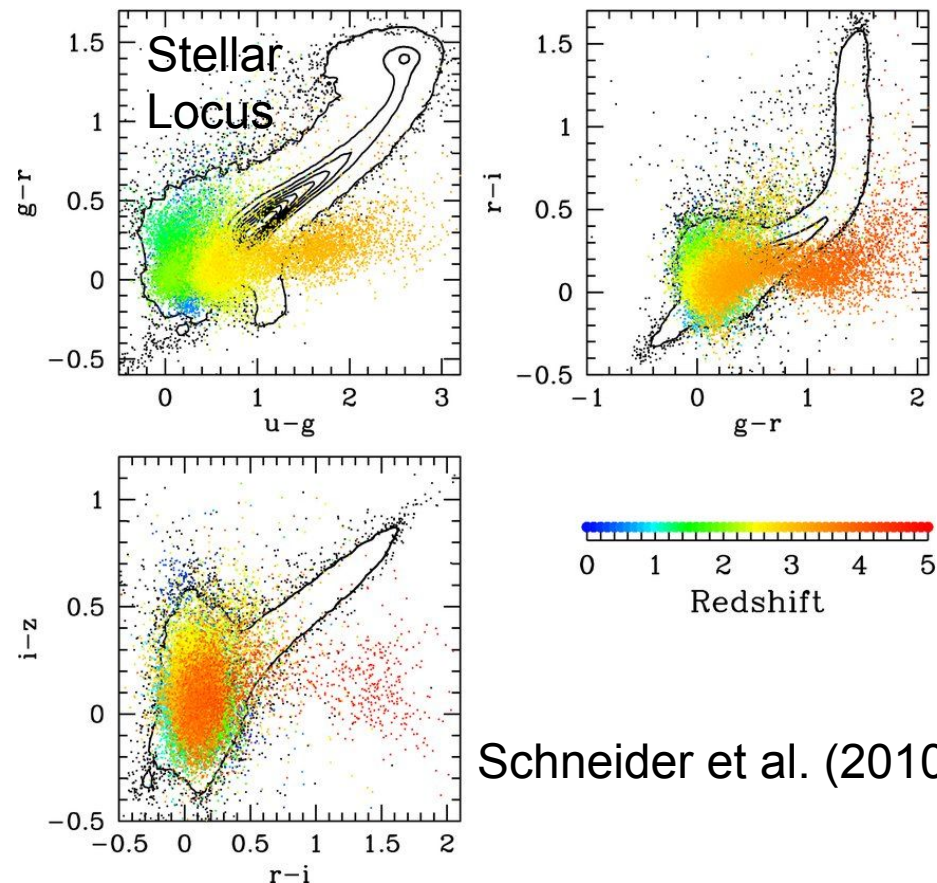
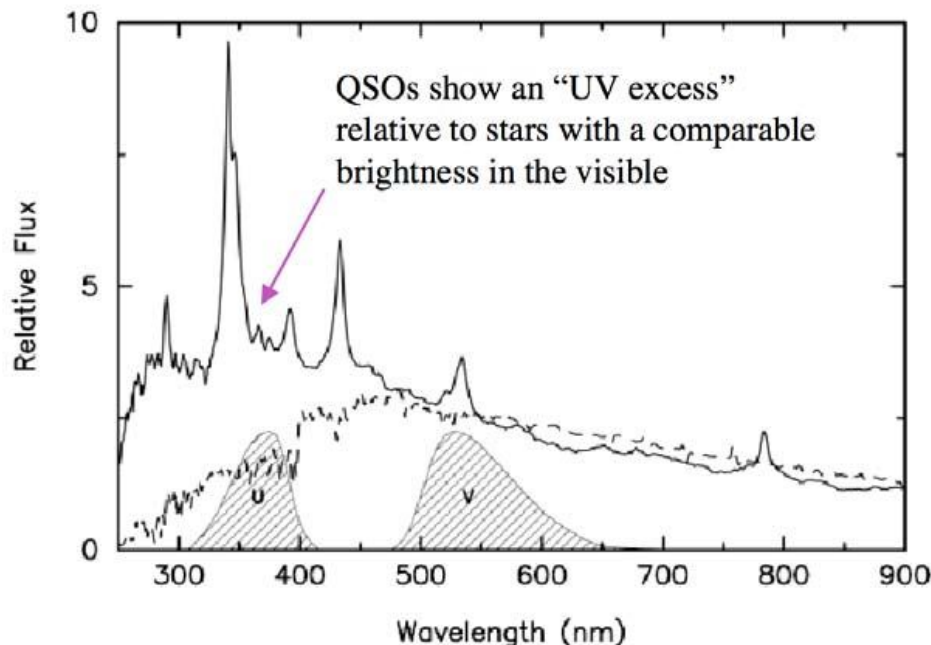
Outline

- Early history
- AGN basics
- Finding AGNs
- AGN terminology
- AGN unification
- Dissecting AGNs
- Focused lecture: Proving the Evidence of a SuperMassive BH

Finding AGNs

- There are many methods for finding AGNs.
- All methods devised for finding AGNs have limitations and selection effects.
- Though some are more effective and give purer samples than others.
- For a complete census, want to apply as many methods as possible enabling cross-checks.
- Need for Multiple Methods.

Optical/UV Colors

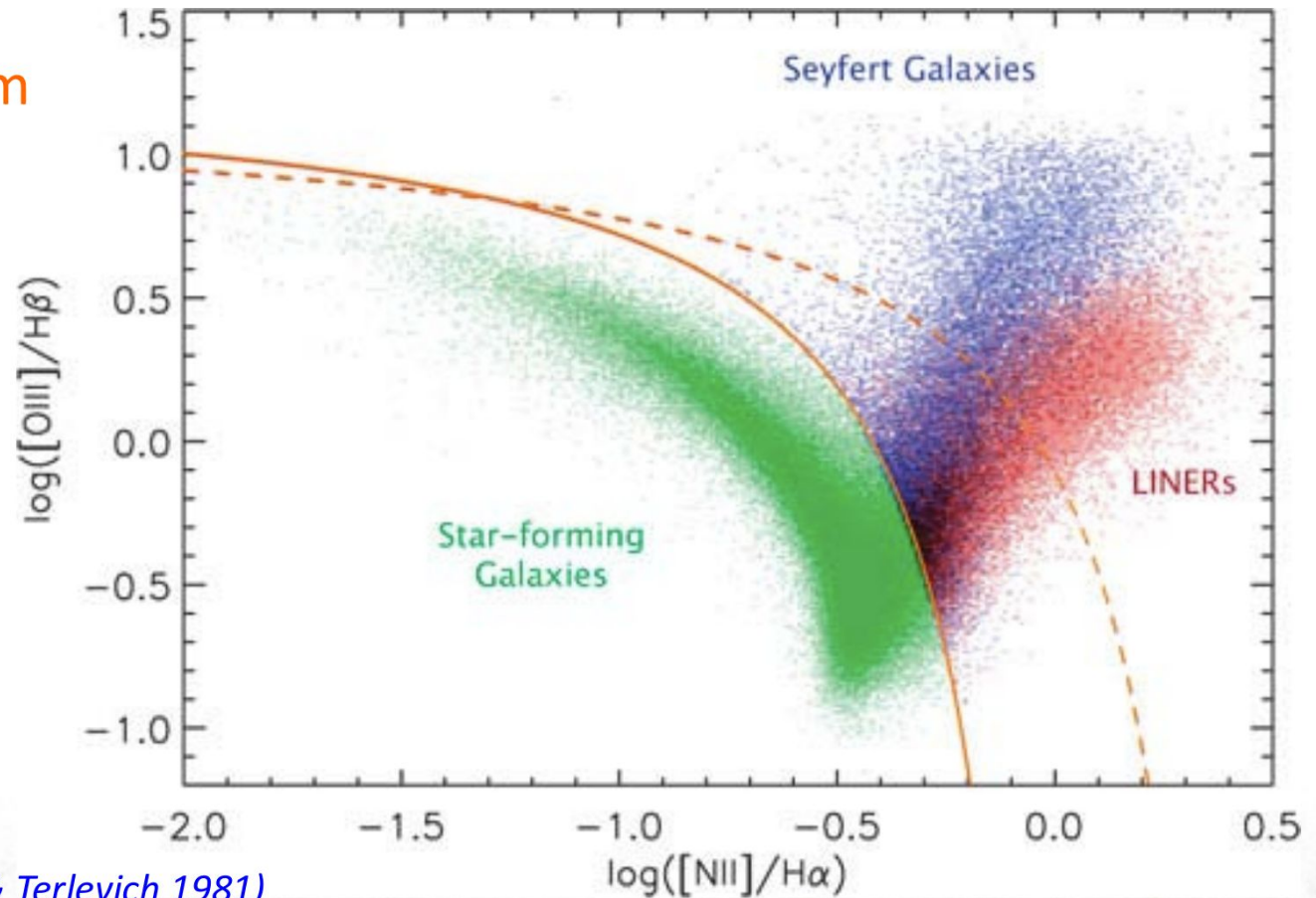


- Look for Point Sources brighter in UV than normal stars – Works to $z \sim 2-2.5$
- At higher redshifts, absorption by the IGM makes Quasars very Red in Blue part of Spectrum
- These methods work best for unobscured quasars; e.g., reddening causes trouble.
- Furthermore, at lower AGN luminosities, host-galaxy light becomes problematic

Schneider et al. (2010)

BPT Diagram

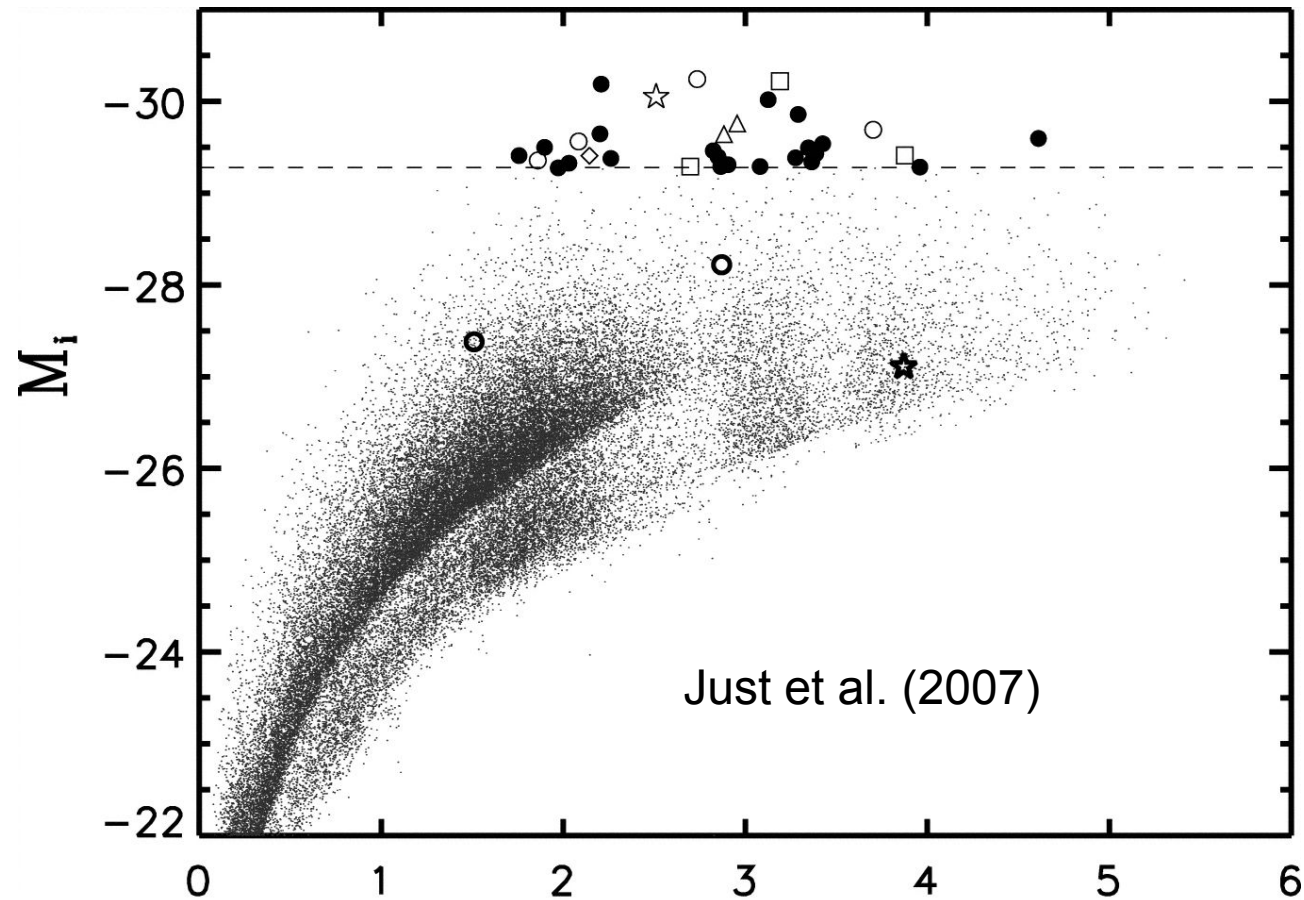
BPT diagram



(Baldwin, Phillips & Terlevich 1981)

Figure 6.1. The spread of emission-line galaxies from the SDSS on one diagnostic diagram that uses four strong optical emission lines, $\text{H}\alpha$, $\text{H}\beta$, $[\text{O III}] \lambda 5007$, and $[\text{N II}] \lambda 6584$, to distinguish galaxies that are dominated by ionization from young stars (green points) from those that are ionized by a typical AGN SED (blue points for high-ionization AGNs and red points for low-ionization AGNs). The AGN and SF groups are well separated, but the division between the two AGN groups is less clear. The curves indicate empirical (solid) and theoretical (dashed) dividing lines between AGNs and star-forming galaxies (courtesy of B. Groves).

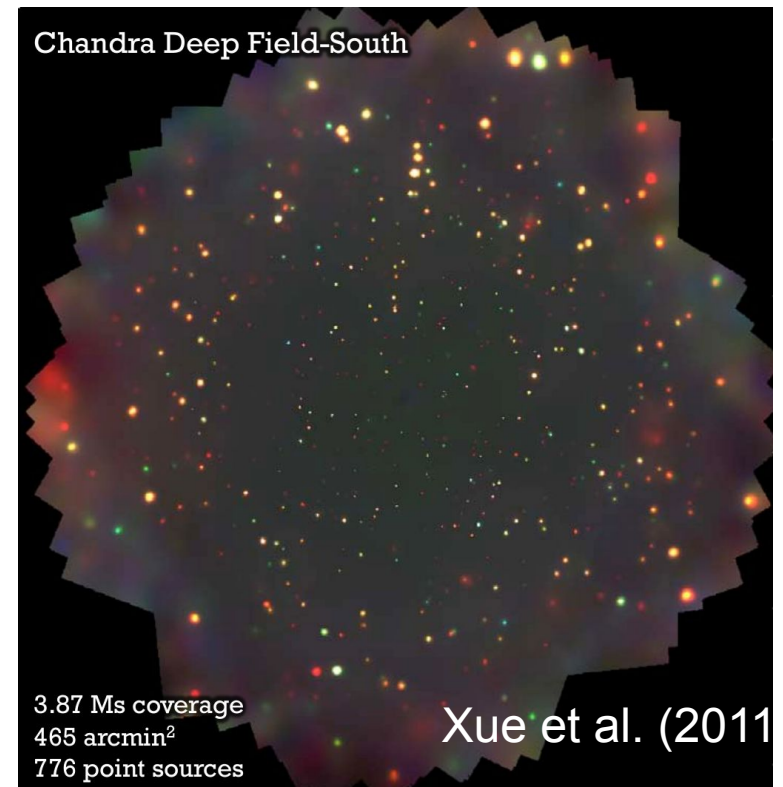
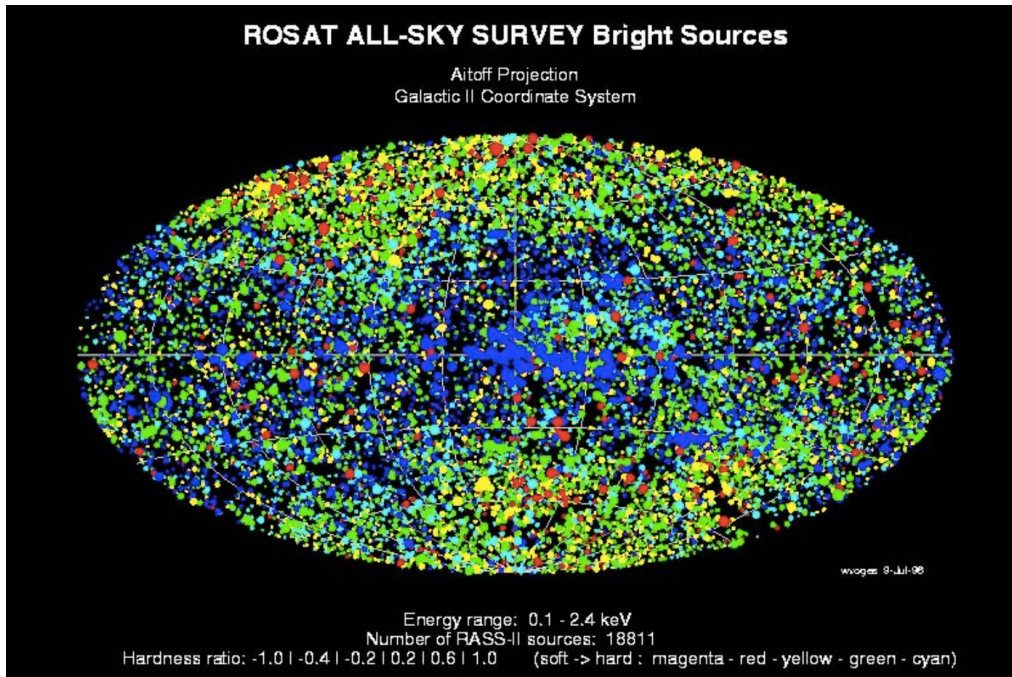
Luminosity-Redshift Coverage from Optical/UV Surveys



- The SDSS has now identified $\sim 300,000$ AGNs^z.
- These span a broad range of luminosity and redshift.
- Note the inevitable luminosity-redshift correlation, common to surveys of all types.

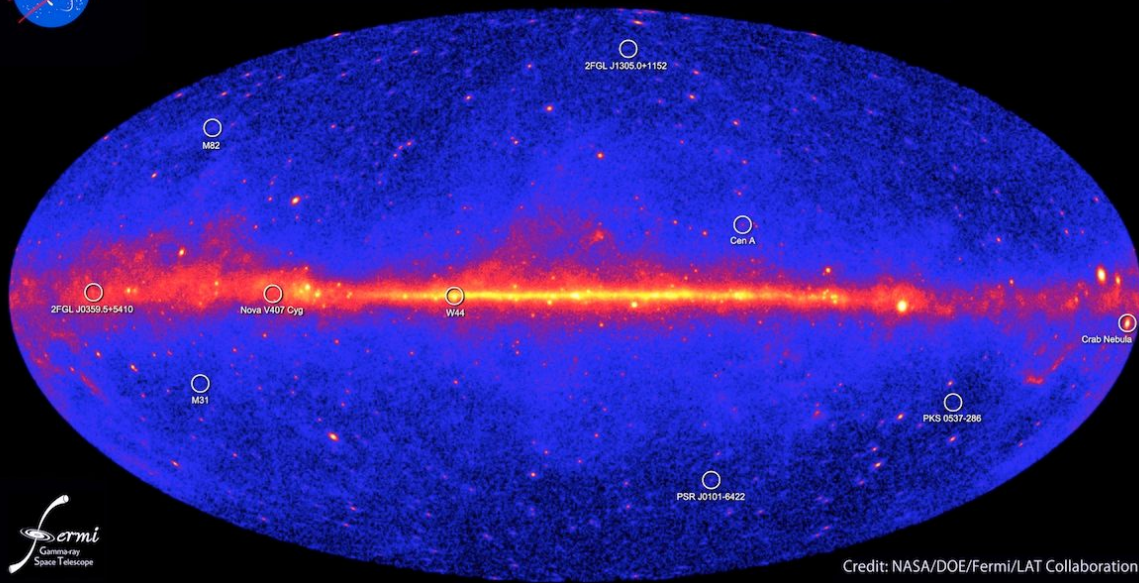
X-ray Surveys for AGNs

- X-ray emission nearly universal from AGNs. Almost all AGNs are STRONG X-ray emission.
- X-rays have reduced absorption bias compared to optical/UV, especially for high-energy X-rays.
- X-rays maximize contrast between black-hole vs. host-galaxy light.
- Can find obscured AGNs and lower luminosity AGNs than in optical/UV.
- Now are a wide variety of X-ray surveys, ranging from shallow all-sky to deep pencil-beam.

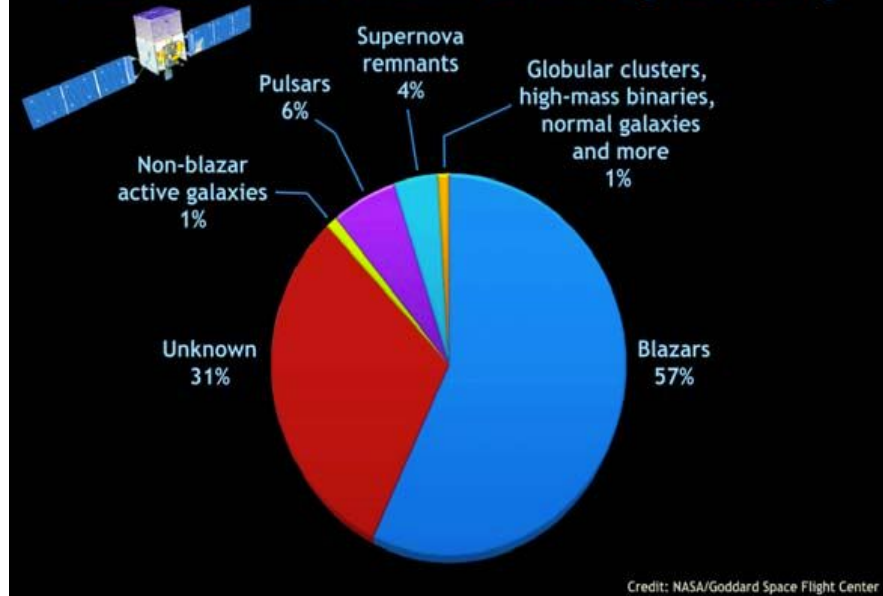


Gamma-Ray Surveys for AGNs

Fermi two-year all-sky map



What has Fermi found: The LAT two-year catalog



Gamma-ray surveys mostly find AGNs with radio jets pointed right at us, commonly called “blazars”.

Infrared Selection of AGNs

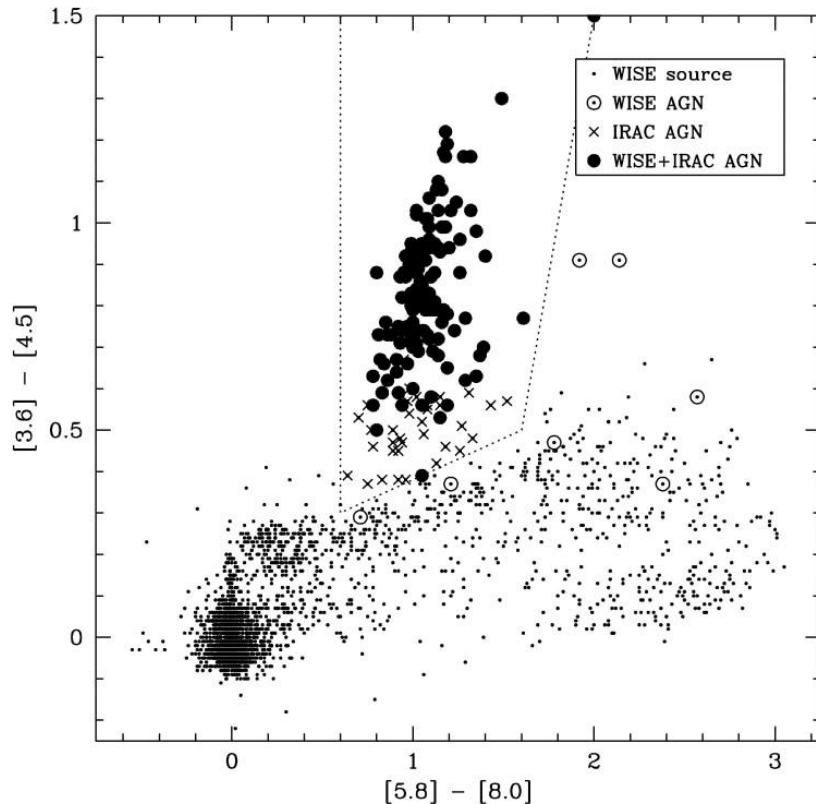
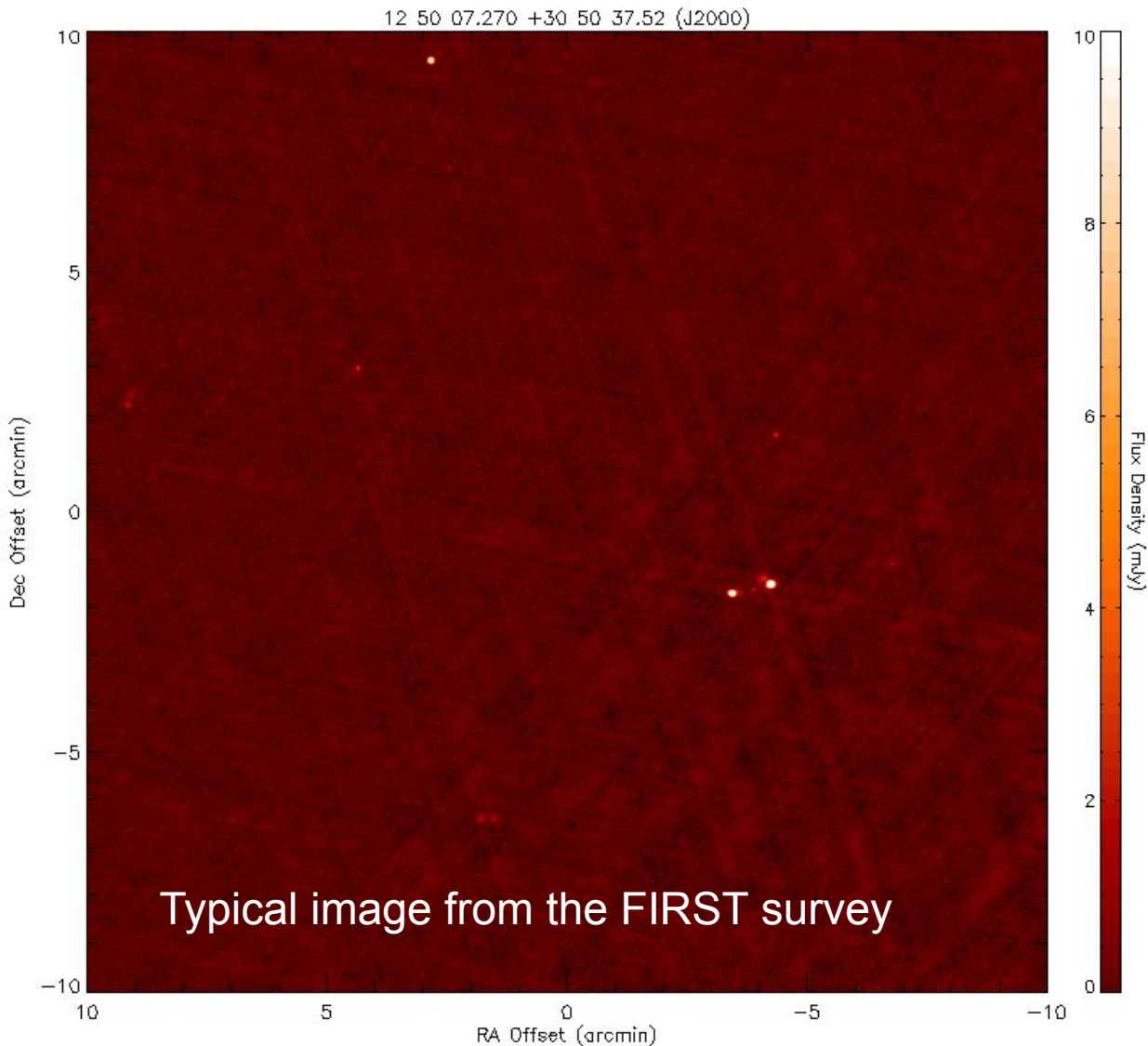


Figure 4. IRAC color-color diagram of *WISE*-selected sources in the COSMOS field. We only plot sources with $S/N \geq 10$ in $W1$ and $W2$, and we require $[3.6] > 11$ to avoid saturated stars. Sources with $W1 - W2 \geq 0.8$ are indicated with larger circles; filled circles indicate sources that were also identified as AGNs using the Stern et al. (2005) mid-infrared color criteria. Sources identified as AGNs using *Spitzer* criteria but not using the *WISE* criterion are indicated with \times 's.

Stern et al. (2012)

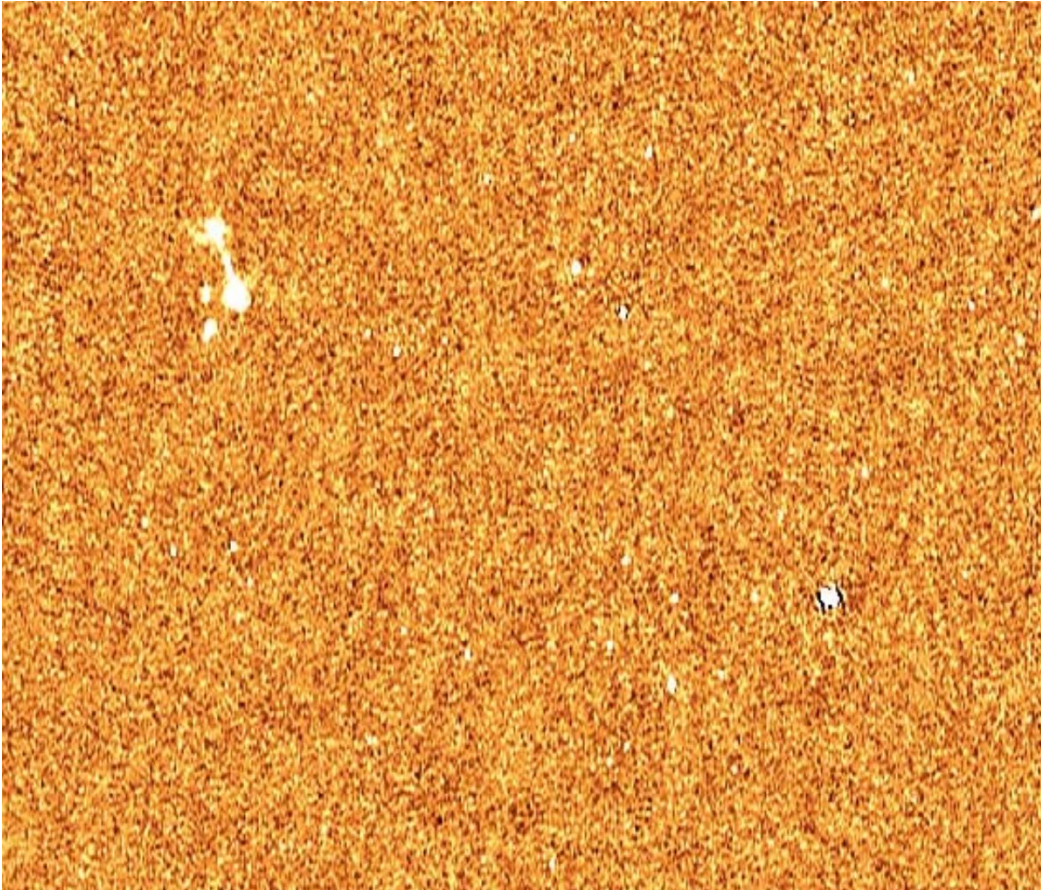
- Several methods have been developed for the effective selection of AGNs in sensitive infrared data.
- Often are seeing infrared power-law emission or “waste heat” from the AGN re-emitted by warm dust.
- These are also relatively resistant against obscuration effects.
- They sometimes even find AGNs missed in X-ray surveys.
- At lower AGN luminosities, such surveys suffer substantial contamination from star-forming galaxies.

Radio Surveys for AGNs



- Many of the first quasars were found via radio selection (3C).
- About 10% of AGNs are radio-loud sources.
- Sensitive radio surveys can detect many radio-quiet AGNs too.
- Stars are usually very weak radio sources, so little stellar contamination.
- Generally good radio positions allow efficient follow-up studies.
- Often quite incomplete, owing to radio-quietness of many AGNs.
- Often involves “human intervention” → Visual inspection

Radio Surveys for AGNs



A cutout of the VLA 1.4 GHz E-CDF-S radio image; Miller et al. 2013

- Many of the first quasars were found via radio selection (3C).
- About 10% of AGNs are radio-loud sources.
- Sensitive radio surveys can detect many radio-quiet AGNs too.
- Stars are usually very weak radio sources, so little stellar contamination.
- Generally good radio positions allow efficient follow-up studies.
- Often quite incomplete, owing to radio-quietness of many AGNs.
- Often involves “human intervention” → Visual inspection

The AGN bestiary

Seyfert 1 galaxy

BAL Quasar

Radio Loud Quasar

FR I

Radio-Quiet Quasar

Blazar

Broad Line Radio galaxy

OVVs

Narrow-Line Radio Galaxy

LLAGN

Seyfert 2 galaxy

Narrow-Line Seyfert 1

FR II

LINER

BL Lac Object

Type 2 Quasar

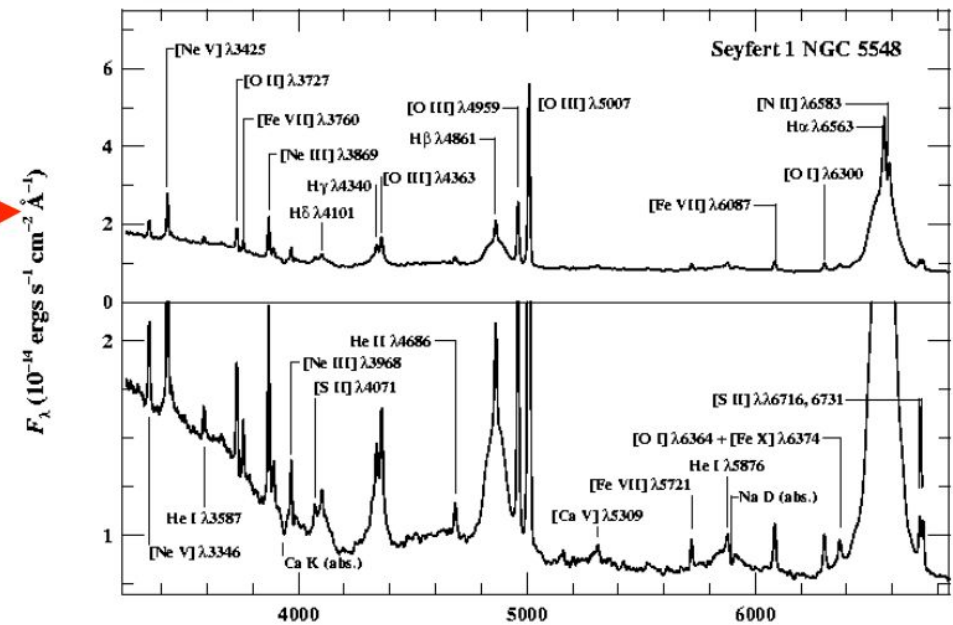
Weak Line Quasars

Galassie di Seyfert

Esistono due tipi di galassie di Seyfert in base alla presenza o meno di righe larghe nello spettro:

Seyfert 1 (Sy1) $\xrightarrow{\sim 20\% \text{ di tutte le Seyfert}}$

- ★ righe larghe (broad ~ 5000 km/s; > 1000 km/s) continuo UV-X forte e variabile;
- ★ luminosità fino a $\sim 10^{45}$ erg/s ($\sim 2 \times 10^{11} L_{\odot}$).



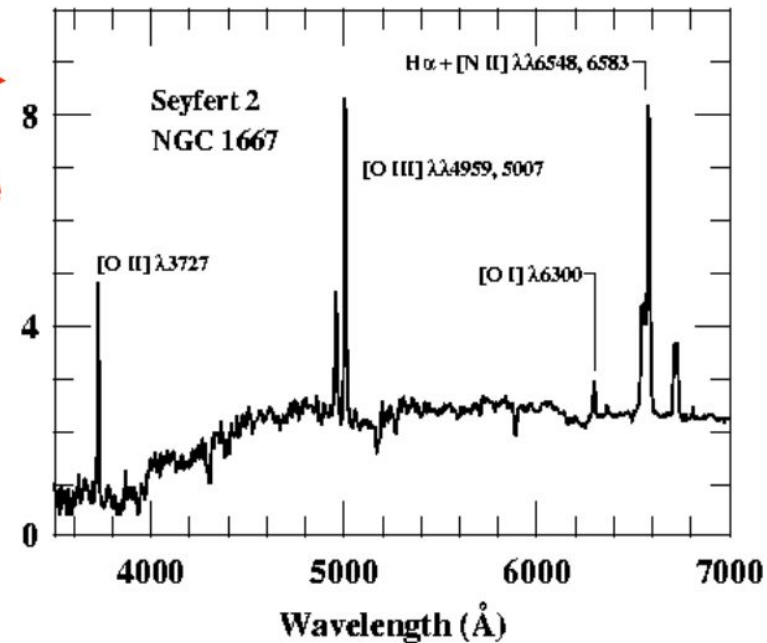
Seyfert 2 (Sy2) $\xrightarrow{\sim 80\% \text{ di tutte le Seyfert}}$

- ★ solo righe strette (narrow ~ 500 km/s; < 1000 km/s);
- ★ continuo UV-X molto debole rispetto a quello stellare della galassia ospite.

$\sim 80\%$
di tutte le
Seyfert

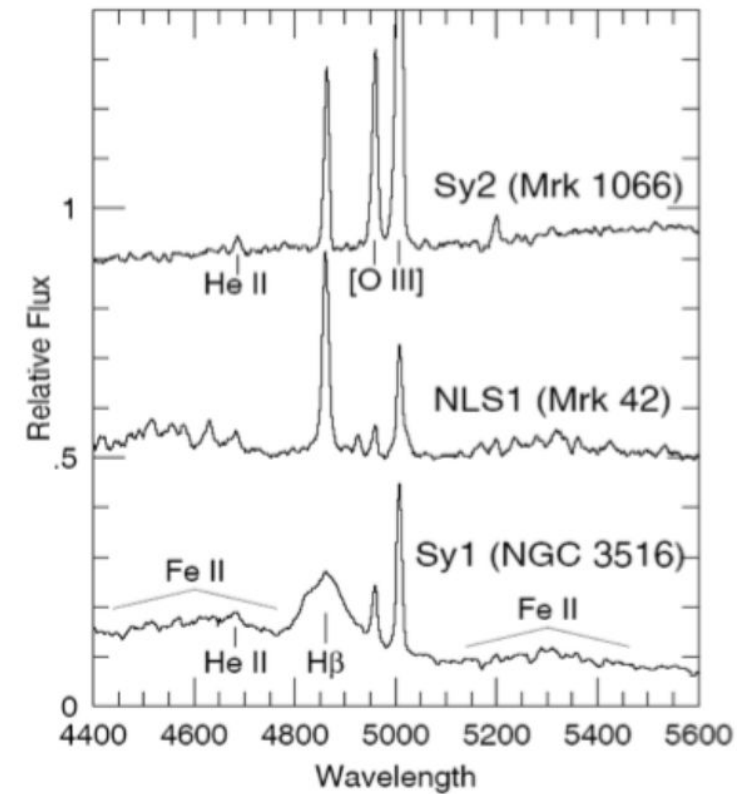
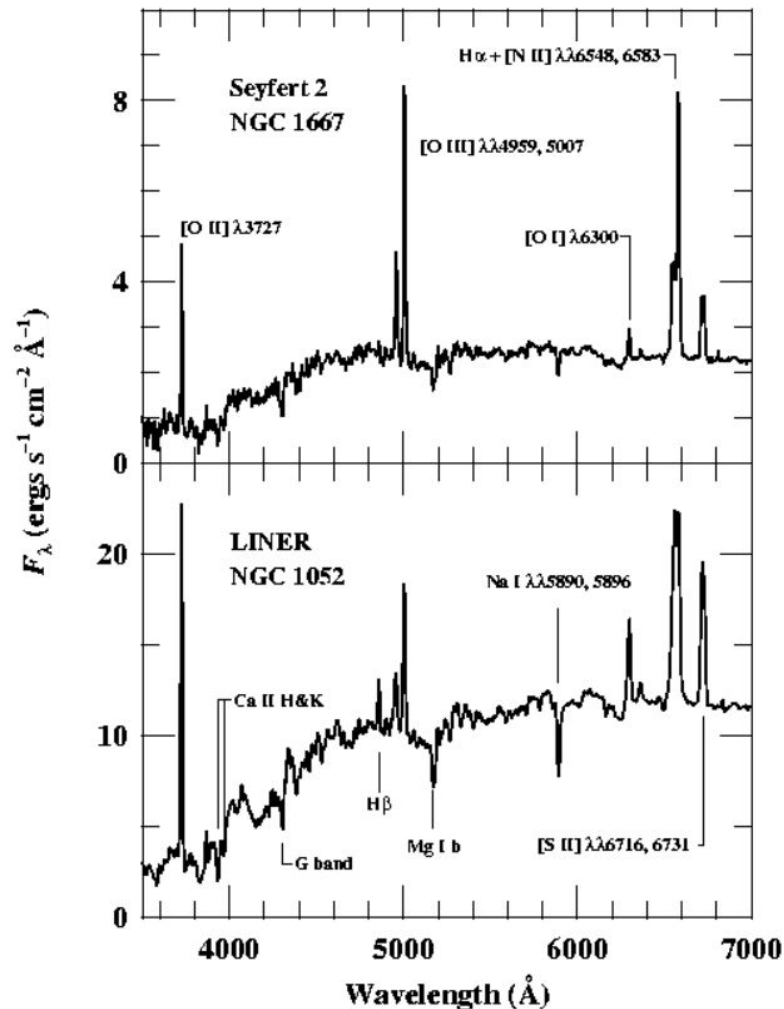
Broad Line Region (BLR): regione compatta, di alta densità ($n > 10^9 \text{ cm}^{-3}$)

Narrow Line Region (NLR): regione estesa di bassa densità ($n \sim 10^2 - 10^6 \text{ cm}^{-3}$)



Altre galassie di Seyfert ...

Le Narrow Line Seyfert 1 Galaxies (NLS1) sono galassie di Seyfert di tipo 1 ma con righe larghe “strette”: $1000 \text{ km/s} < \text{FWHM} < 2000 \text{ km/s}$

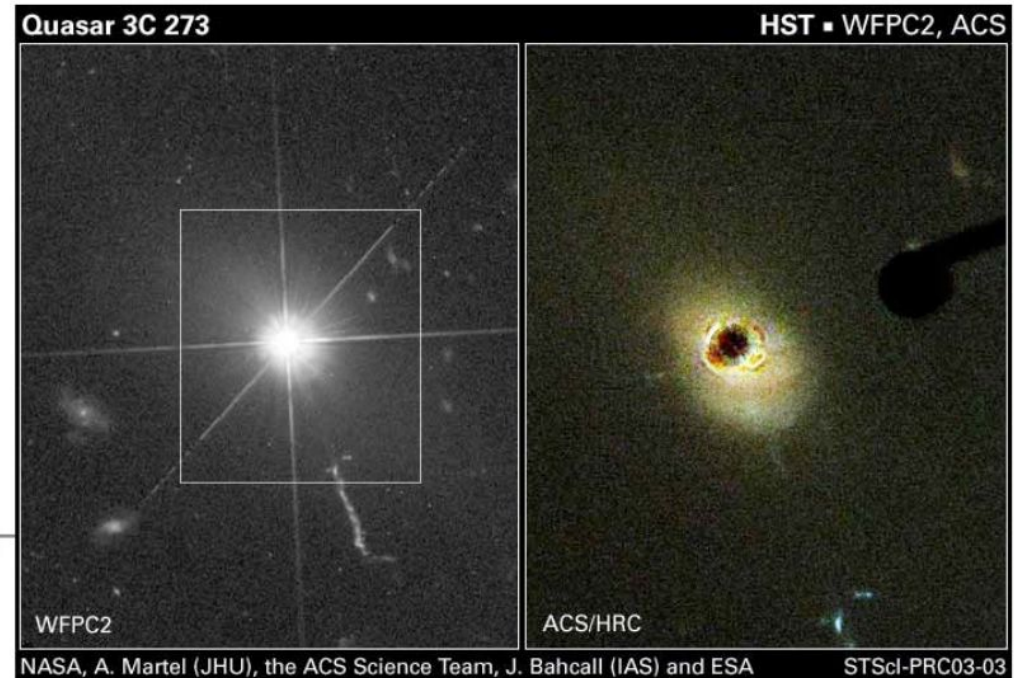
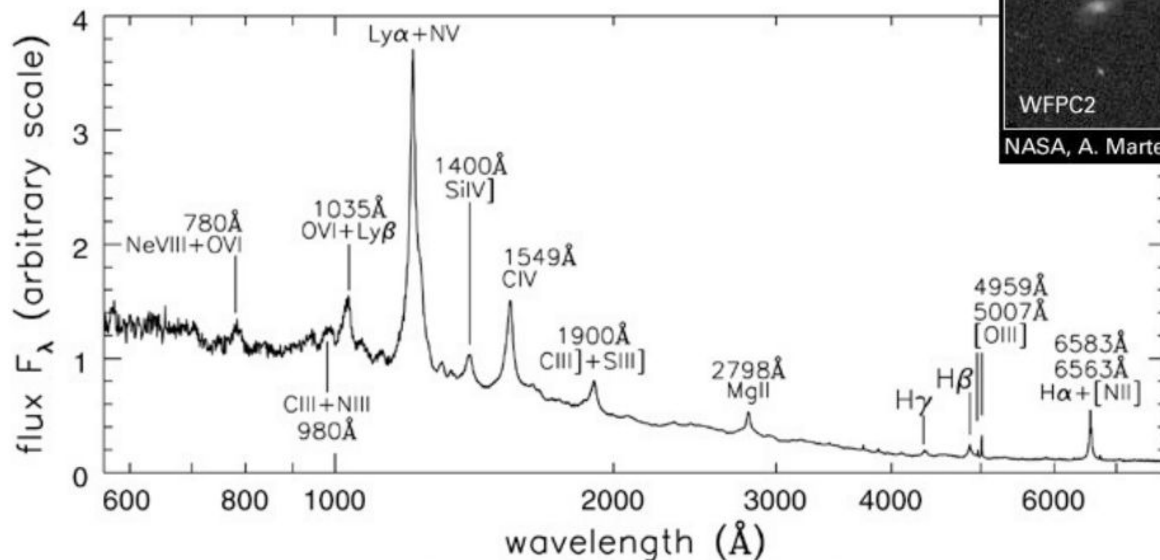


I LINER (Low Ionization Narrow Line Region) sono analoghi delle Seyfert 2 ma con righe molto forti di bassa ionizzazione.

I Quasar

Scoperti nel 1960 come sorgenti radio (Quasar = Quasi stellar radio source)
Identificati nel 1963 (Marteen Schmidt). Sono più luminosi delle galassie più
luminoose note.

La loro luminosità “nasconde” la
galassia ospite ed hanno
un'apparenza stellare.



**3C 273 - il quasar più vicino
e la sua galassia ospite.**

Spettro tipico di un quasar.

Esistono due tipi di sorgenti radio (galassie o quasar) classificate in base alla loro apparenza radio:

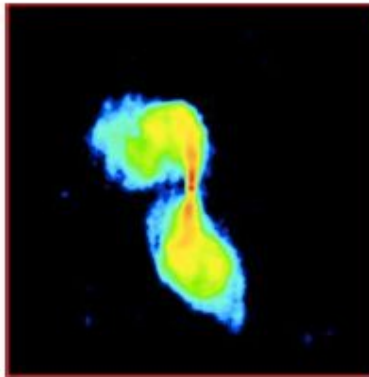
Sorgenti Fanaroff-Riley I (FR I)

Sorgenti Fanaroff-Riley II (FR II)

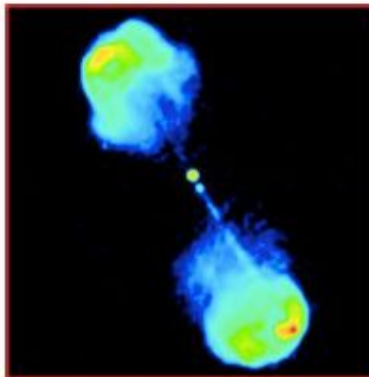
$< 2 \times 10^{25} \text{ W}$ **FR I**

Radio
Loudness
 $L(178\text{MHz})$

$> 2 \times 10^{25} \text{ W}$ **FR II**



Getti radio gemelli, molti
“blob” di emissione,
estesi, oscurate ai bordi
(edge darkened)

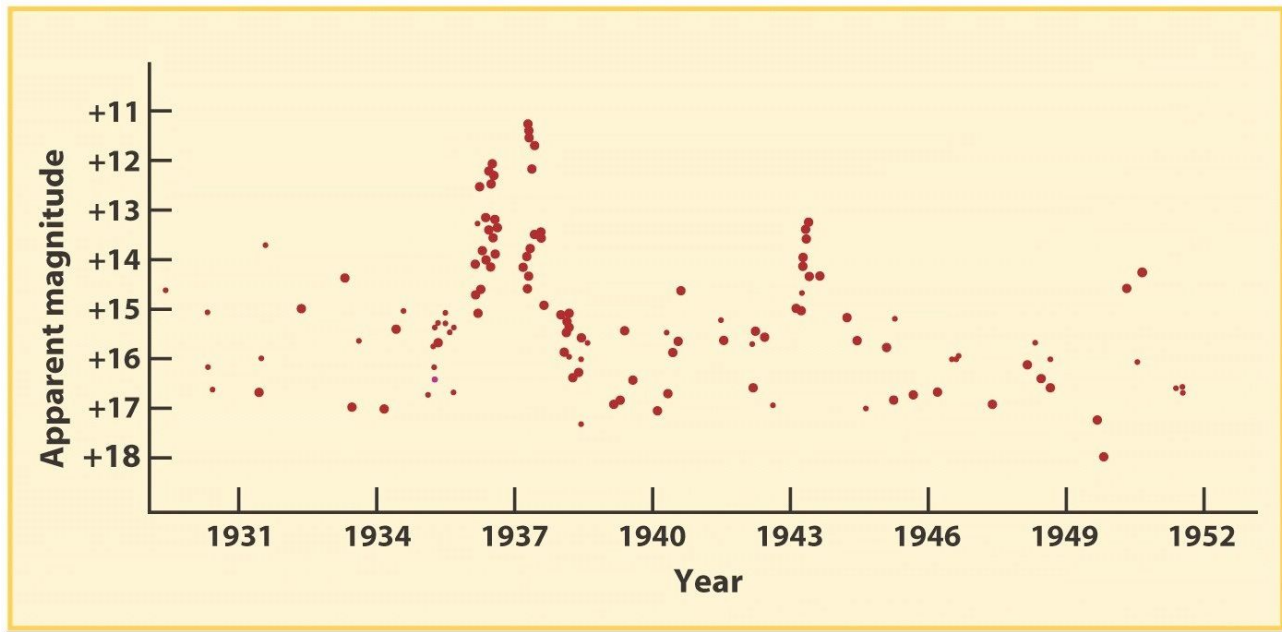


Getti radio singoli e
altamente collimati,
brillanti ai bordi
(edge brightened)

BL Lac e Blazars

Alcuni AGN sono peculiari nel senso che sono caratterizzati da:
sorgenti radio compatte (no lobi) e molto potenti;
spesso “blob” di emissione radio mostrano moti superluminali (velocità apparenti sul piano del cielo $> c$);
hanno spettri dominati da continuo fortemente polarizzato privo di righe di emissione;
la SED è più piatta di quella degli altri AGN;
sono estremamente variabili in luminosità.

Questi AGN sono detti BL Lac o Blazars.



The AGN bestiary

Seyfert 1 galaxy

BAL Quasar

Radio Loud Quasar

FR I

Radio-Quiet Quasar

Blazar

Broad Line Radio galaxy

OVVs

Narrow-Line Radio Galaxy

LLAGN

Seyfert 2 galaxy

Narrow-Line Seyfert 1

FR II

LINER

BL Lac Object

Type 2 Quasar

Weak Line Quasars

The AGN Zoo – Key Classification

- **Strength of Radio Emission**
 - Radio-Loud Quasar vs. Radio-Quiet Quasar
- **Optical/UV Emission-Line Properties**
 - Seyfert 1 galaxy vs. Seyfert 2 galaxy
 - Type 1 Quasar vs. Type 2 Quasar
 - Broad Line vs. Narrow Line Radio Galaxy
 - Also intermediate Seyfert types, Narrow-Line, Seyfert 1, BL Lac, Weak-Line Quasar
- Also **Variability** and **UV Absorption-Line Properties**
- **Luminosity** is also often used in classifications for largely historical reasons; usually not so fundamental (e.g., Seyferts are just low-luminosity quasars).

Table 1.2: The AGN Bestiary

Beast	Pointlike	Broad-band	Broad Lines	Narrow Lines	Radio	Variable	Polarized
Radio-loud quasars	Yes	Yes	Yes	Yes	Yes	Some	Some
Radio-quiet quasars	Yes	Yes	Yes	Yes	Weak	Weak	Weak
Broad line radio galaxies (FR2 only)	Yes	Yes	Yes	Yes	Yes	Weak	Weak
Narrow line radio galaxies (FR1 and FR2)	No	No	No	Yes	Yes	No	No
OVV quasars	Yes	Yes	Yes	Yes	Yes	Yes	Yes
BL Lac objects	Yes	Yes	No	No	Yes	Yes	Yes
Seyferts type 1	Yes	Yes	Yes	Yes	Weak	Some	Weak
Seyferts type 2	No	Yes	No	Yes	Weak	No	Some
LINERs	No	No	No	Yes	No	No	No

Krolik (1999)

AGN zoo: 3 dimensional classification: optical spectral type, radio properties, and L

Name	Optical spectral type?	Radio Loud?	Luminosity?
Seyferts	1, 1.2, 1.5, 1.8, 1.9, 2.0	No	Moderate
Quasars	1, 2	No	High
LINERs or low-luminosity AGN	1, 2	Yes and No	Low
Broad-line Radio Galaxies (BLRGs)	1	Yes	Moderate
Narrow-line Radio Galaxies (NLRGs)	2	Yes	Moderate
Radio-loud quasars	1, 2	Yes	High
FRIs	1	Yes	Low
FRILs	1, 2	Yes	Low-High
Blazars	0!!!	Yes	Low-High

Radio sub types

Classification Scheme

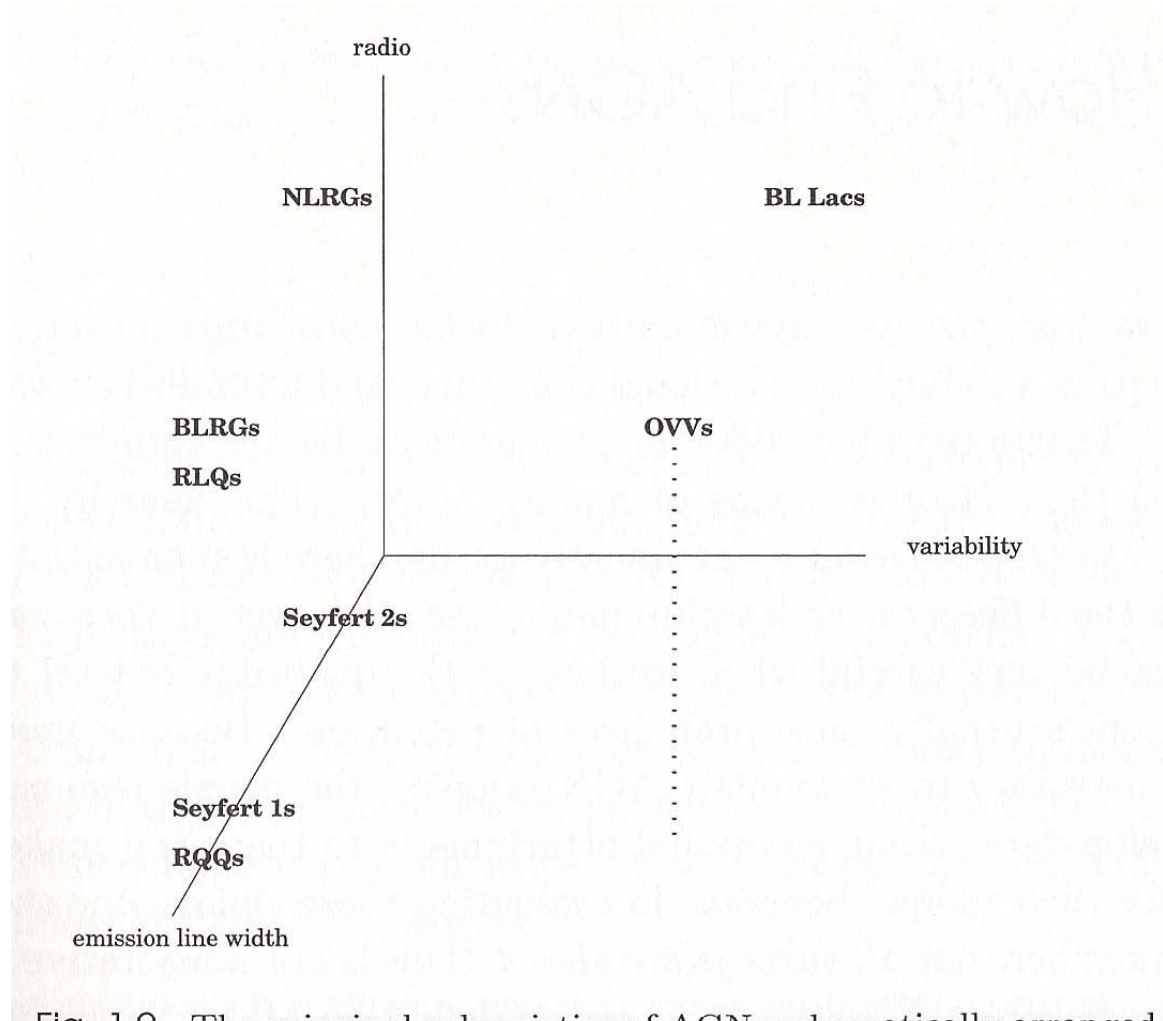
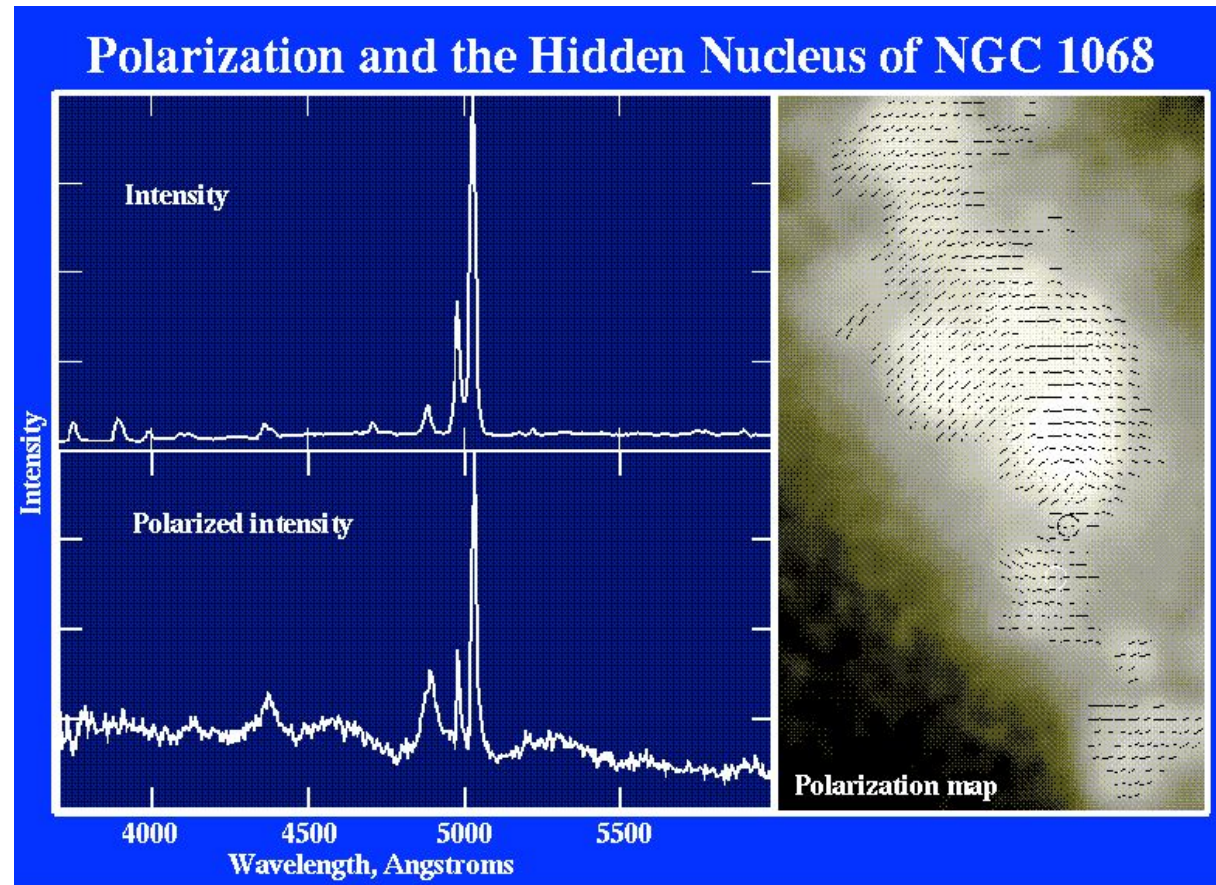


Fig. 1.9 The principal subvarieties of AGNs schematically arranged according to relative power in the radio band, emission line width, and variability. All combinations are possible except that there are no highly variable radio-quiet objects.

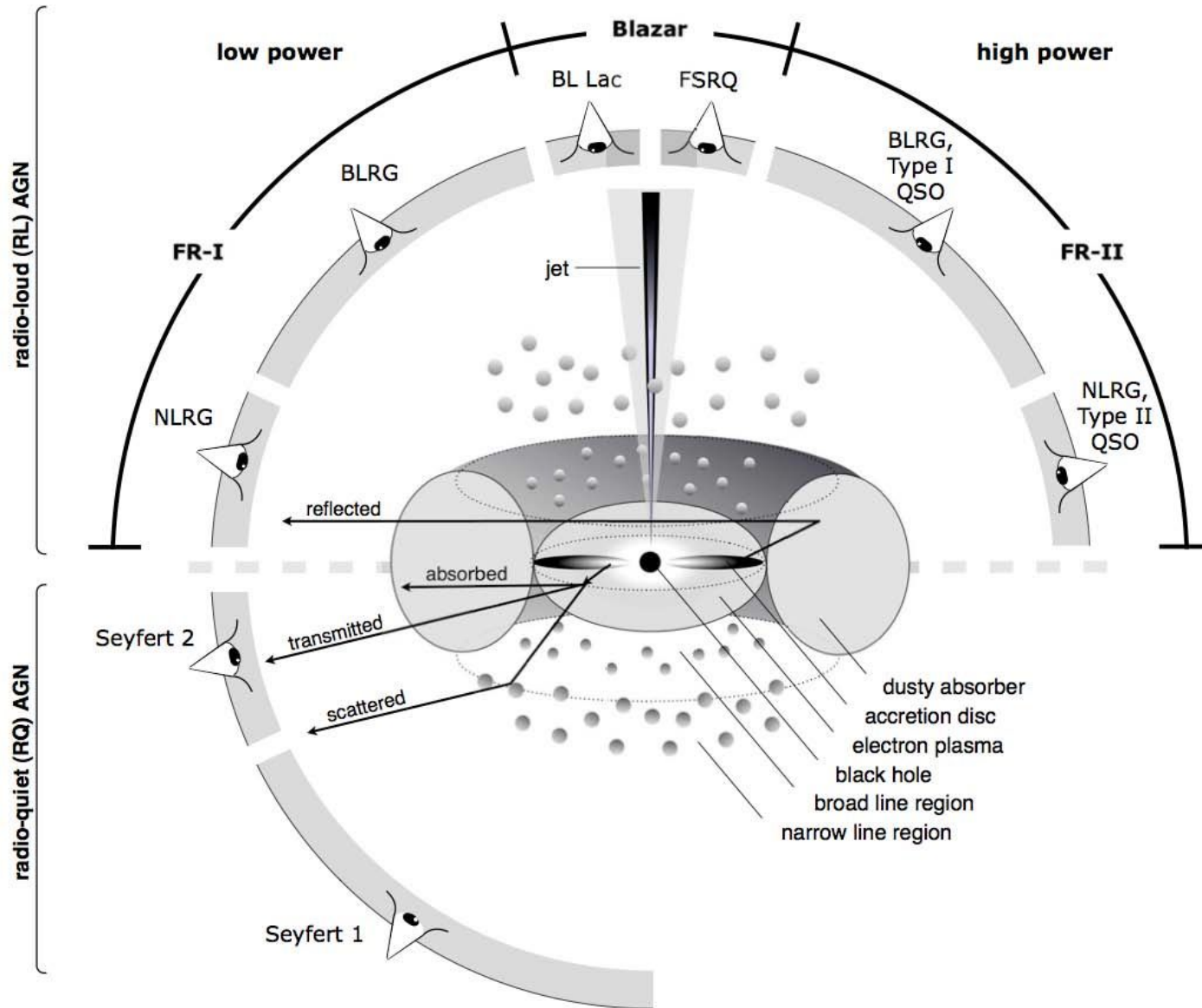
Krolik (1999)

Evidence for Unification

- Key Observation:
Polarized Spectrum of NGC 1068 (Seyfert 2 archetype) → Shows clear Broad Lines!
- Polarized light enhance the presence of broad lines.
- BL in intensity are 100 times fainter than Continuum and NL (impossible to detect)

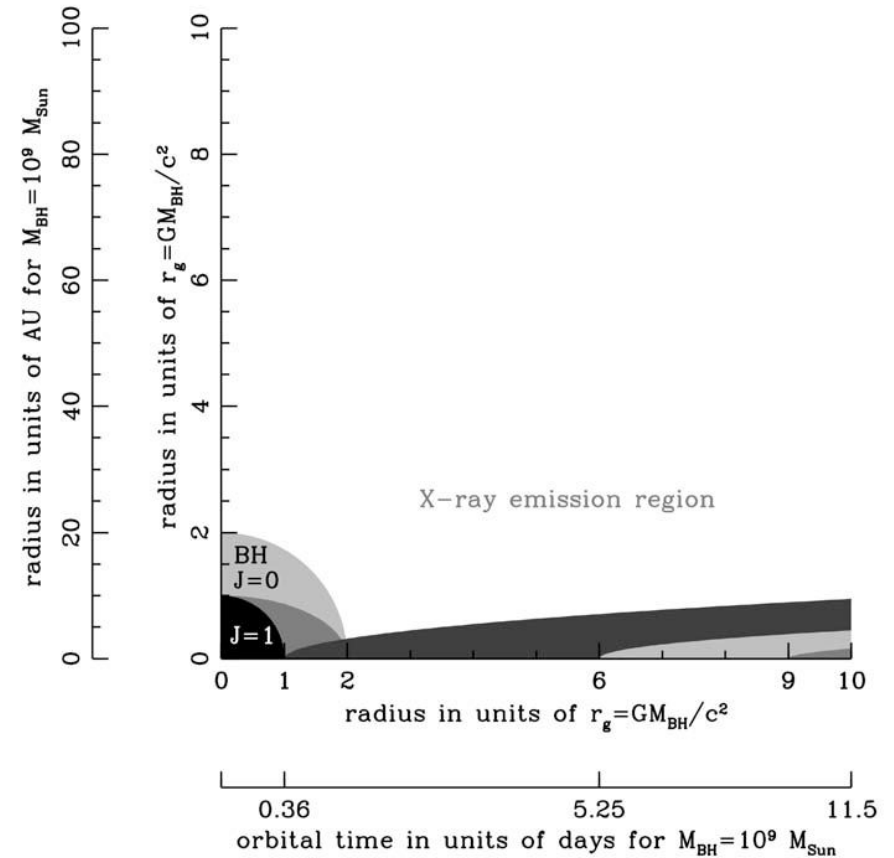
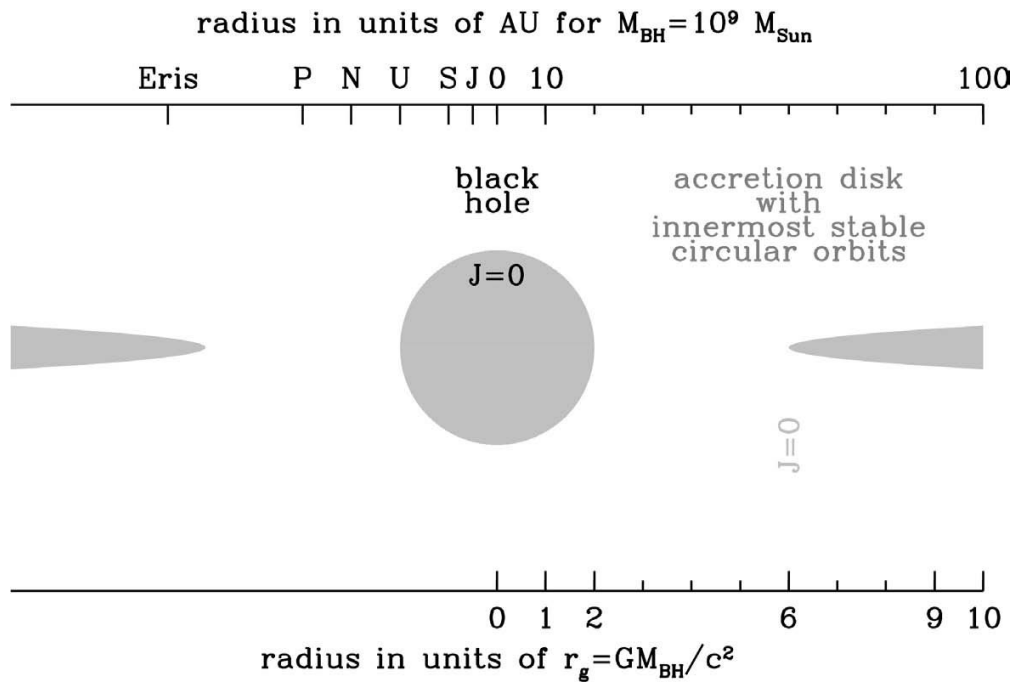


The Unifying Model



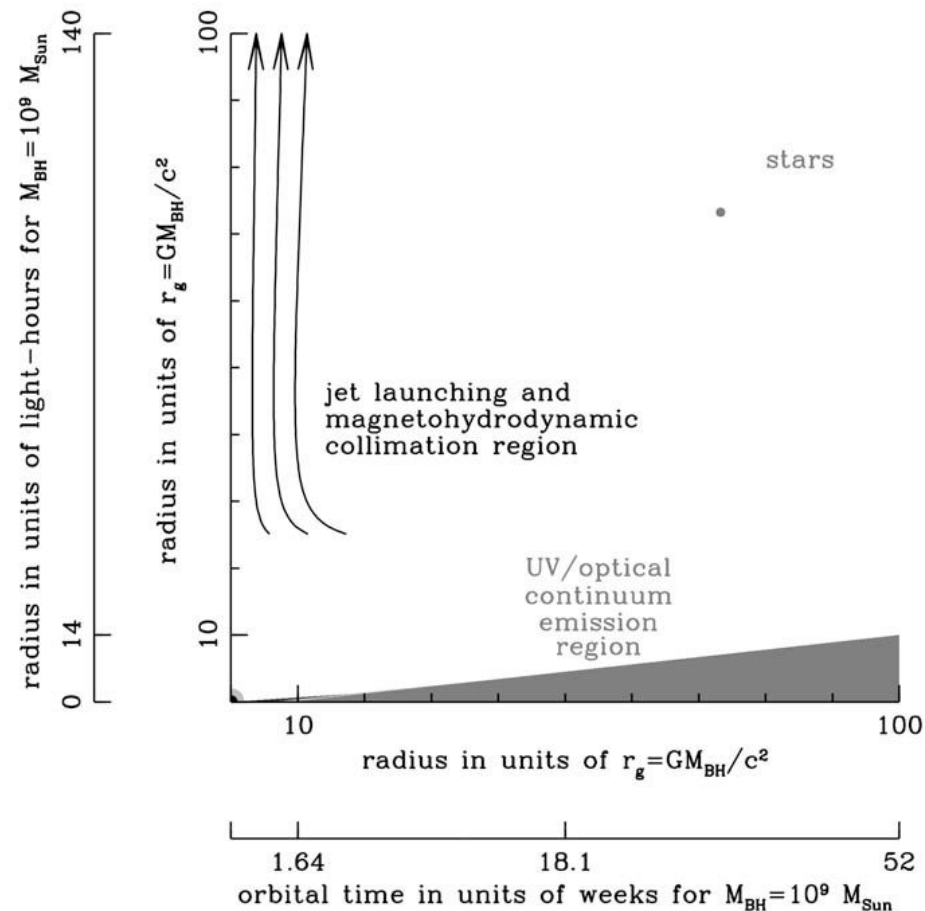
Dissecting AGNs emission

1) The BH region



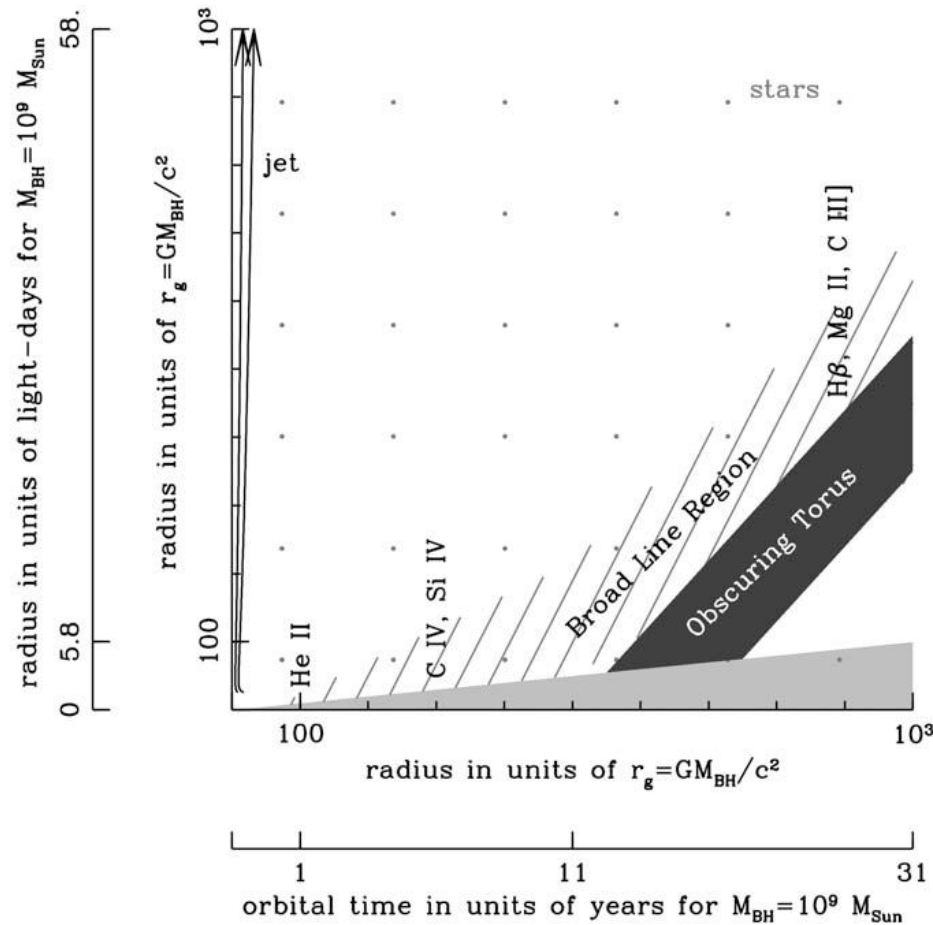
Dissecting AGNs emission

2) The UV/Optical Continuum Emission Region



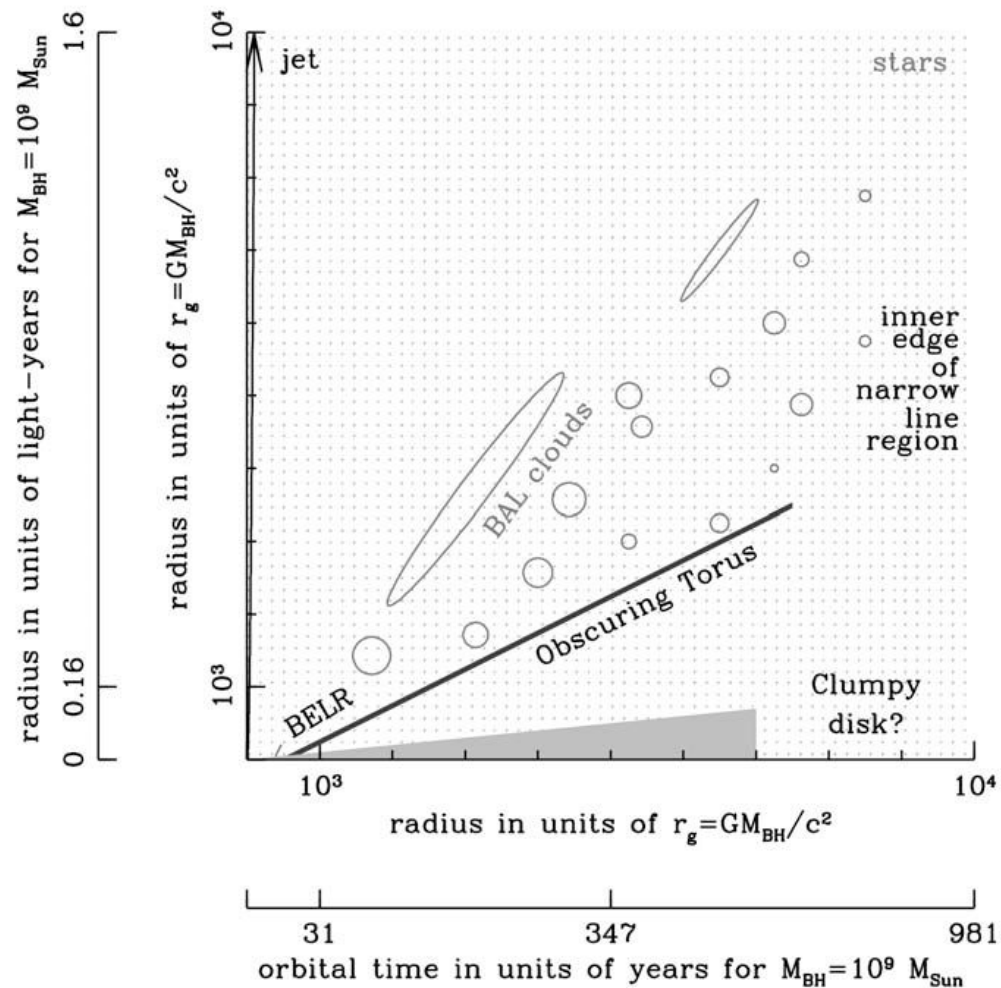
Dissecting AGNs emission

3) The Broad Line Region



Dissecting AGNs emission

4) The Outflow Region



The Black Hole Region

- Inner $\sim 50 R_S$

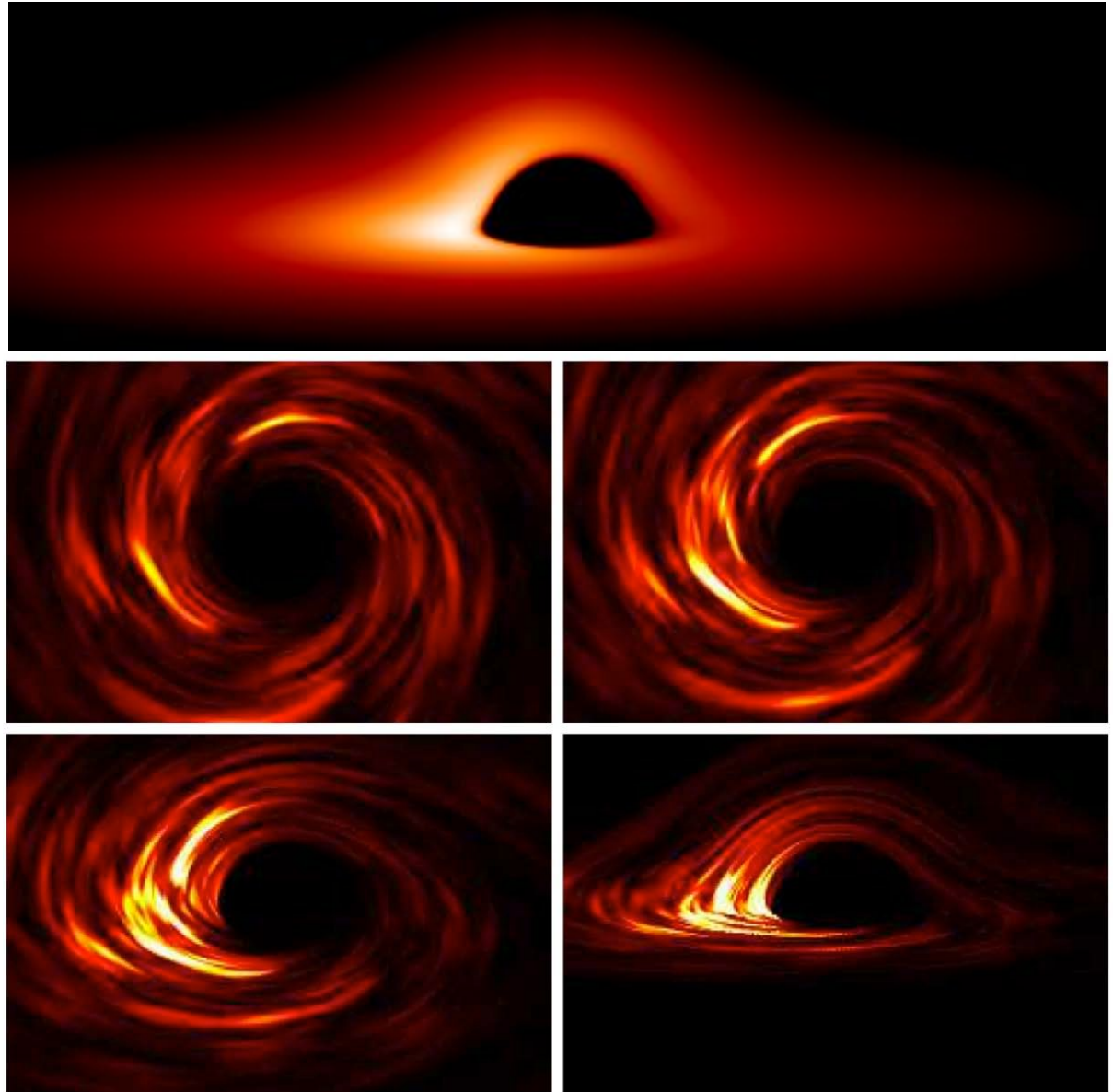
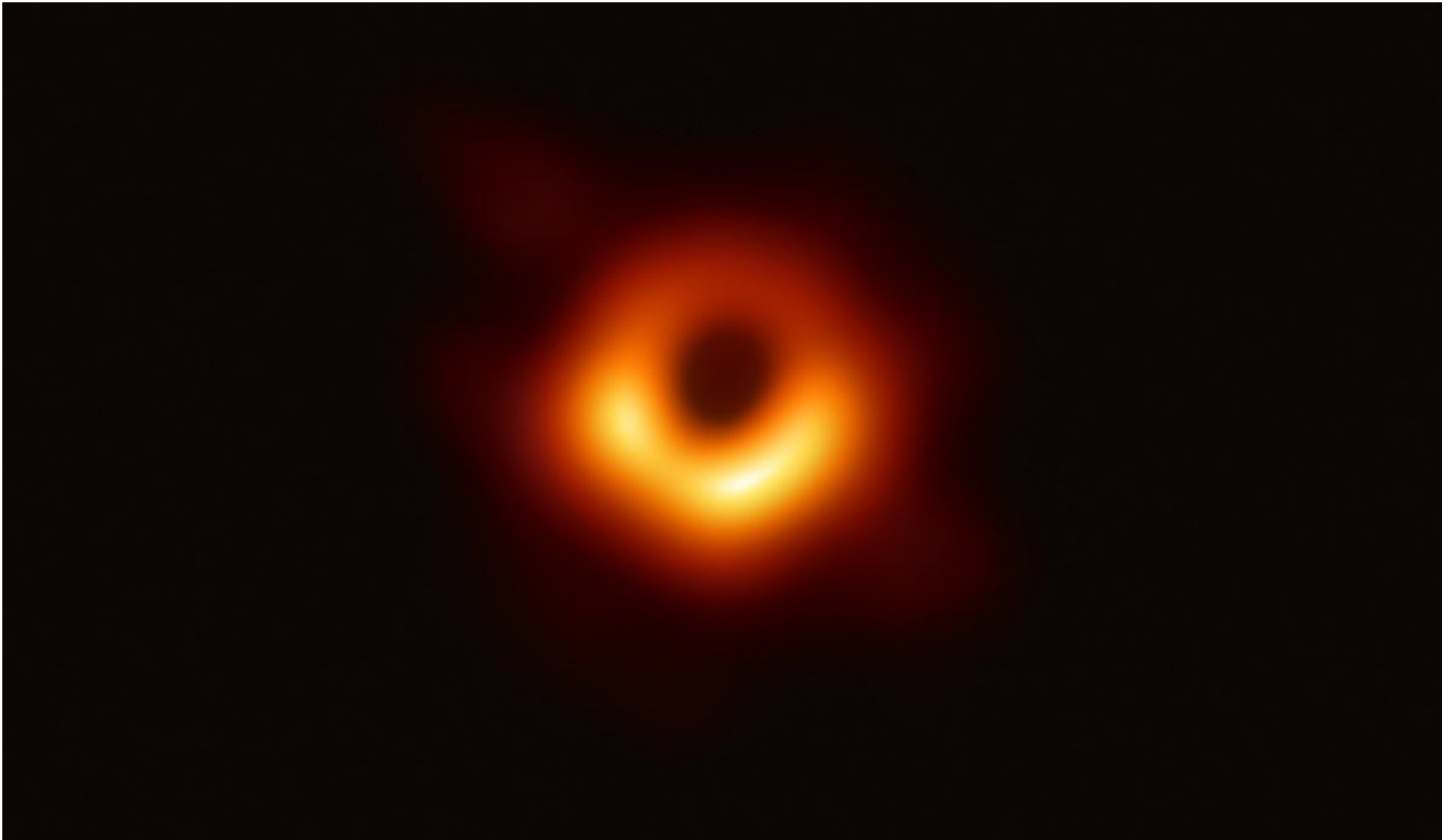


Figure 4. View of the disc as seen by a distant observer at an inclination angle of 5° (upper left), 30° (upper right), 55° (lower left) and 80° (lower right). In these raw images, note the presence of stress extending to the inner boundary of the computational domain, within the marginally stable circular orbit. Movies showing the evolution of the simulated disc are available at <http://jilawww.colorado.edu/~pja/black.hole.html>

The Black Hole Region

- EHT



The Black Hole Region

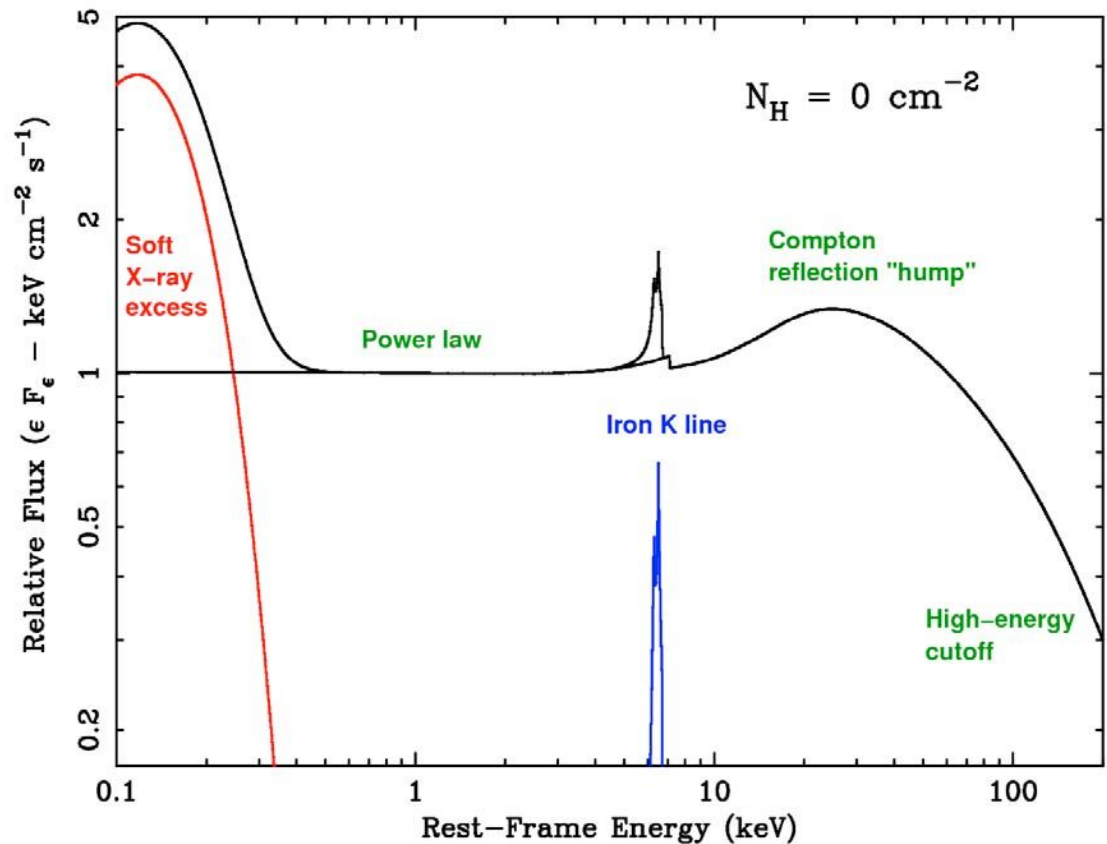
Schematic AGN X-ray Spectral Energy Distribution

Continuum components

- Power law
- Soft X-ray excess
- Compton reflection hump

Discrete atomic features

- Iron K α Line
- Other line emission



The Black Hole Region

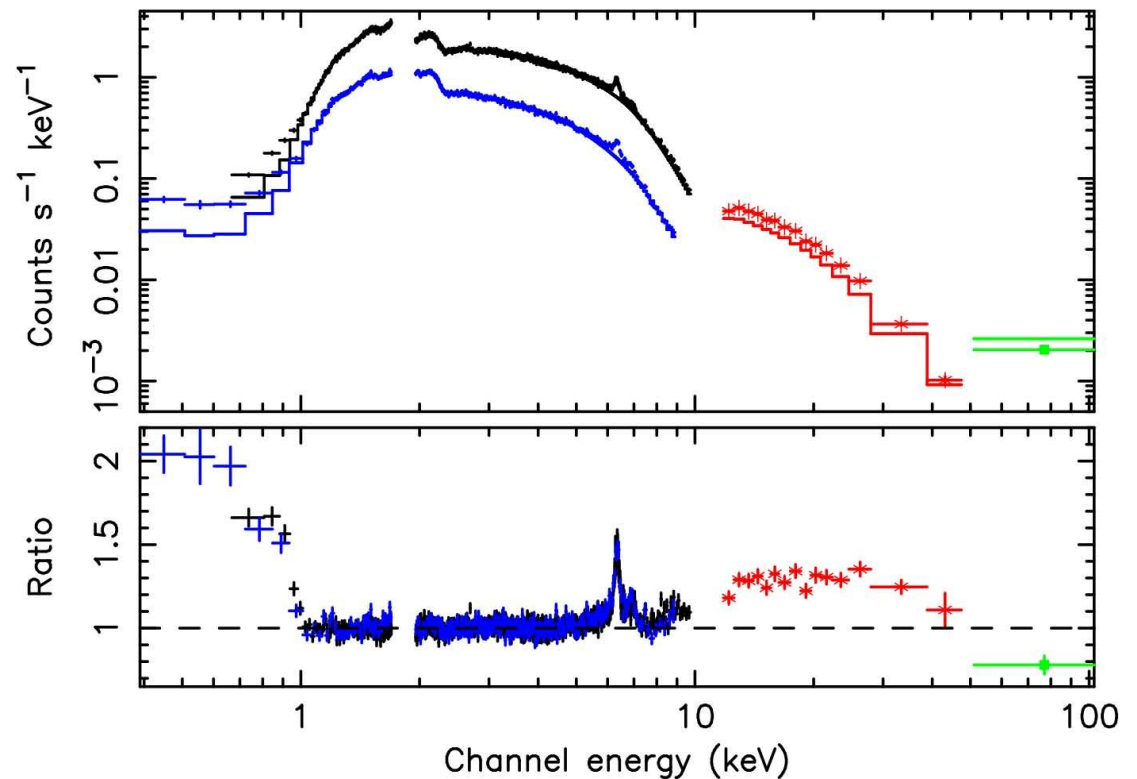
Schematic AGN X-ray Spectral Energy Distribution

Continuum components

- Power law
- Soft X-ray excess
- Compton reflection hump

Discrete atomic features

- Iron $K\alpha$ Line
- Other line emission

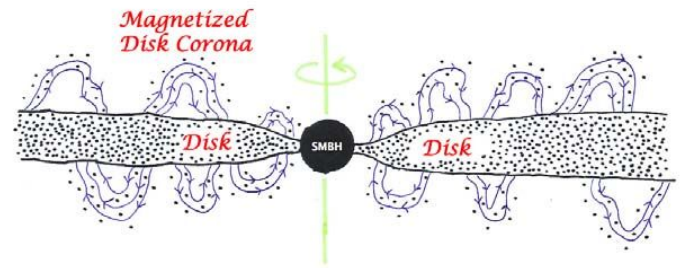


Suzaku Spectrum

Reeves et al. (2007)

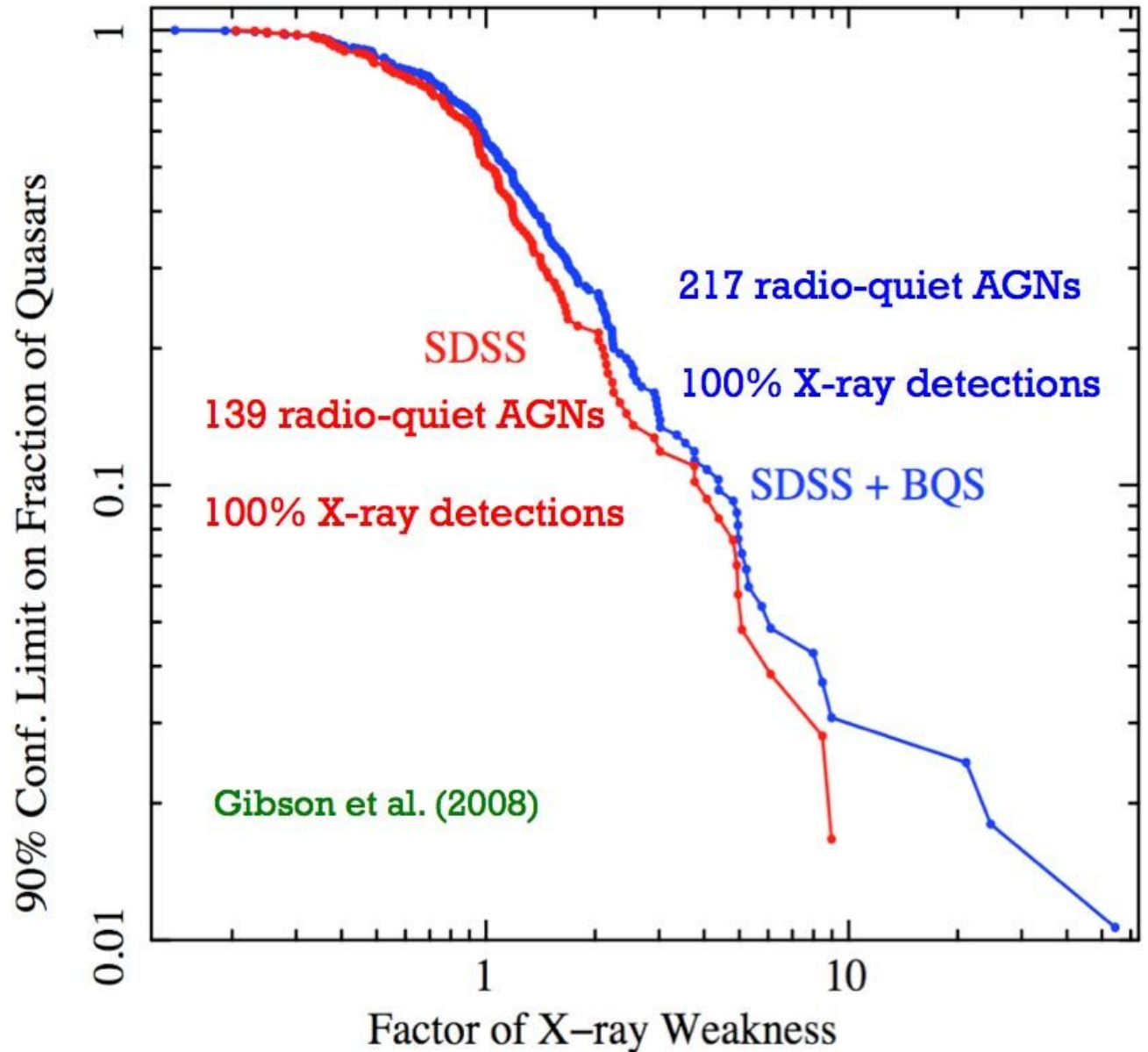
X-ray Power Law

- Power law $N(E) \propto E^{-\Gamma}$ has a photon index of $\Gamma = 1.7-2.2$.
- The “corona” Compton up-scatters UV/optical photons from the disk to create the power law.
- Corona likely heated by magnetic flares.
- Corona has a temperature of ~ 150 keV, beyond which an \sim exponential cutoff is observed.
- 150 keV “reasonable” \rightarrow 511 keV pair production
- The corona’s properties cannot yet be computed from first principles, but progress being made.
- Thus the corona’s nature remains uncertain.
 - Sandwiching the disk?
 - Base of a jet?



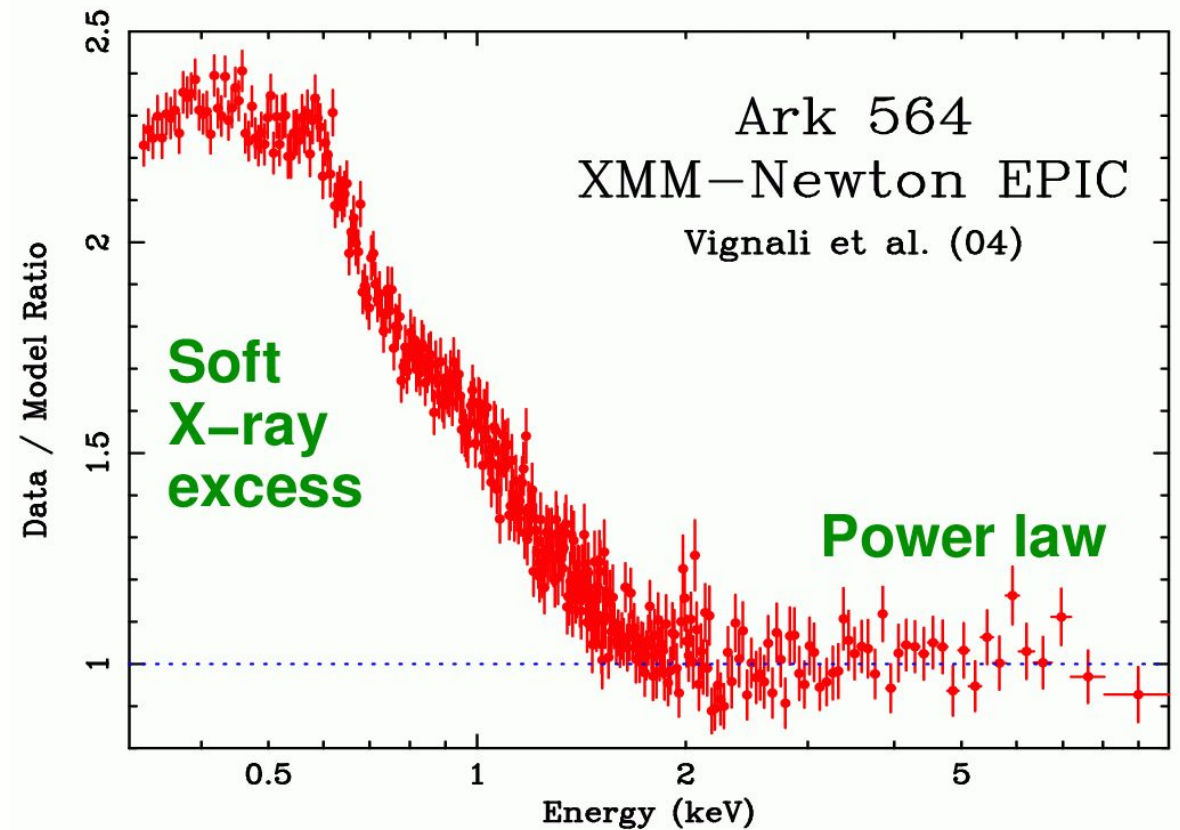
X-ray signature

- Almost all AGNs show some X-ray emission

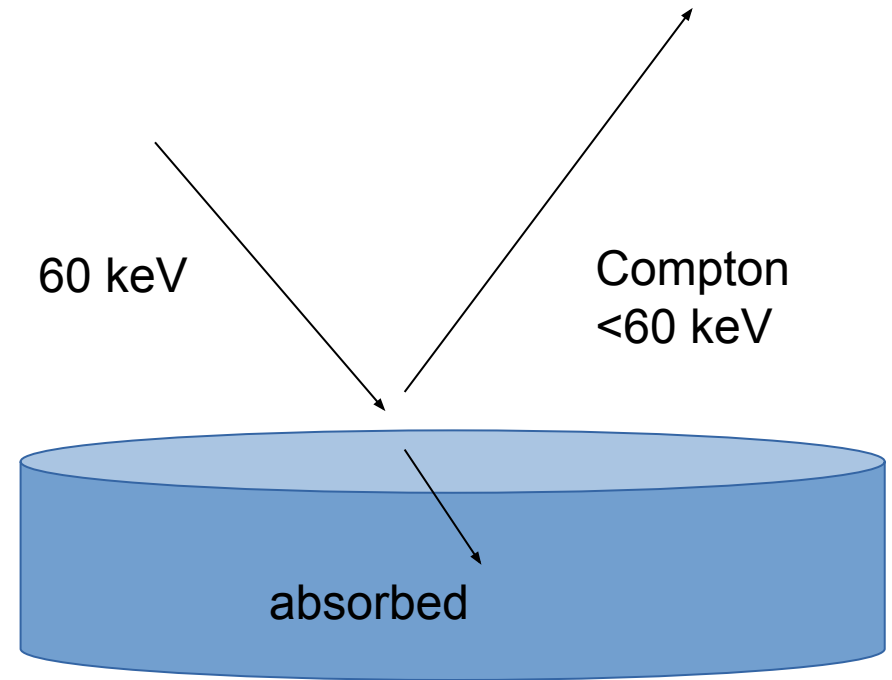
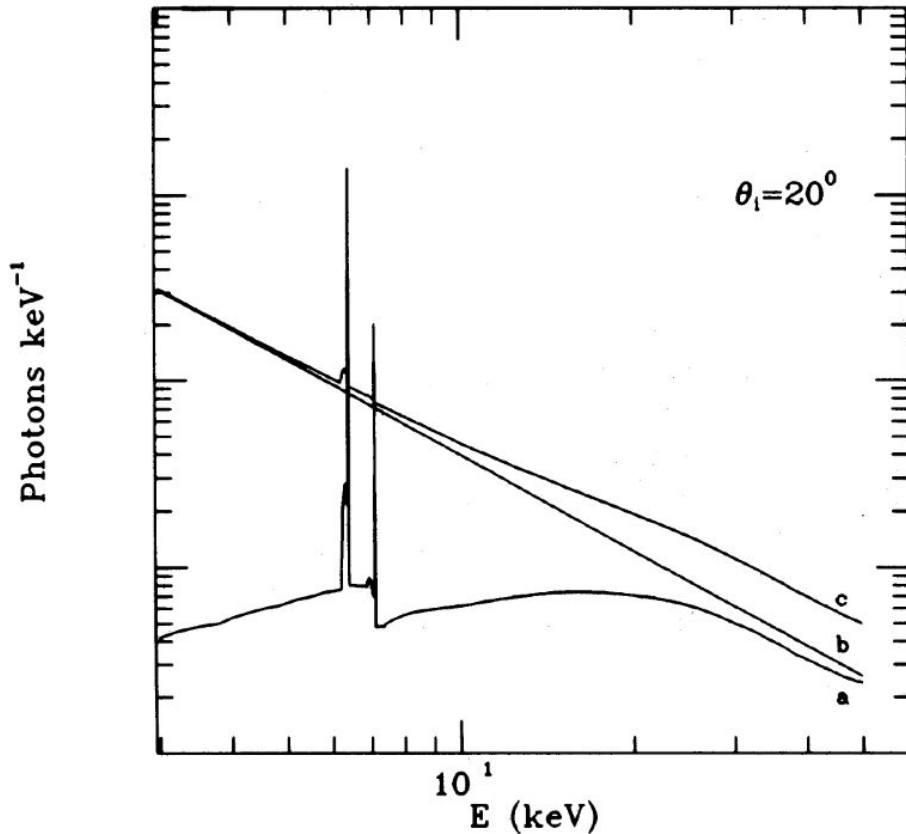


Soft X-ray Excess

- Strong soft emission of a \sim blackbody spectral form seen from some objects below ~ 1.5 keV.
- Too hot and too variable to be entirely from standard accretion disk.
- Likely a combination of disk emission at lowest energies plus a cool Compton-scattered component and disk reflection.



Compton Reflection Hump

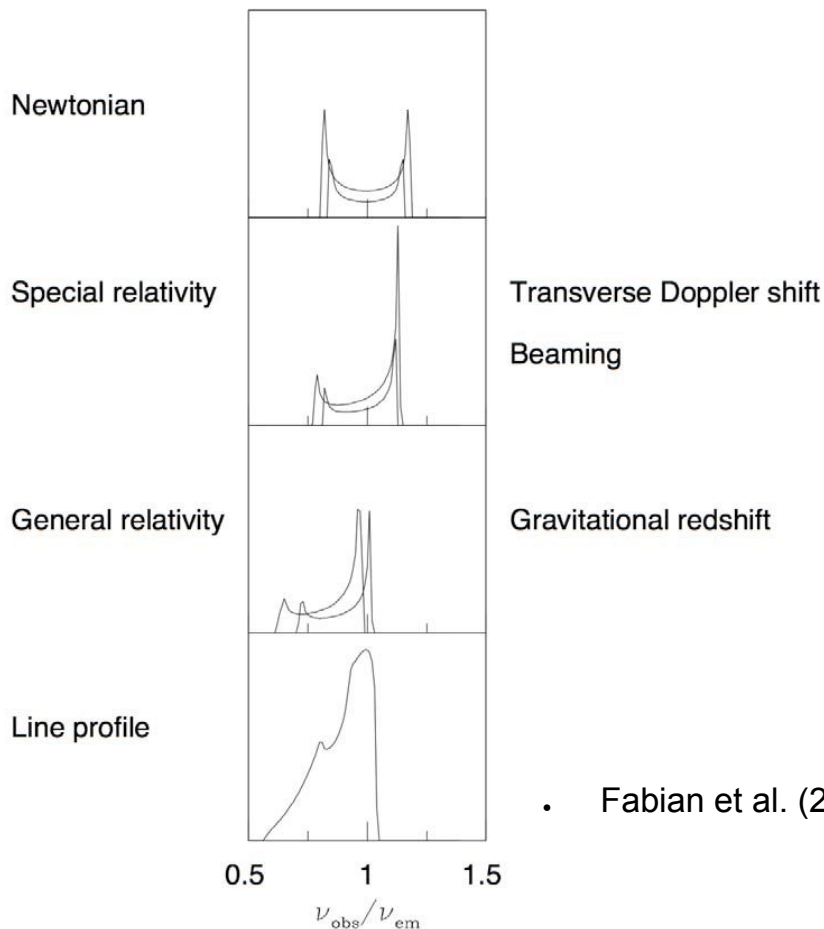


- Broad band hump peaking at 20-40 keV.
- Produced when X-rays shine upon the accretion disk or other material.
- At low energies have a competition between Compton scattering and photoelectric absorption.
- Photoelectric absorption dominates below 10-15~ keV
- At high energies drops off due to e.g. Compton recoil, and the power-law cutoff.
- Affected by Doppler shifts, beaming, GR



Iron K α Line

$\sim 2\text{keV} \sim c/3$



• Fabian et al. (2000)

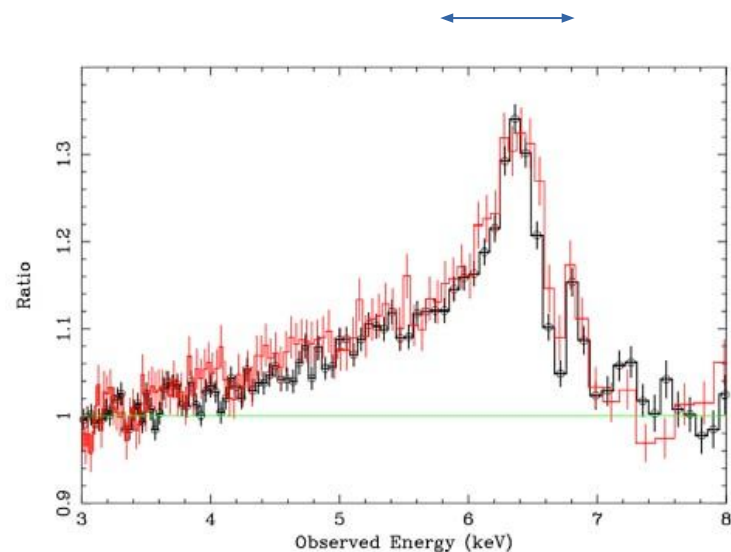
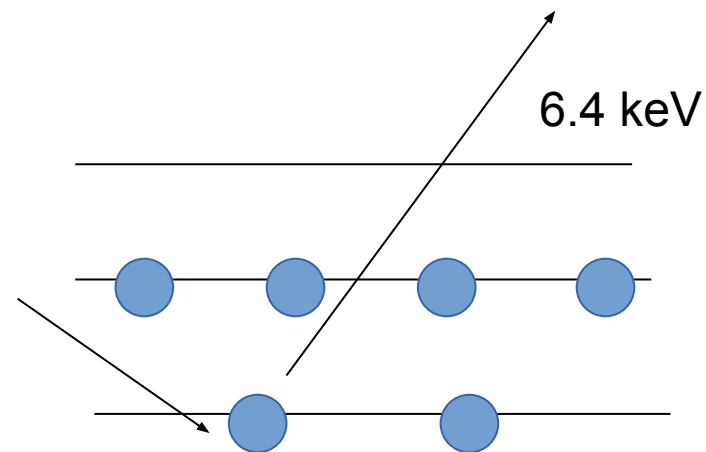
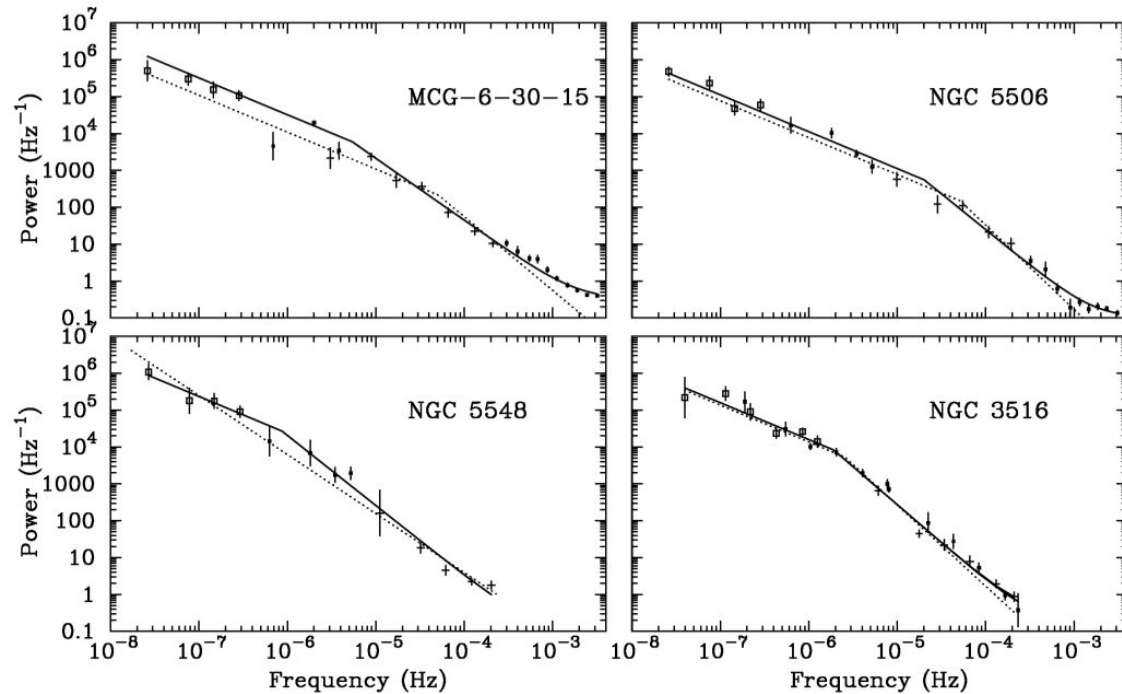
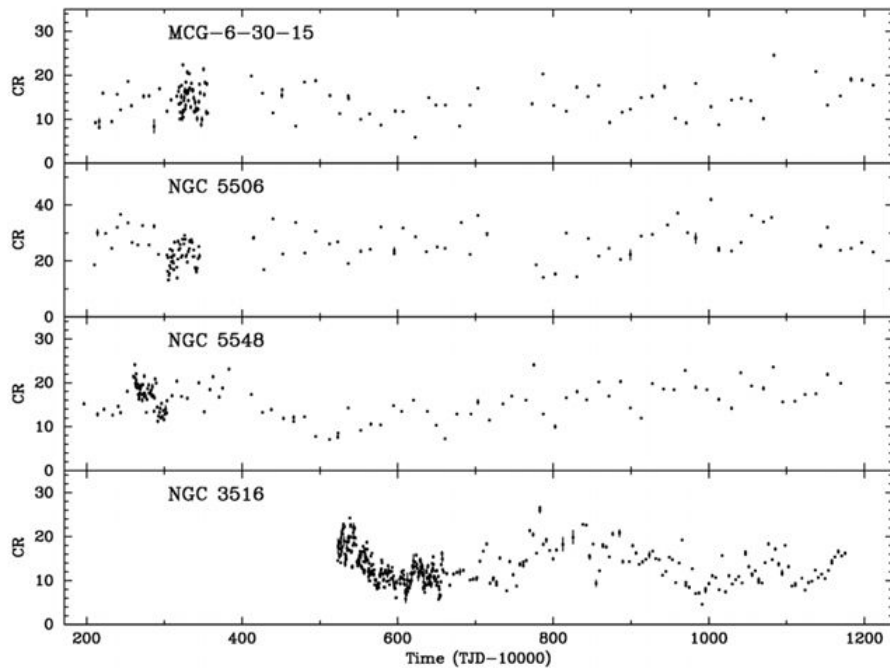


Figure 4: The figure above shows the relativistic disk line profile revealed in MCG-6-30-15 after fitting for the continuum. (Adapted from Miniutti et al. 2007 and Reeves et al. 2006.) The line in MCG-6-30-15 is the best example known presently, and these spectra above are the best yet obtained. The spectrum in black was obtained with *Suzaku*, and the spectrum in red was obtained with *XMM-Newton*.

- Made via iron fluorescence when disk irradiated by X-rays.
- Iron has best product of abundance and fluorescent yield.
- With very high-S/N data, can use to estimate disk inclination, disk emissivity, and black-hole spin.

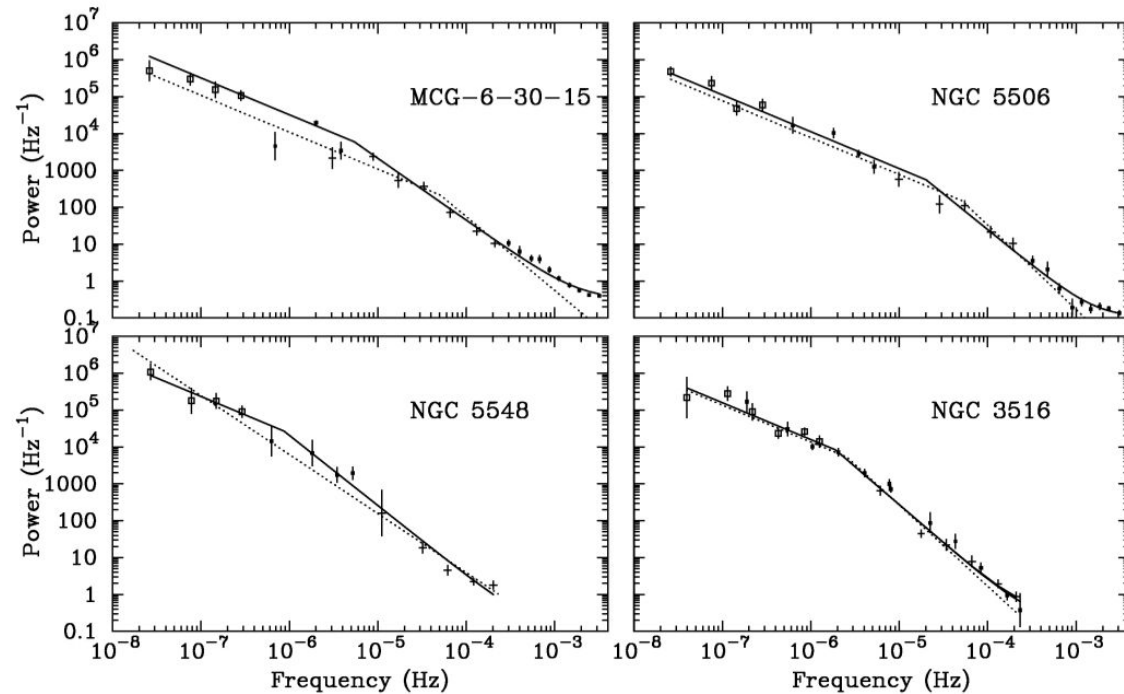
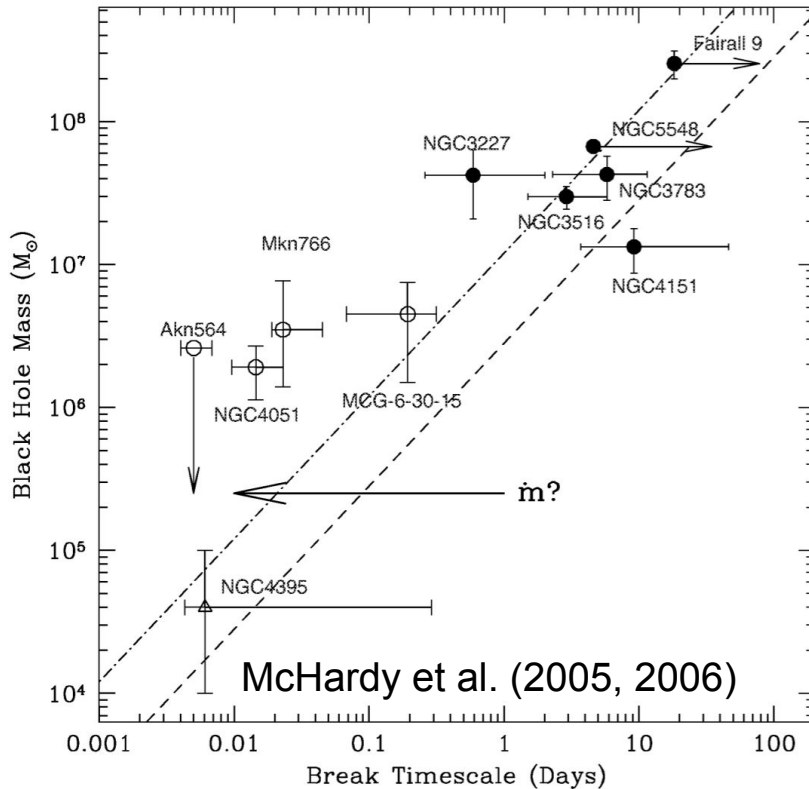


X-ray Variability



- AGN variability power spectra usually do not show periodicity or quasi-periodicity.
- Observe noise power spectra with a bend/break at ~ 0.1 -100 days.
- The bend/break timescale can be correlated with other AGN physical properties.

X-ray Variability



- AGN variability power spectra usually do not show periodicity or quasi-periodicity.
- Observe noise power spectra with a bend/break at ~ 0.1 -100 days.
- The bend/break timescale can be correlated with other AGN physical properties.

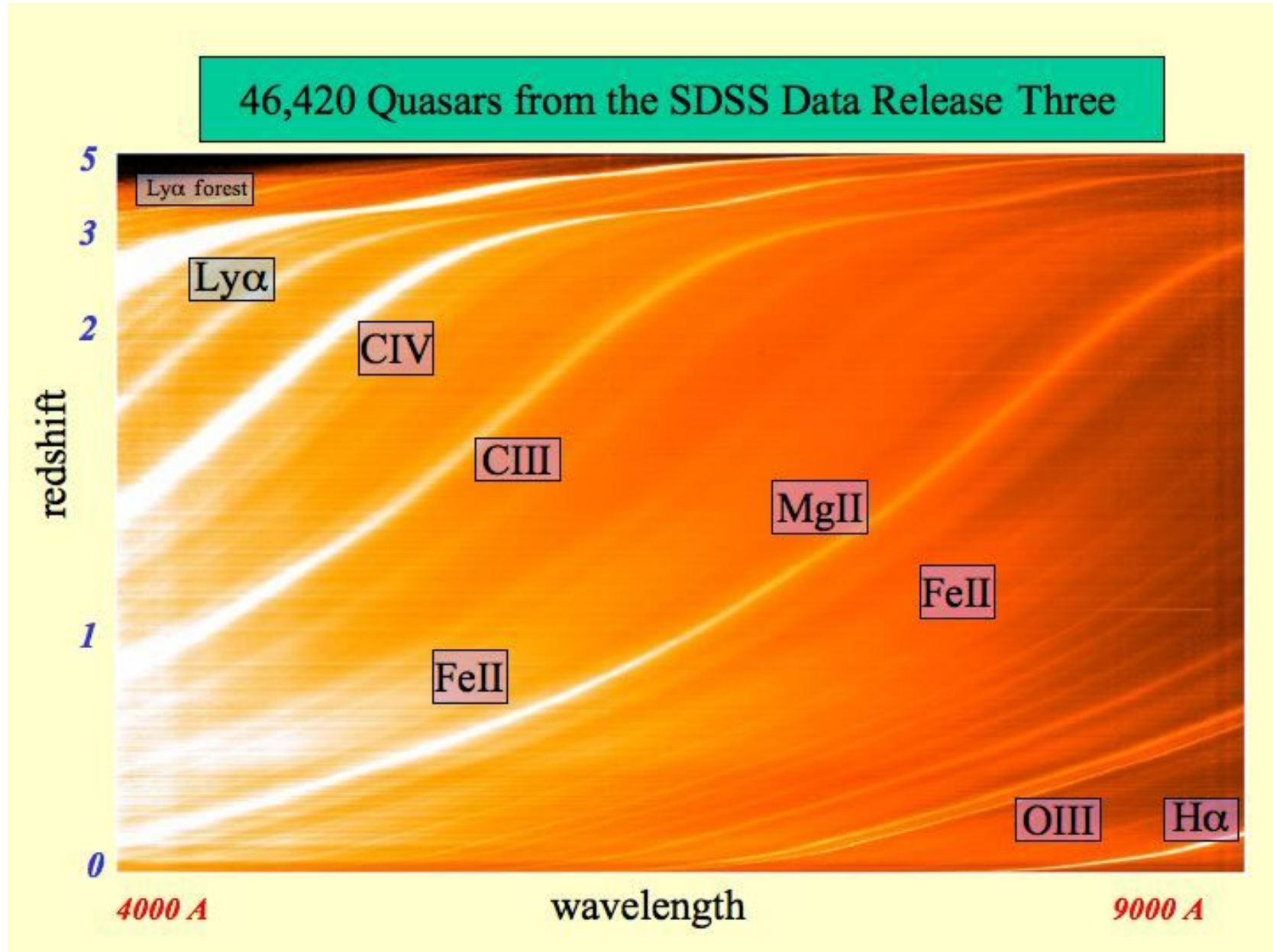
The Broad Line Region (BLR)

- Relative strengths of emission lines in AGN spectra indicate we are observing gas in photoionization equilibrium at $\sim 10^4$ K.
- Abundances about solar or slightly supersolar.
- Lines are kinematically composite:
 - Broad components
 - Doppler widths of 1000-25000 km/s.
 - Arise in gas with density $n_e \sim 10^9 - 10^{11} \text{ cm}^{-3}$ (as determined from strengths (missing) of certain density sensitive lines like [O III] and CIII).
 - We called it the “Broad Line Region”
 - Narrow components:
 - Doppler widths typically less than 900 km/s .
 - Arise in relatively low-density gas ($n_e \sim 10^3 \text{ cm}^{-3}$).
 - We called it the “Narrow Line Region”

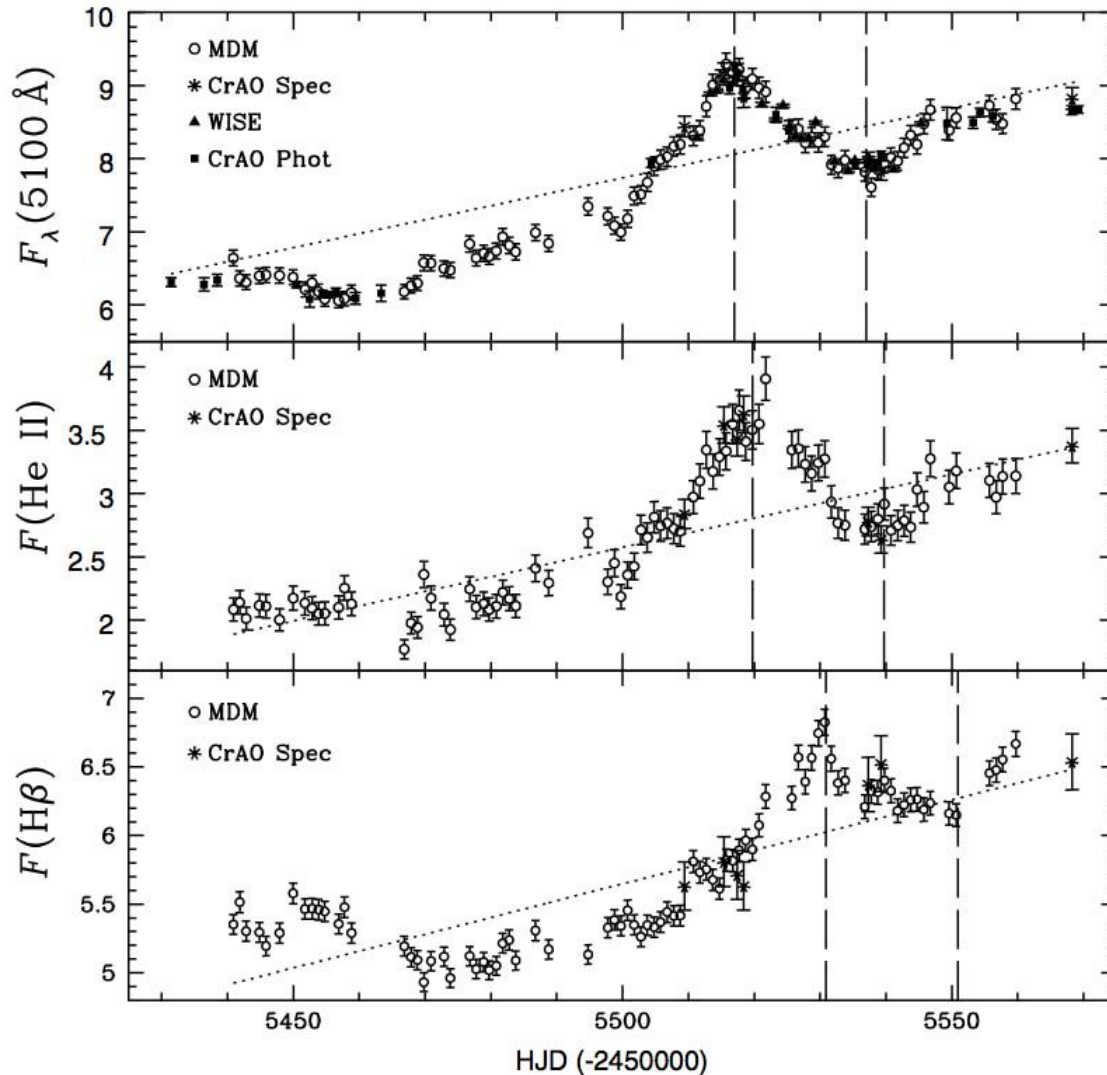
The Broad Line Region (BLR)

- Relative strengths of emission lines in AGN spectra indicate we are observing gas in photoionization equilibrium at $\sim 10^4$ K.
- Abundances about solar or slightly supersolar.
- Lines are kinematically composite:
 - Broad components
 - Doppler widths of 1000-25000 km/s.
 - Arise in gas with density $n_e \sim 10^9 - 10^{11} \text{ cm}^{-3}$ (as determined from strengths (missing) of certain density sensitive lines like [O III] and CIII).
 - We called it the “Broad Line Region”
- These motions are not thermal (~ 10 km/s for 10^4 K).
- Rather are supersonic bulk motions.
- The larger Doppler widths of the broad lines indicate they arise deeper in the gravitational potential.

Strong and Broad Lines Common



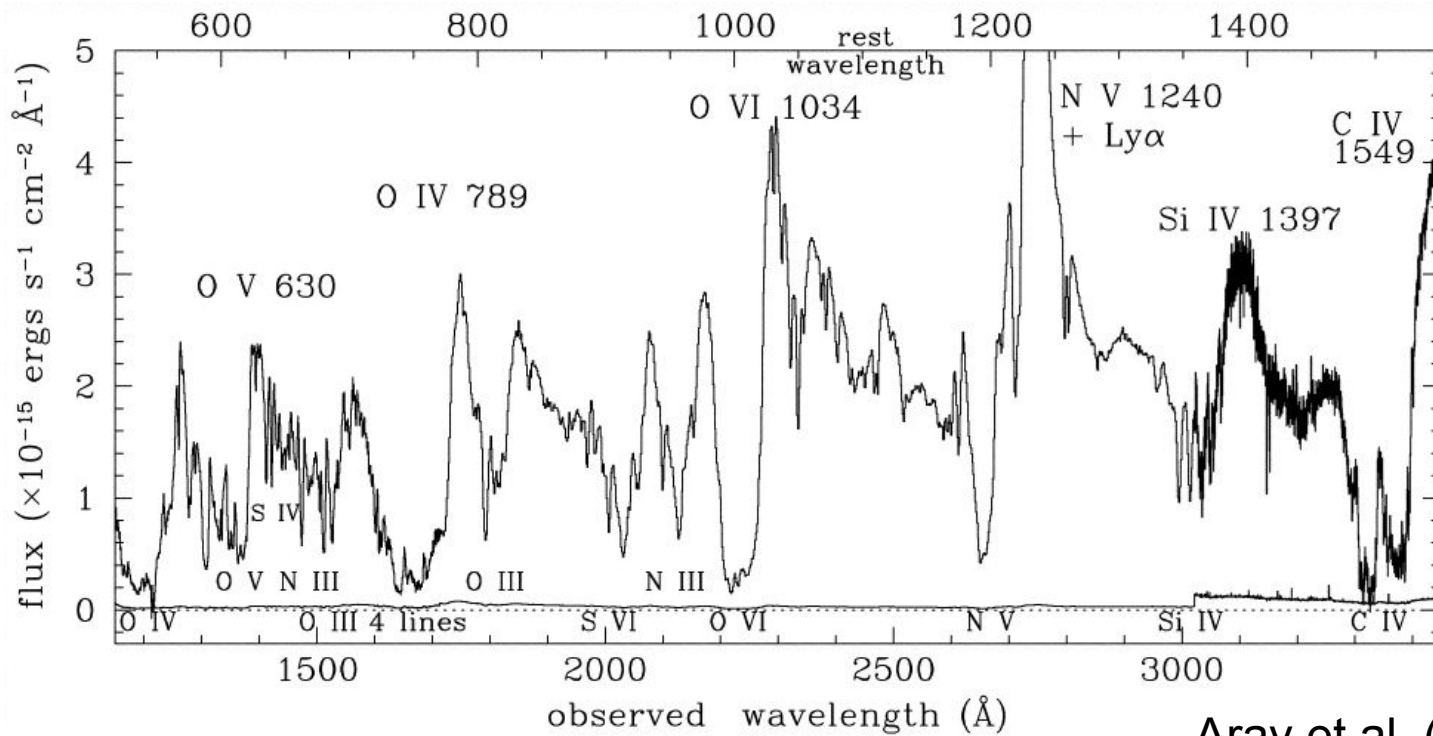
Broad Lines Lag Continuum



- The broad lines vary on short timescales, usually following the continuum variations with a time delay.
- Thought to be the light travel time across the BLR, leading to the idea of “reverberation mapping”.
- Provides a way to measure the BLR size, which is $\sim 5\text{-}500$ light days depending upon luminosity.
- The narrow lines do not vary on short timescales, indicating they are from a much larger region.

Outflowing Winds

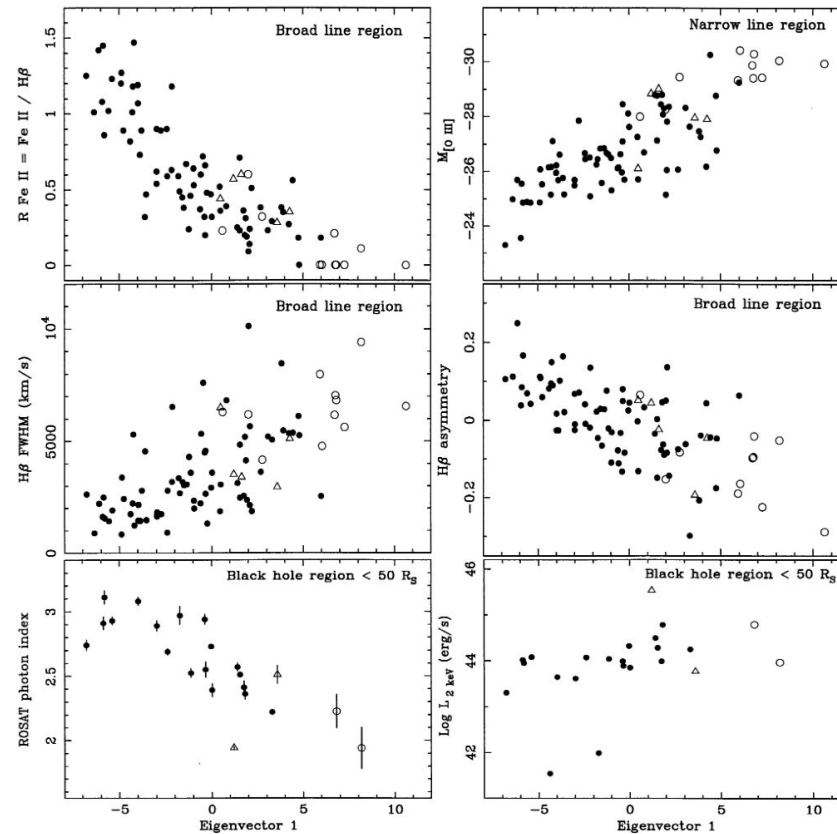
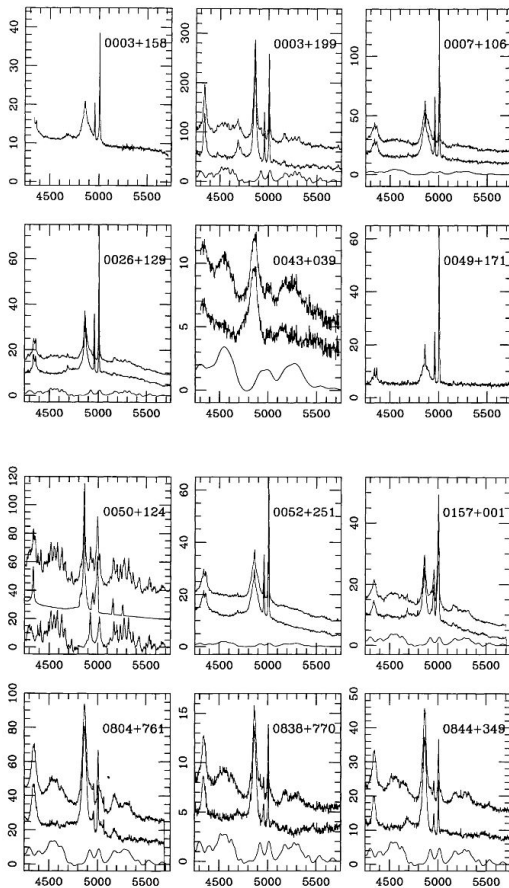
- Blueshifted UV **Broad Absorption Lines** (BAL) in Quasars
- Seen in 10-15 % of sources, but thought to be associated to 20-30% of sources (due to selection effects)
- Complex and multiple absorption features
- Defined to be broader than 2000 km/s
- Smaller are often defined as mini-BALs



Arav et al. (2001)

Object-to-Object Differences in Broad Line Properties

- There are significant object-to-object differences in broad-line properties.
- There is a set of emission-line properties that vary in a correlated manner called “Eigenvector 1”.
- Likely related to L / L_{Edd} .



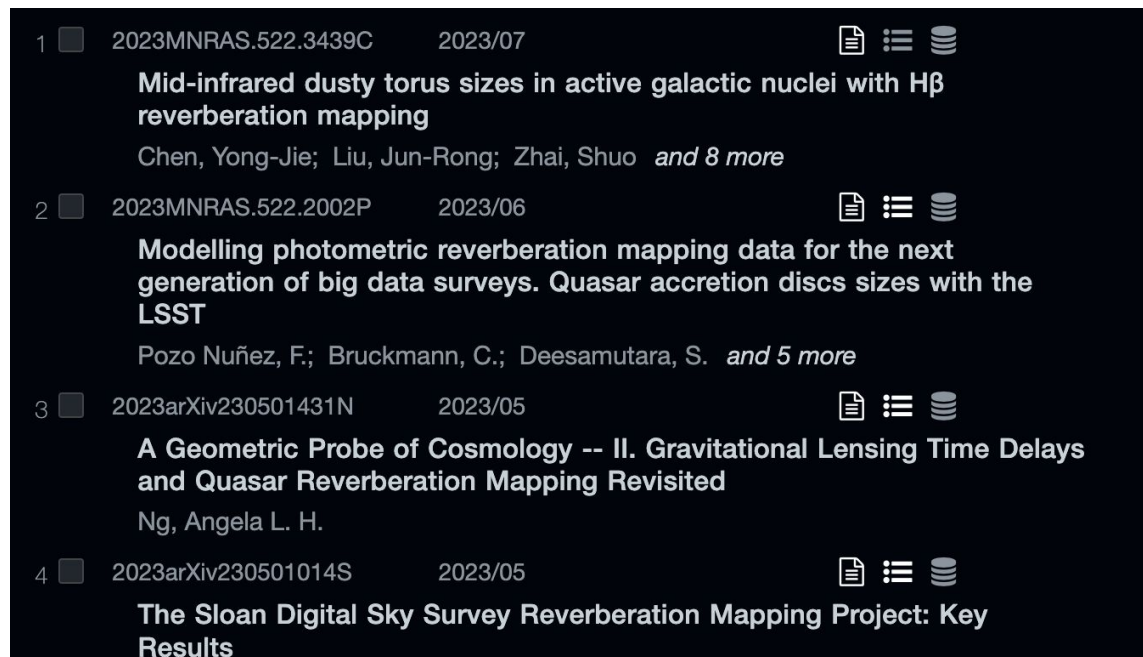
Eigenvector 1 from PCA

Boroson & Green (1992)

Reverberation Mapping: Stratification and Virialization

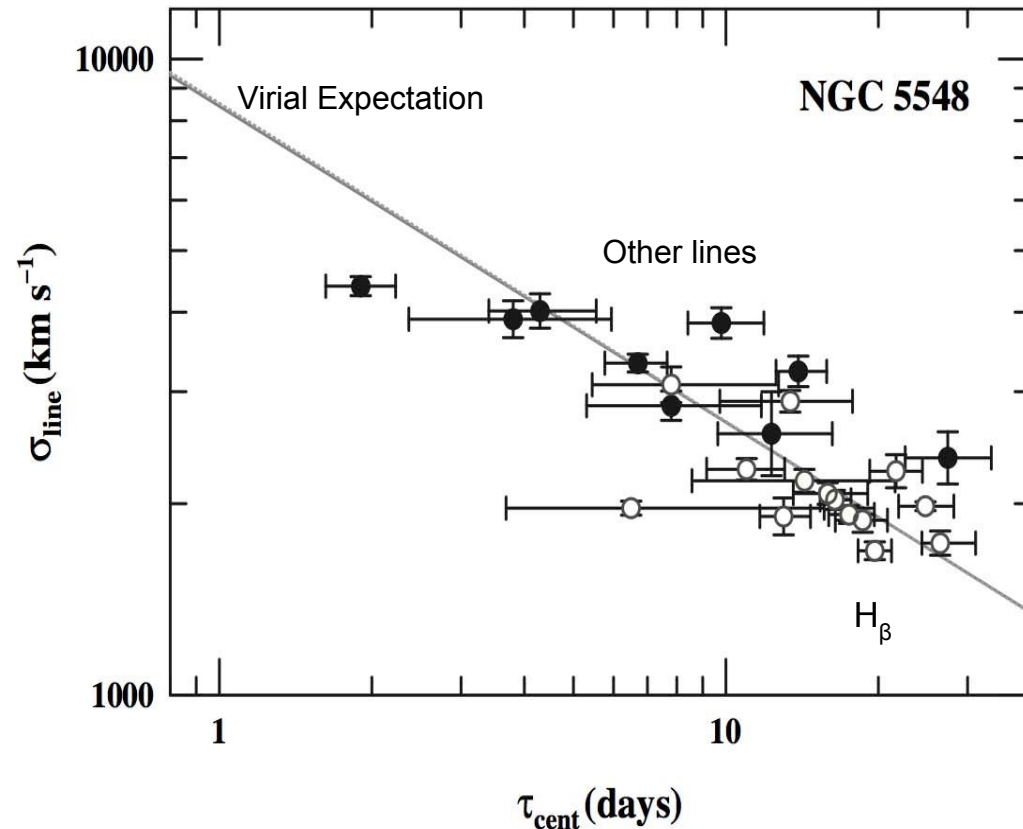
- Reverberation lags have now been measured for ~ 50 -100 AGNs.
- The current sample is biased toward AGNs with relatively strong lines.
- Mostly measured for H_{β} , but in some cases for multiple lines.
- The highest ionization emission lines respond most rapidly to continuum changes, indicating ionization stratification.
- A plot of line width vs. lag (τ) shows that $v \sim \tau^{-0.5}$, as expected for virialized gas dominated by the gravitational potential of the central source.

About 70 papers in 2023 →



1	2023MNRAS.522.3439C	2023/07	Mid-infrared dusty torus sizes in active galactic nuclei with H_{β} reverberation mapping Chen, Yong-Jie; Liu, Jun-Rong; Zhai, Shuo <i>and 8 more</i>
2	2023MNRAS.522.2002P	2023/06	Modelling photometric reverberation mapping data for the next generation of big data surveys. Quasar accretion discs sizes with the LSST Pozo Nuñez, F.; Bruckmann, C.; Deesamutara, S. <i>and 5 more</i>
3	2023arXiv230501431N	2023/05	A Geometric Probe of Cosmology -- II. Gravitational Lensing Time Delays and Quasar Reverberation Mapping Revisited Ng, Angela L. H.
4	2023arXiv230501014S	2023/05	The Sloan Digital Sky Survey Reverberation Mapping Project: Key Results

Estimating Black Hole Masses



- Can estimate black-hole masses following the virial theorem:

$$M_{\text{BH}} = \frac{f c \tau \Delta V^2}{G}$$

- Where f is a factor that includes (unknown) BLR geometry and inclination.
- Comparison with other mass-estimation methods indicates an average value of $f \sim 4-5$.
- Masses measured this way appear accurate to within a factor of ~ 3 when H_{β} is used.
- Note this method can be used, if patient, for masses at high redshifts.

Mass-Luminosity Relationship

Peterson et al. (2004)

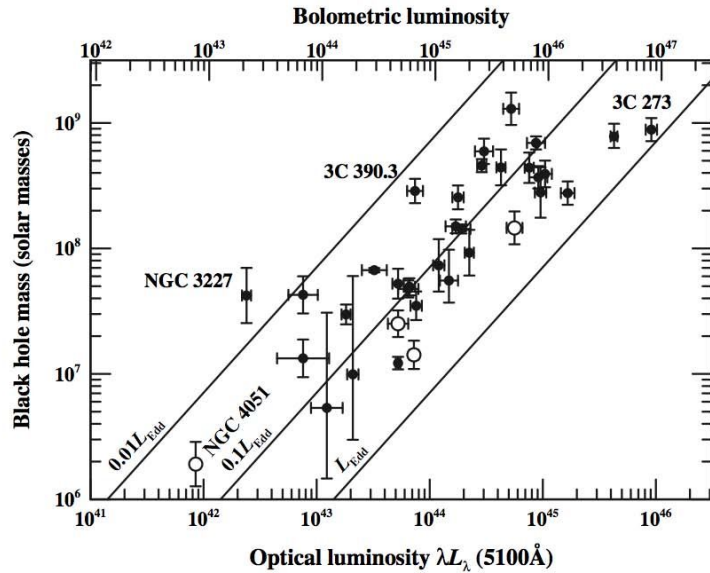


Fig. 9. The mass–luminosity relationship for reverberation-mapped AGNs. The luminosity scale on the lower x-axis is $\log \lambda L_\lambda$ in units of ergs s^{-1} . The upper x-axis shows the bolometric luminosity assuming that $L_{\text{bol}} \approx 9\lambda L_\lambda(5100 \text{ \AA})$. The diagonal lines show the Eddington limit L_{Edd} , $0.1L_{\text{Edd}}$, and $0.01L_{\text{Edd}}$. The open circles represent NLS1s. From [25]

- Can combine the $R_{\text{BLR}}-L$ relation with the virial theorem to estimate single-epoch masses. For example...

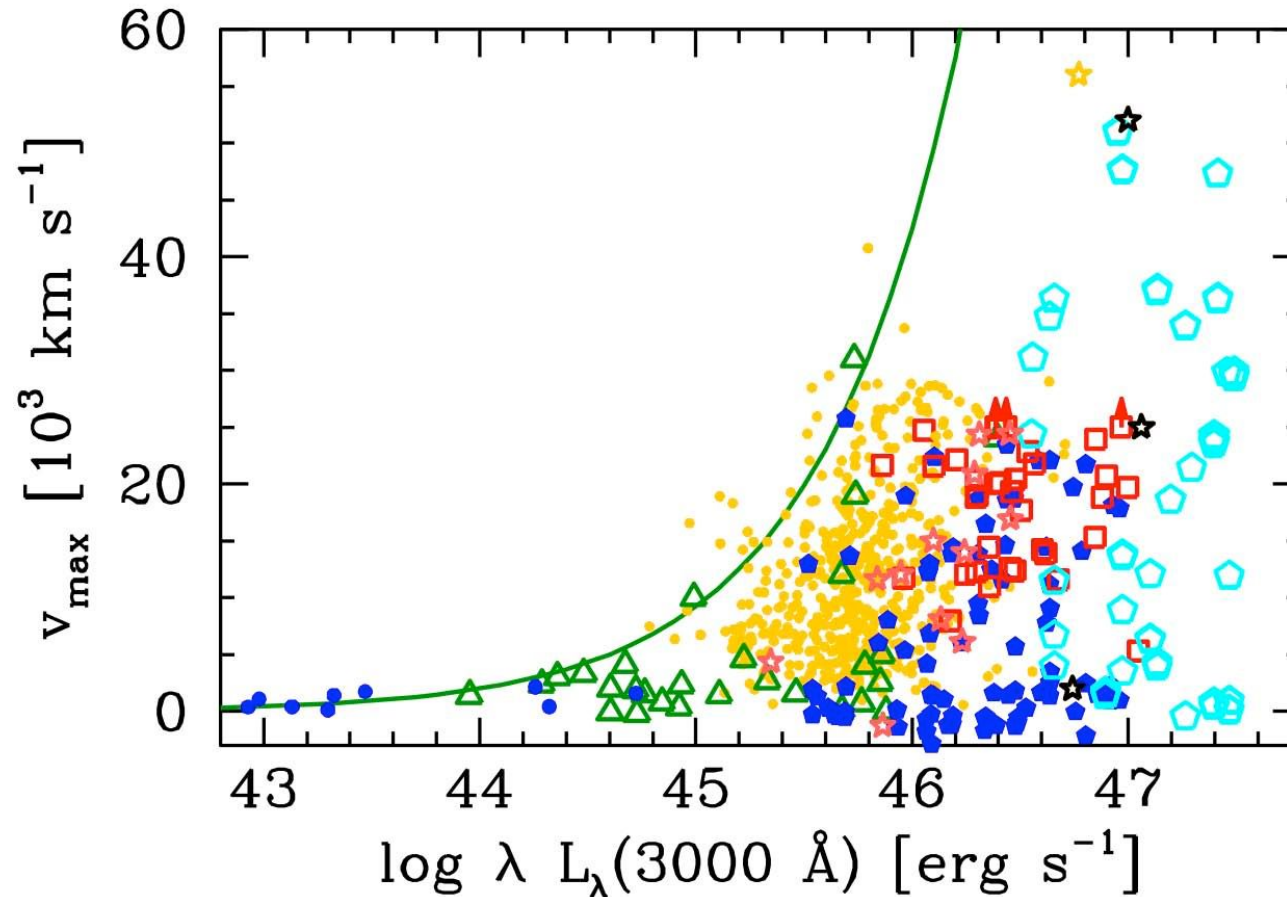
$$\frac{M_{\text{BH}}}{10^6 M_\odot} = 4.35 \left[\frac{\nu L_\nu(5100 \text{ \AA})}{10^{44} \text{ ergs s}^{-1}} \right]^{0.7} \left[\frac{\text{FWHM}(\text{H}\beta)}{10^3 \text{ km s}^{-1}} \right]^2$$

- Similar relations exist for Mg II and C IV.
- These allow quick estimates for large AGN samples, but their accuracy is no better than a factor of several. The main challenge is characterizing the line widths, where caution is needed.
- Statistical use of such masses in large samples is probably OK, but individual mass estimates may be unreliable.

What is the Nature of the BLR?

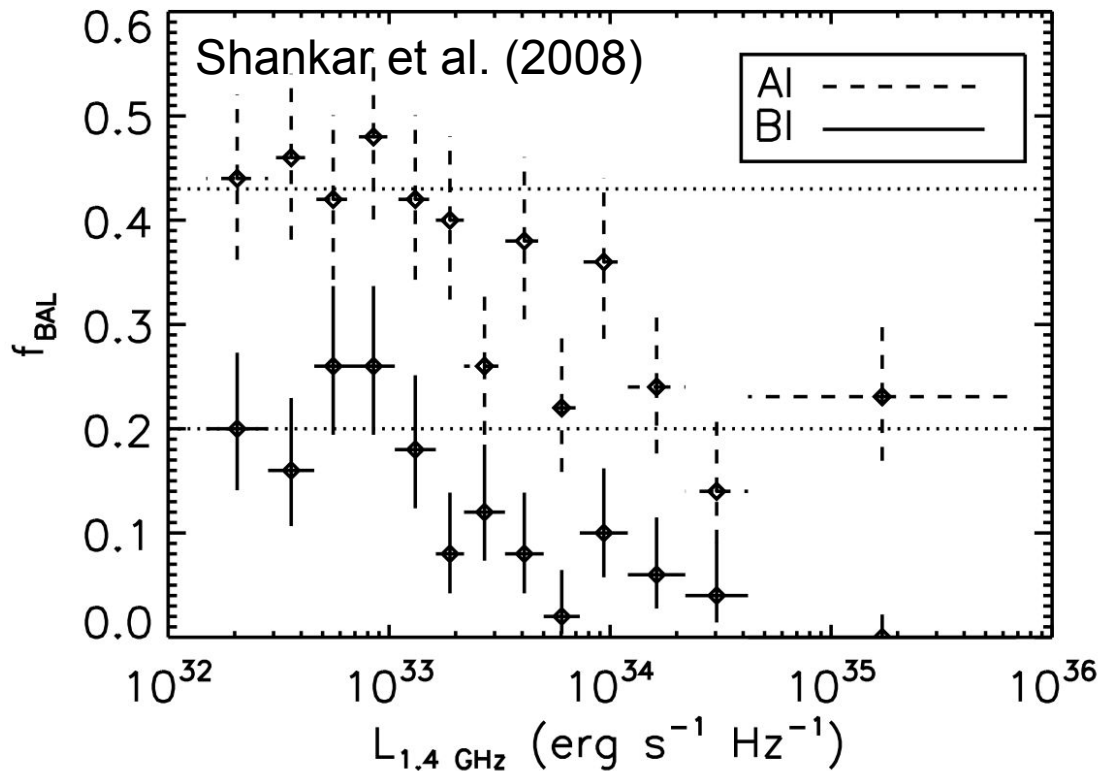
- After much research, it is appearing increasingly likely that the BLR itself has a composite nature:
- Moderate-ionization and high-optical-depth region
 - Largely responsible for the Balmer-line emission and Mg II
 - Accretion disk itself?
 - A disk with a large line-emitting region can make single-peaked profiles consistent with most objects
- High-ionization and moderate-optical-depth region
 - Largely responsible for the high-ionization lines
 - Accretion-disk wind?
 - Helps explain blueshifts of high-ionization lines and blueward line asymmetries

UV Outflows Found Over a Wide AGN Luminosity Range



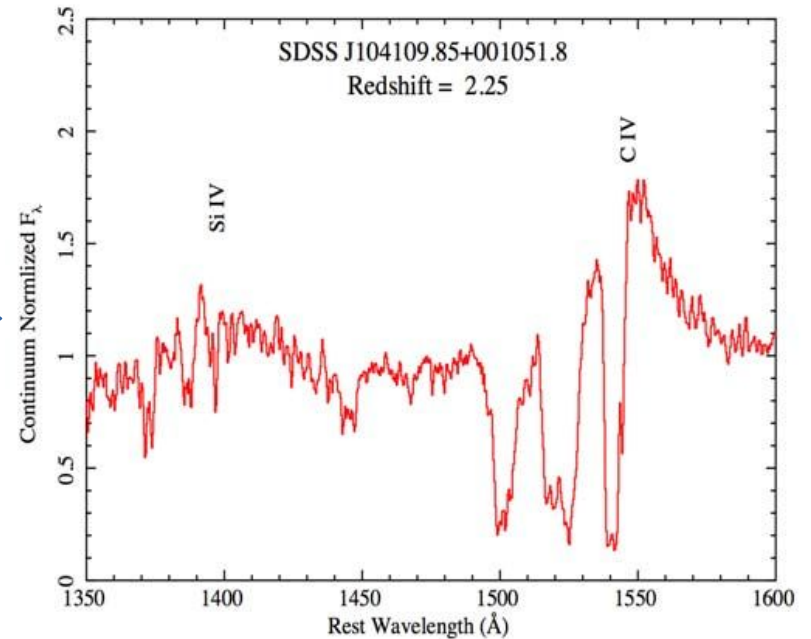
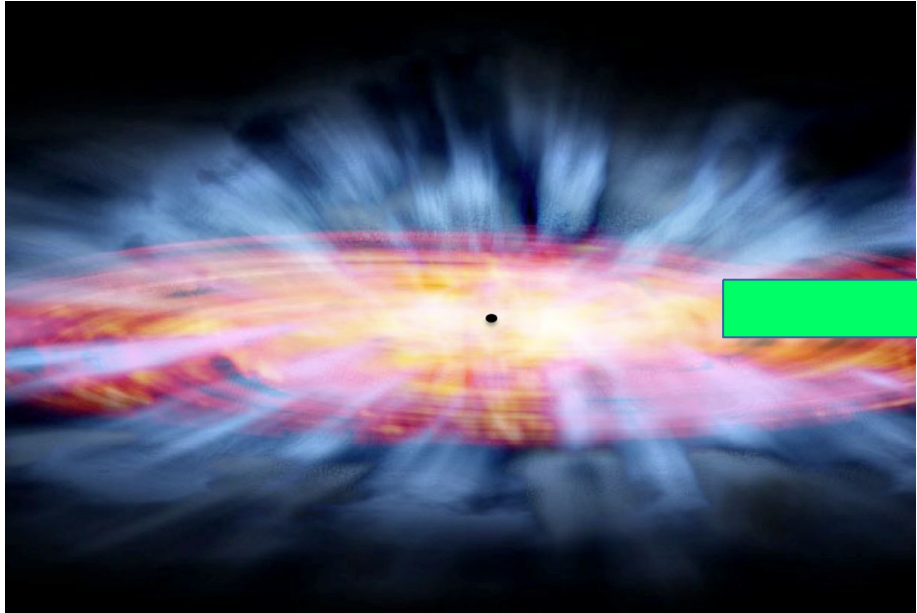
- There's seem to be a correlation with L:
 - The larger the luminosity, the larger the wind velocity

BAL Fraction Depends Upon Radio Power



- BALs generally avoid highly radio-luminous quasars (though not entirely).
- Reason for this is still not entirely clear.
- Wind-jet connection?
 - Connection with Eddington Rate (ER)?
 - Lower ER \rightarrow Radio Mode
 - Higher ER \rightarrow Quasar Mode
- Orientation effects?

Wind Model

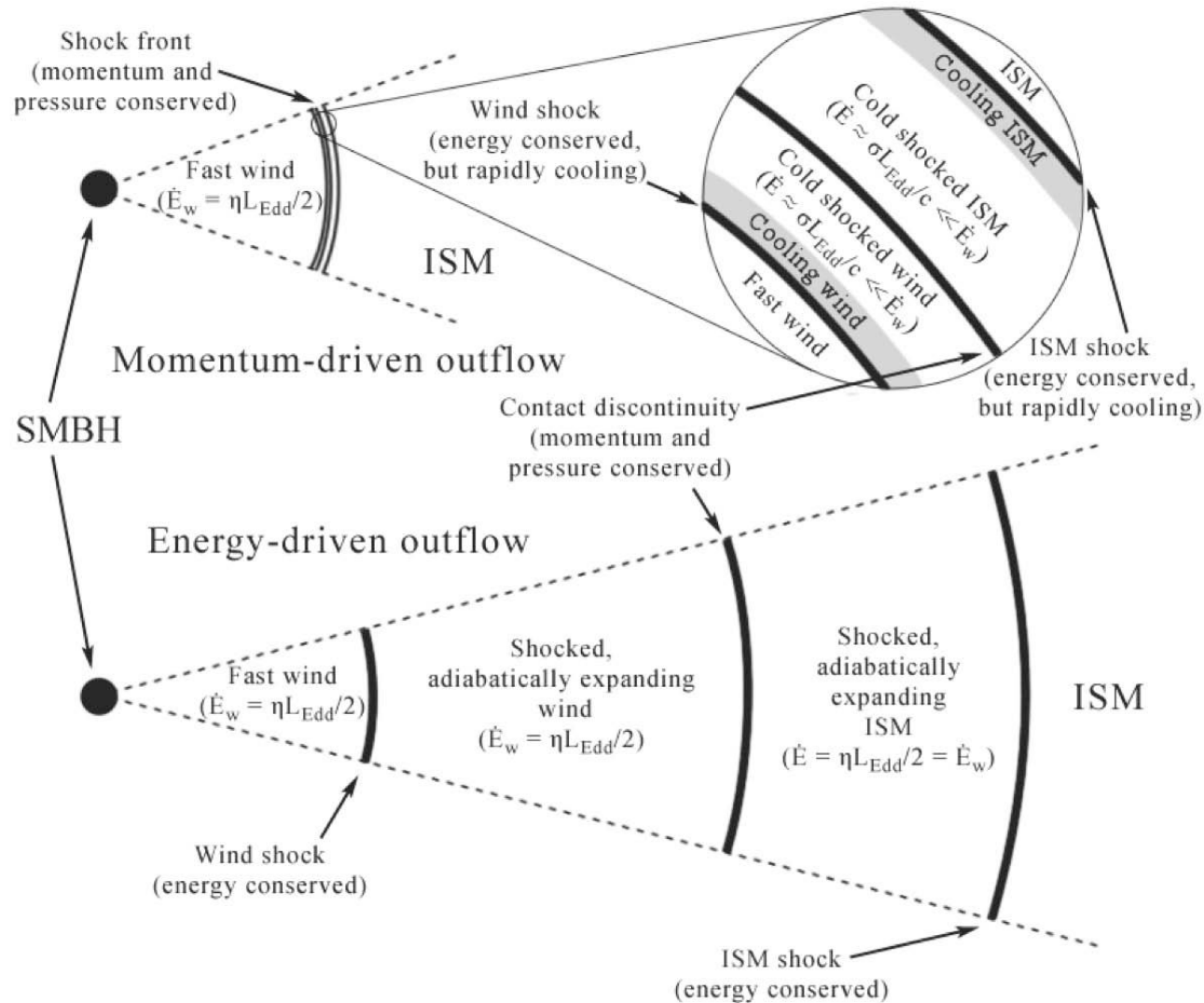


- Most AGNs likely drive winds – orientation effect.
- Multiple lines from same transition probe distinct wind components.
- Wind material exists over a wide range of radii from 0.01 pc to kpc scales. Often outside the BLR.
- Lines often saturated with partial covering.
- Wind is driven by radiative pressure on the lines from the Equatorial Accretion-Disk or Torus to Velocities of $\sim 100\text{-}30000$ km/s

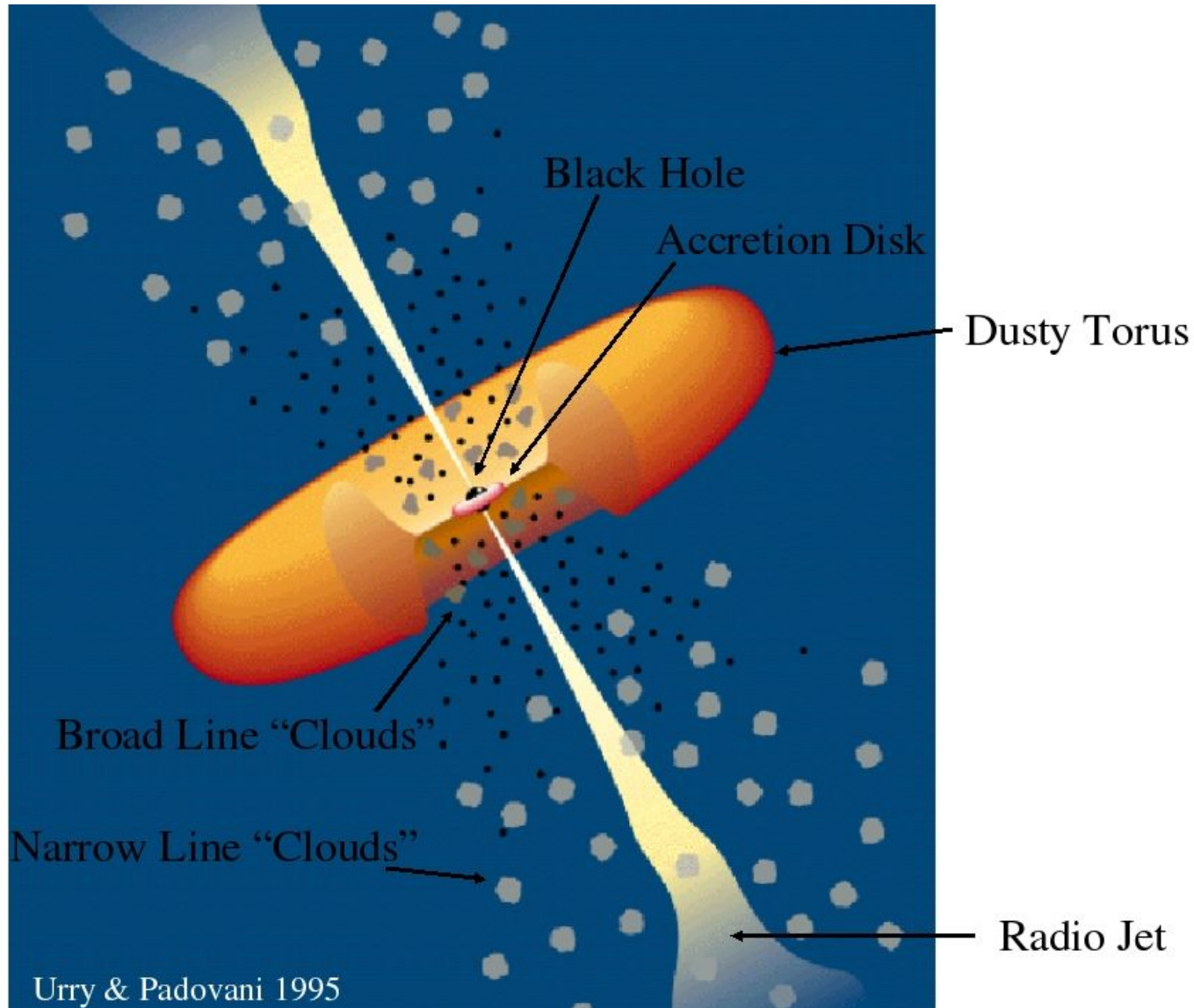
Effect of Winds

- Why Care About AGN Winds?
- Significantly affect observed AGN properties (UV line absorption, high-ionization line emission, reddening, polarization, X-ray absorption).
- Substantial part of typical AGN nuclear regions; seen in absorption in $\sim 30+\%$ of AGNs.
- Help black-hole accretion to proceed by removing angular momentum from the disk.
- Can evacuate gas from the host galaxy, likely affecting black-hole growth and galaxy evolution.

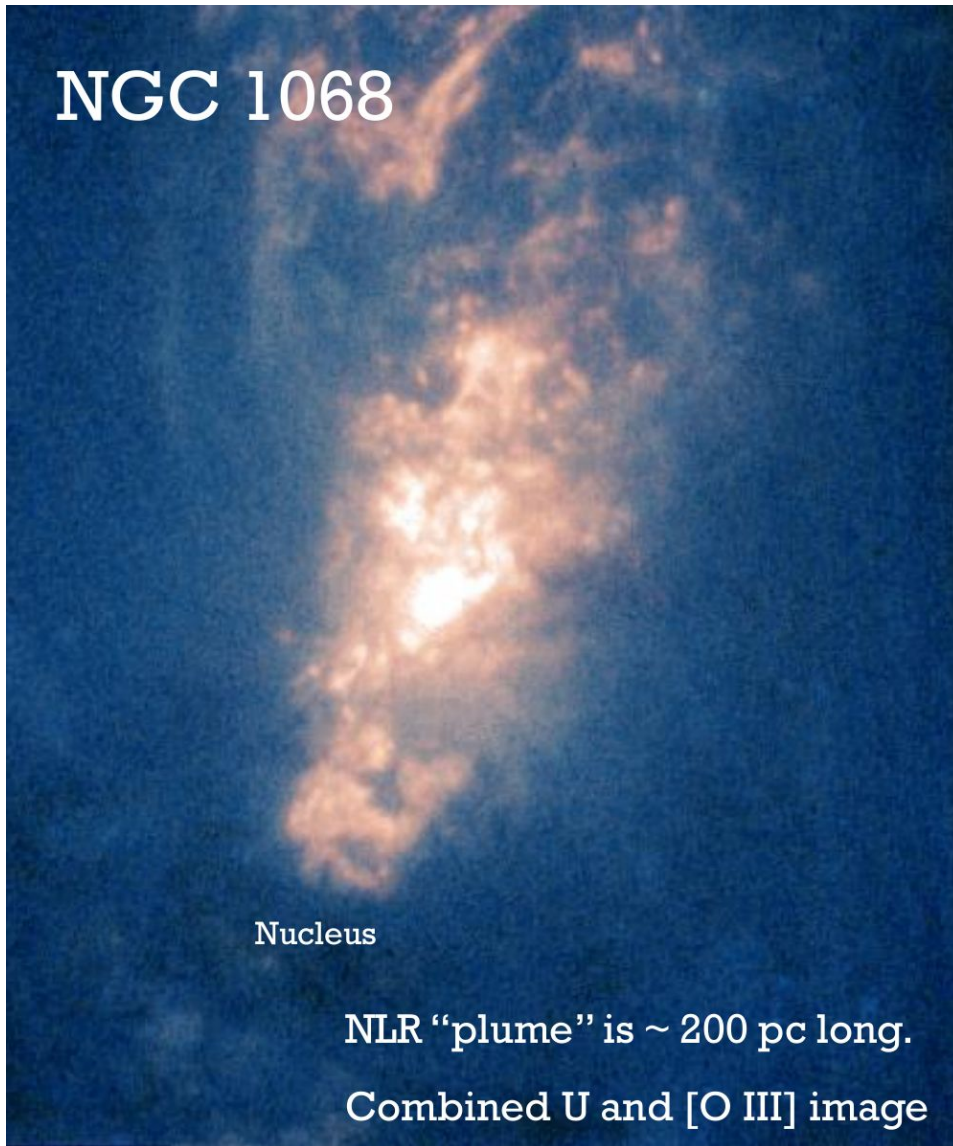
Wind Feedback into the ISM



The Narrow Line Region



Imaging the NLR



- NGC 1068 (Fath 1908)
- The line emission region is clumpy and complex.
- NLR is clearly not spherically symmetric, but rather is roughly axisymmetric.
- NLR axis generally coincides with radio axis in cases where extended linear radio emission is detected.
- In some sources, we see strong line emission from regions where the radio jet is colliding with the ISM and causing shocks – an additional source of ionization.

HST - Macchetto et al. (1994)

The Narrow Line Region

- Narrow components
 - Doppler widths typically less than 900 km/s.
 - Arise in relatively low-density gas ($n_e \sim 10^3 \text{ cm}^{-3}$) (**Forbidden Lines!!**)
 - From the “Narrow Line Region”.
- Largest spatial scale where ionizing radiation from the AGN dominates.
- NLR can be spatially resolved in the optical; has sizes of $\sim 100+$ pc in local Seyferts (and even larger in quasars).
- Can map out physical and kinematic properties directly to some extent.
- FWHM values are 200-900 km s/1 , with line profiles varying across NLR.
- See a wide range of ionization states:
 - Low ionization (e.g., [O I] $\lambda 6300$)
 - High ionization (e.g., [O III] $\lambda 4959, 5007$)
 - Sometimes even very highly ionized species (e.g., iron coronal lines)
- From line ratios, infer that the NLR is mostly photoionized by the AGN continuum (with some likely additional ionization by shocks from radio jets).
- NLR line EWs drop with increasing continuum luminosity, and are often undetectable in high-luminosity quasars.
- **NLR becoming larger than the host galaxy?**
- If ionization parameter ξ is constant $\rightarrow \xi = L/(n R^2) \rightarrow R$ Can exceed the Galaxy (running out of gas)

Importance of NLR

- Line peaks provide useful systemic redshifts for AGNs.
- Useful as a bolometer for inferring AGN total power.
 - NLR lines can be used to estimate rough bolometric luminosities, even for obscured AGNs.
 - Emitted from a region larger than any nuclear obscuration → Vary on longer timescales (decades).
- Connection with Eigenvector 1.
- NLR line widths are correlated with host-galaxy bulge luminosity (and bulge gravitational potential).
- Anisotropic illumination provides clues about AGN geometry and orientation.

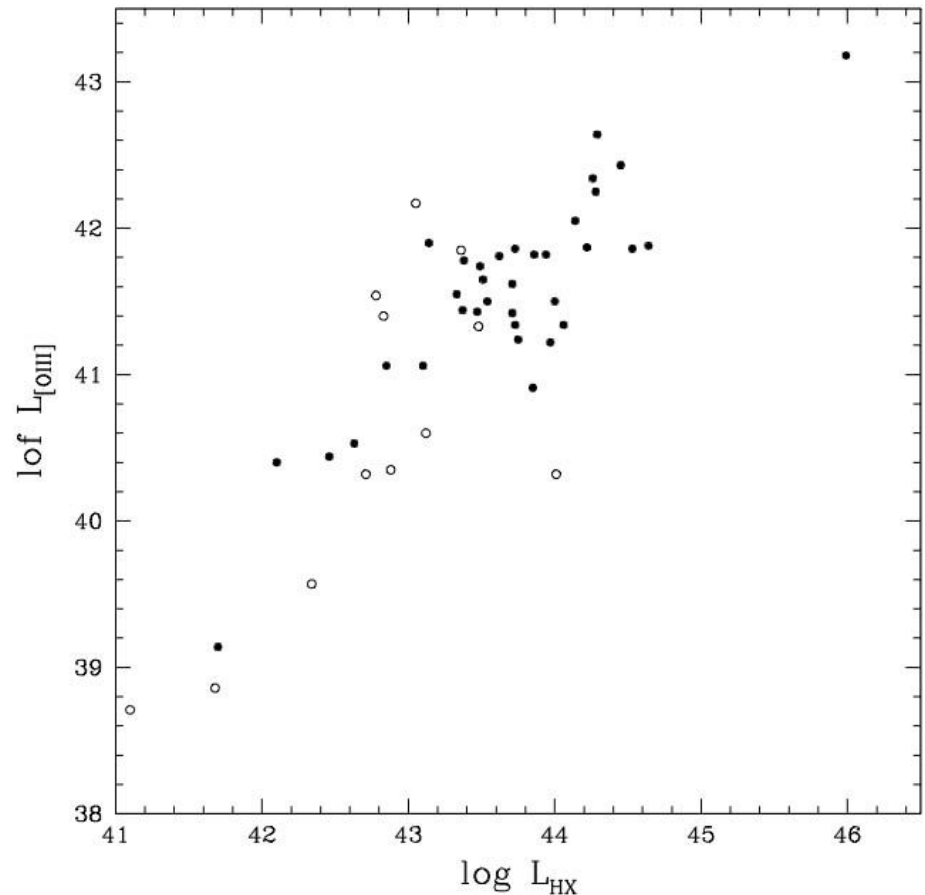


FIG. 2.—Plot of the hard X-ray (3–20 keV) vs. the [O III] $\lambda 5007$ luminosities for the AGNs in Fig. 1. The Type 1 AGNs are plotted as filled circles and the Type 2 AGNs as hollow circles. Luminosities are in units of ergs s^{-1} .

Importance of NLR

- Line peaks provide useful systemic redshifts for AGNs.
- Useful as a bolometer for inferring AGN total power.
 - NLR lines can be used to estimate rough bolometric luminosities, even for obscured AGNs.
 - Emitted from a region larger than any nuclear obscuration.
- Connection with Eigenvector 1.
- NLR line widths are correlated with host-galaxy bulge luminosity (and bulge gravitational potential).
- Anisotropic illumination provides clues about AGN geometry and orientation.

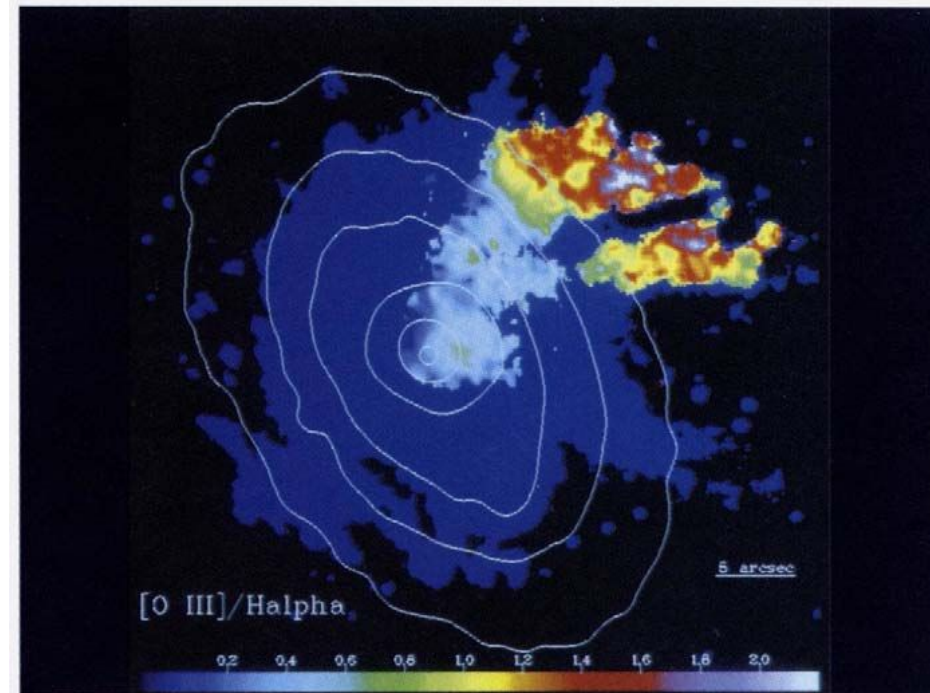
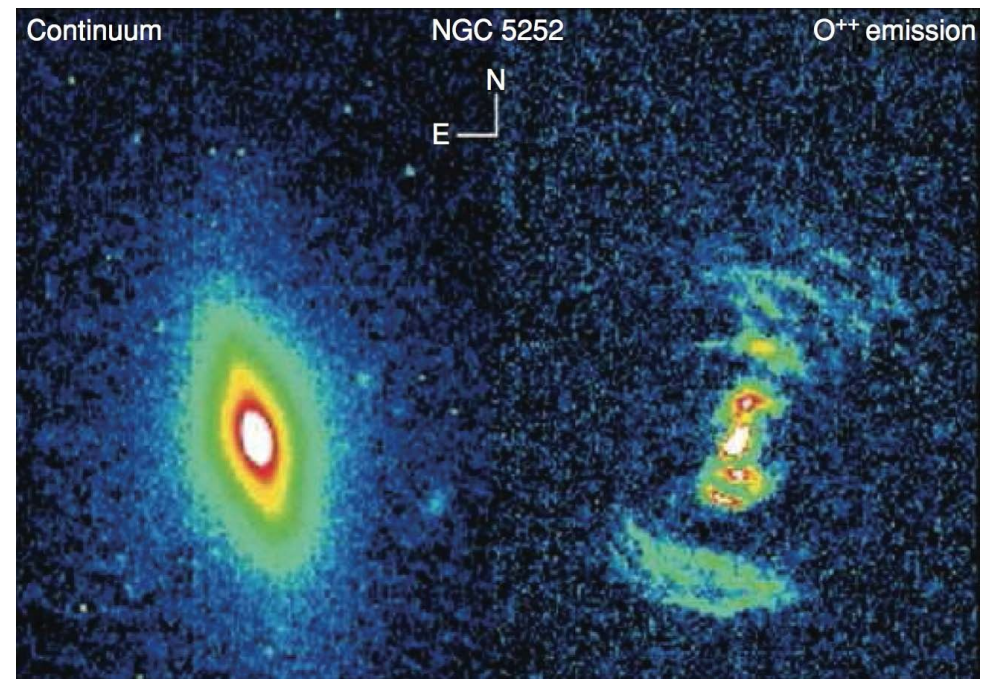


Figure 6: $[O\text{ III}]/(H\alpha + [N\text{ II}])$ showing the ionization structure of the cone. The uniform dark blue region is where $H\alpha + [N\text{ II}]$ but not $[O\text{ III}]$ was detected at more than 10σ .

Marconi et al. (1994)

Importance of NLR

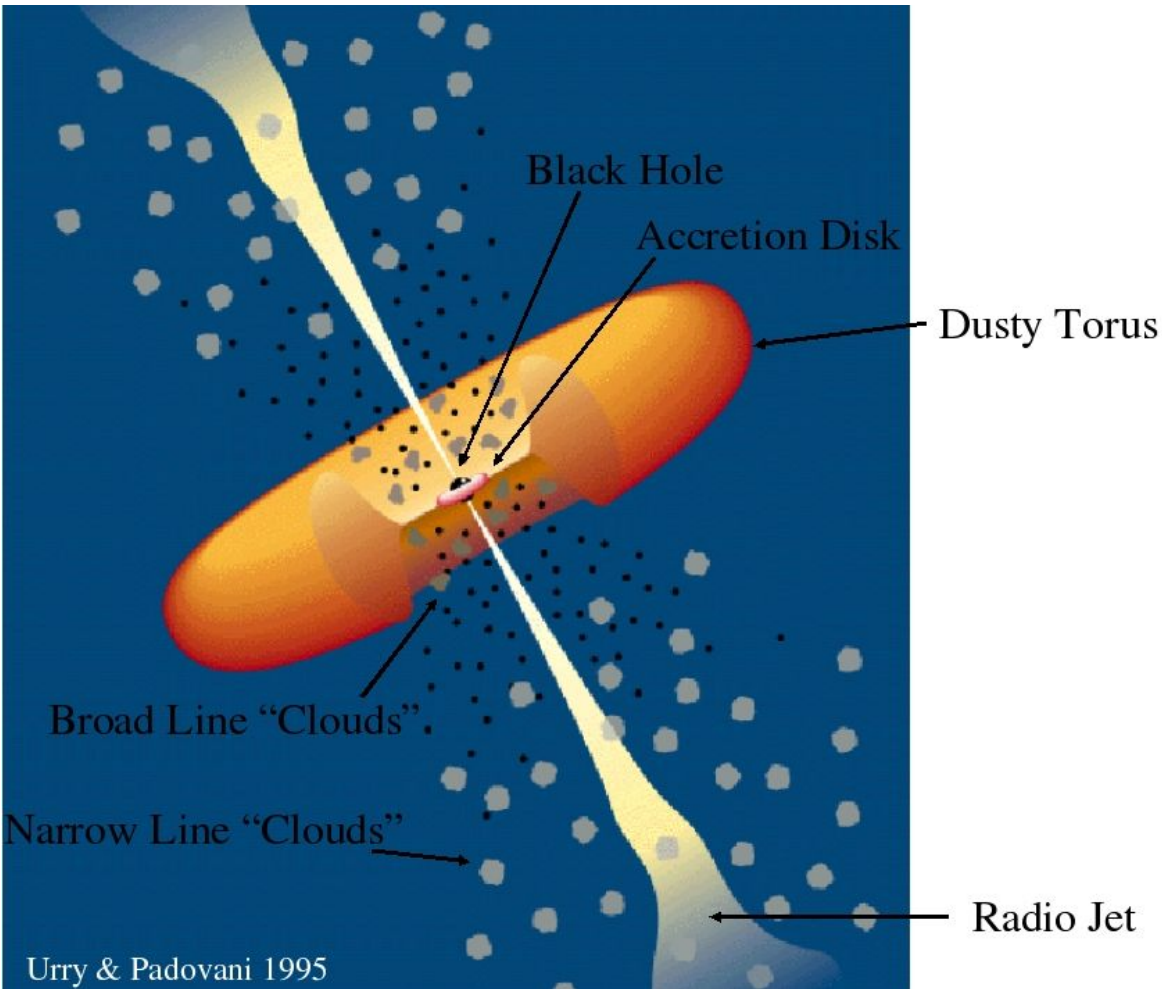
- Line peaks provide useful systemic redshifts for AGNs.
- Useful as a bolometer for inferring AGN total power.
 - NLR lines can be used to estimate rough bolometric luminosities, even for obscured AGNs.
 - Emitted from a region larger than any nuclear obscuration.
- Connection with Eigenvector 1.
- NLR line widths are correlated with host-galaxy bulge luminosity (and bulge gravitational potential).
- Anisotropic illumination provides clues about AGN geometry and orientation.



Netzer (2013)

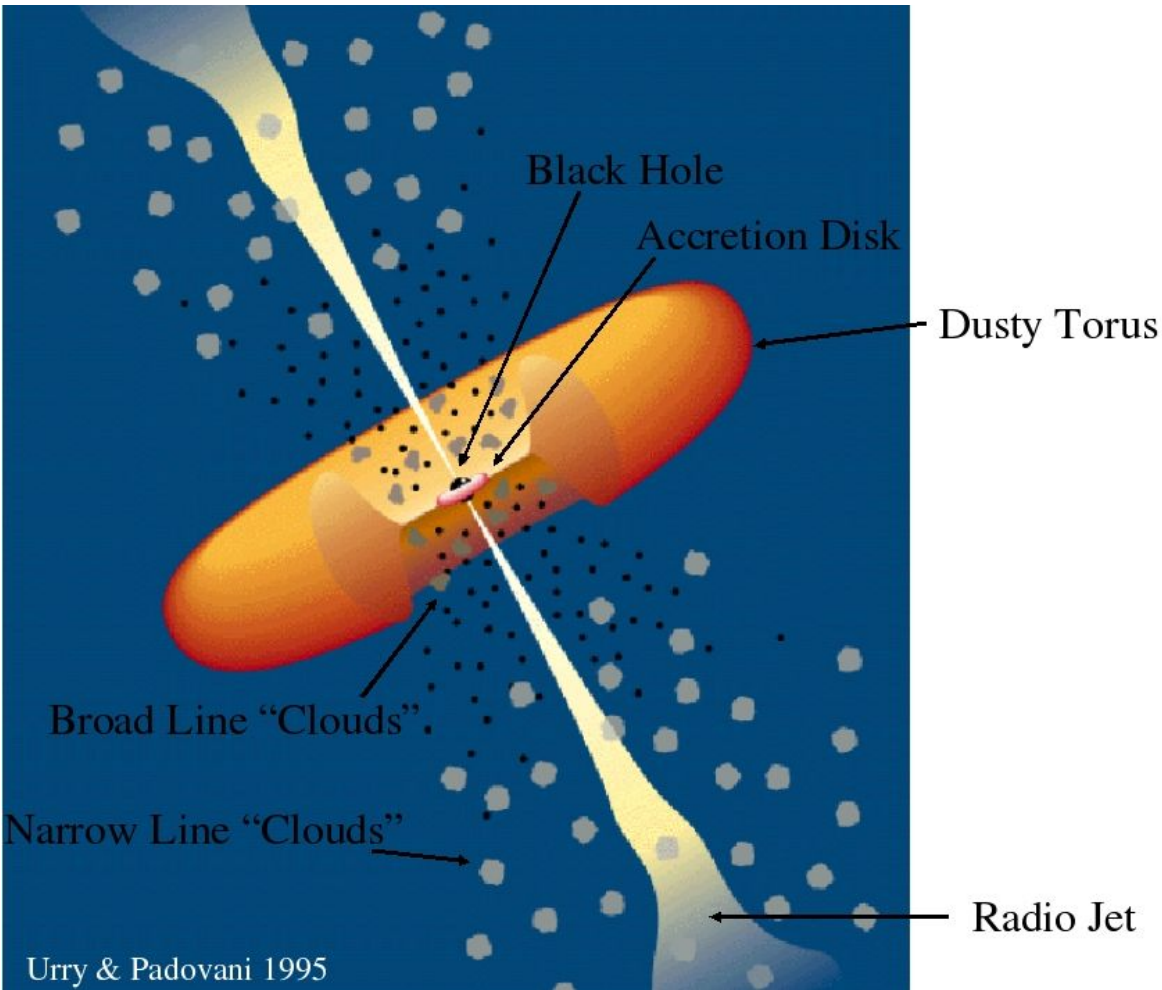
Orientation of the Cone not correlated with host galaxy

The Torus and the Unifying Model



- To first approximation, the optical/UV spectra of AGNs separate into two broad spectral types:
- Type 1:
 - Broad permitted emission lines, particularly the Balmer lines
 - Permitted lines clearly broader than forbidden lines
 - Moderate EW forbidden lines
- Type 2:
 - Narrow permitted emission lines, particularly the Balmer lines
 - Permitted lines have similar widths to forbidden lines
 - High EW forbidden lines
- There are additional complications to this simple scheme (e.g., intermediate type classifications, narrow-line Type 1 AGNs).
- These optical spectral differences have come to be understood as (often) due to orientation-dependent central obscuration by a so-called "**TORUS**".

The Torus and the Unifying Model



- The torus is presumed to be an axisymmetric structure of large height so that, at least at low luminosities, the majority of AGNs are obscured by it.
- It is made of a combination of dusty atomic and molecular gas.
- The dust causes large extinction in the optical/UV and sometimes even in the NIR.
- The torus lies between the BLR and the NLR.
- Type 2 AGNs are those obscured by the torus, and emission on the scale of the BLR and smaller is obscured by it.
- Models explaining differences between Type 1 and Type 2 AGNs this way are referred to as "unification models".
- These models have had much success, though they are not complete and there are likely exceptions.
- There appear to be substantial object-to-object variations in the covering factor and geometry of the torus.
- Keplerian velocities at the torus distance are ~ 1000 km/s
- Density of torus "clumps" are $\sim 10^5 - 10^7$ cm⁻³.
- The estimated mass of the torus is only a small fraction of the SMBH mass.
- The torus is likely a dynamic system (maybe clumpy) being part of the general flow of matter from the galaxy's center to the SMBH. But the details remain unclear.

Size of the Torus

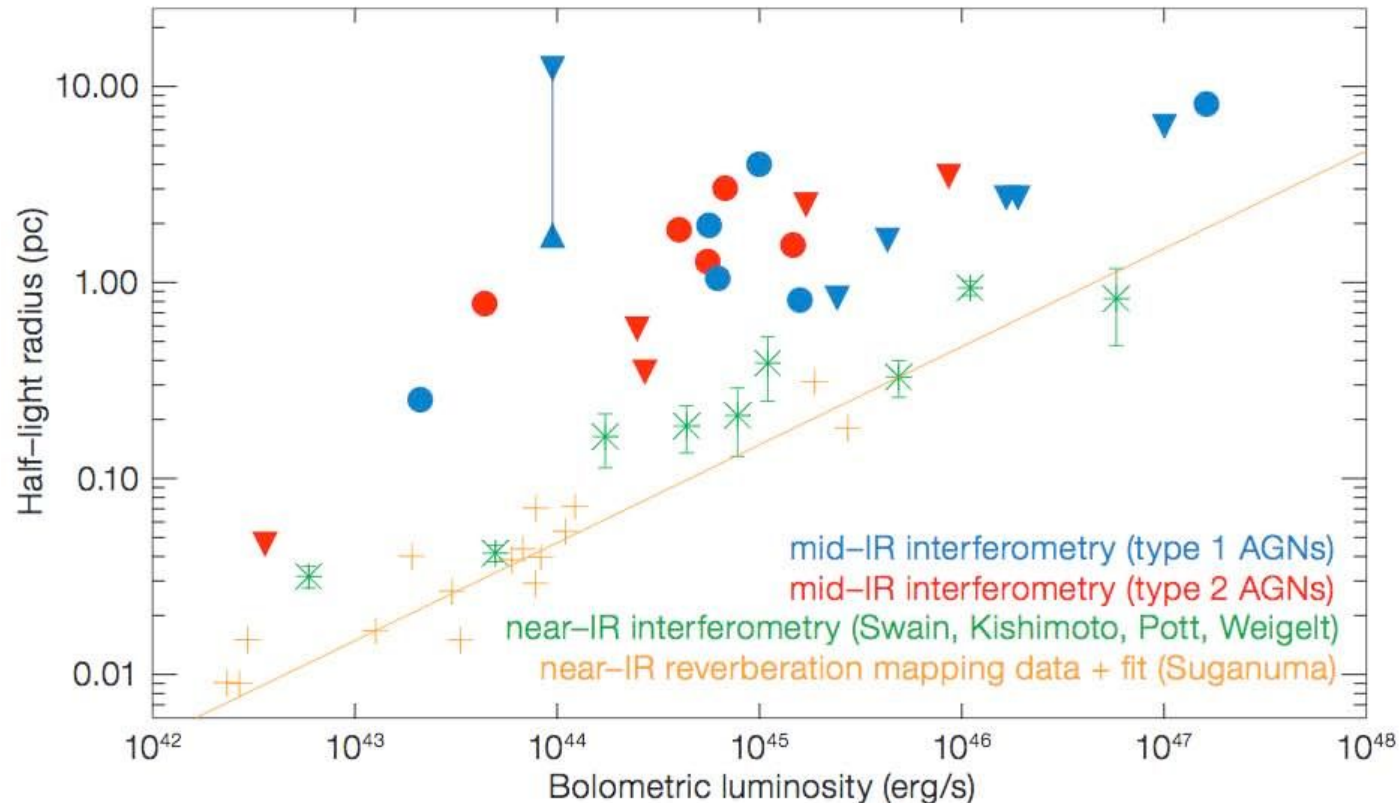
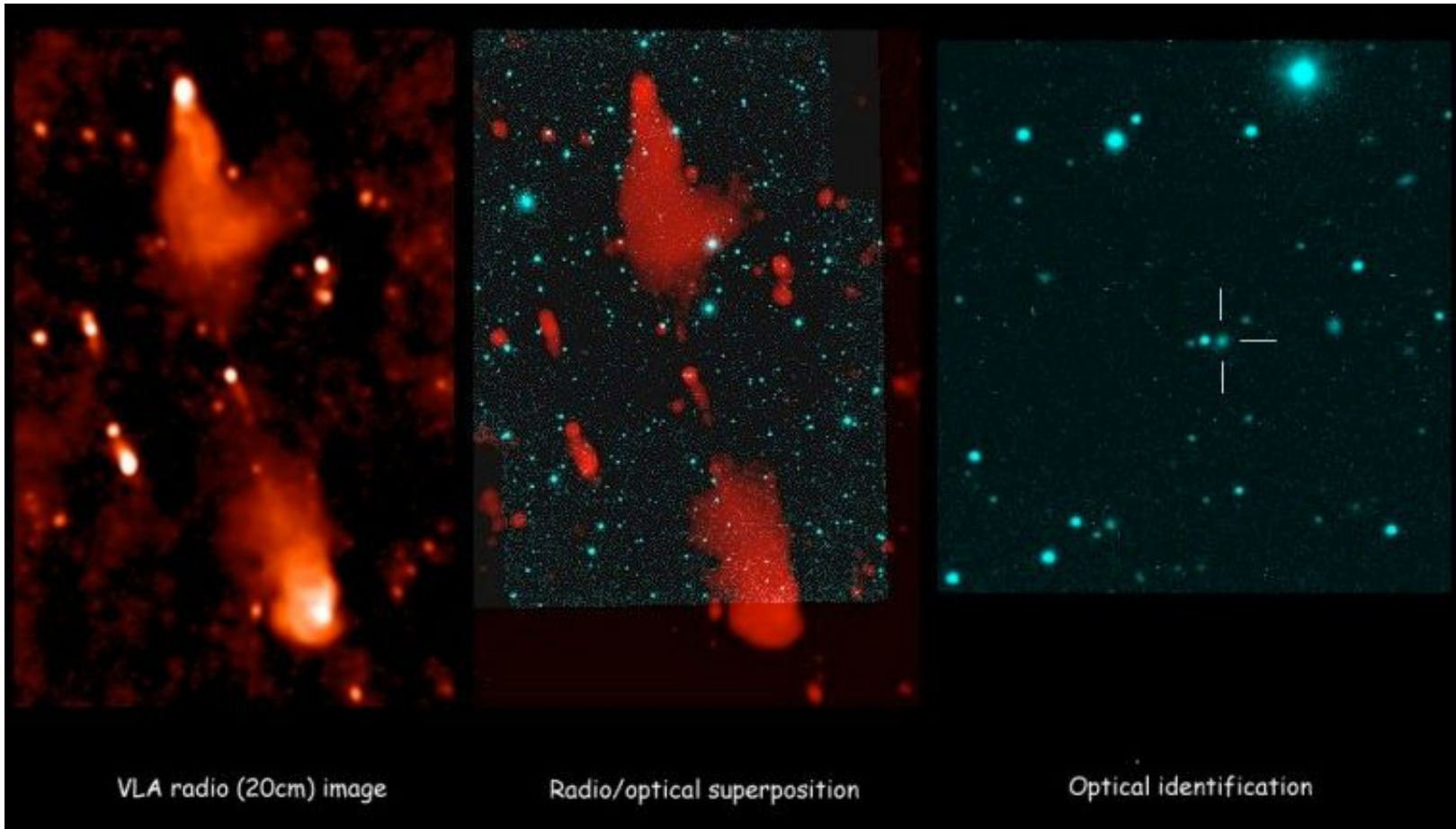


Figure 5. Size–luminosity relation for AGNs probing different regions of the torus: blue/ red points are MIDI measurements from the MIDI AGN Large Programme + archive for type 1/type 2 sources (statistical errors are smaller than symbol sizes); green crosses are NIR interferometry with both the Keck-Interferometer and AMBER/VLTI; orange pluses are from NIR dust reverberation mapping. Filled triangles show limits. Taking both the limits and the determined half-light radii into account shows that the mid-infrared size is less strictly correlated with luminosity than the innermost radius of dust that is seen in the NIR.

Burtscher et al. (2013)

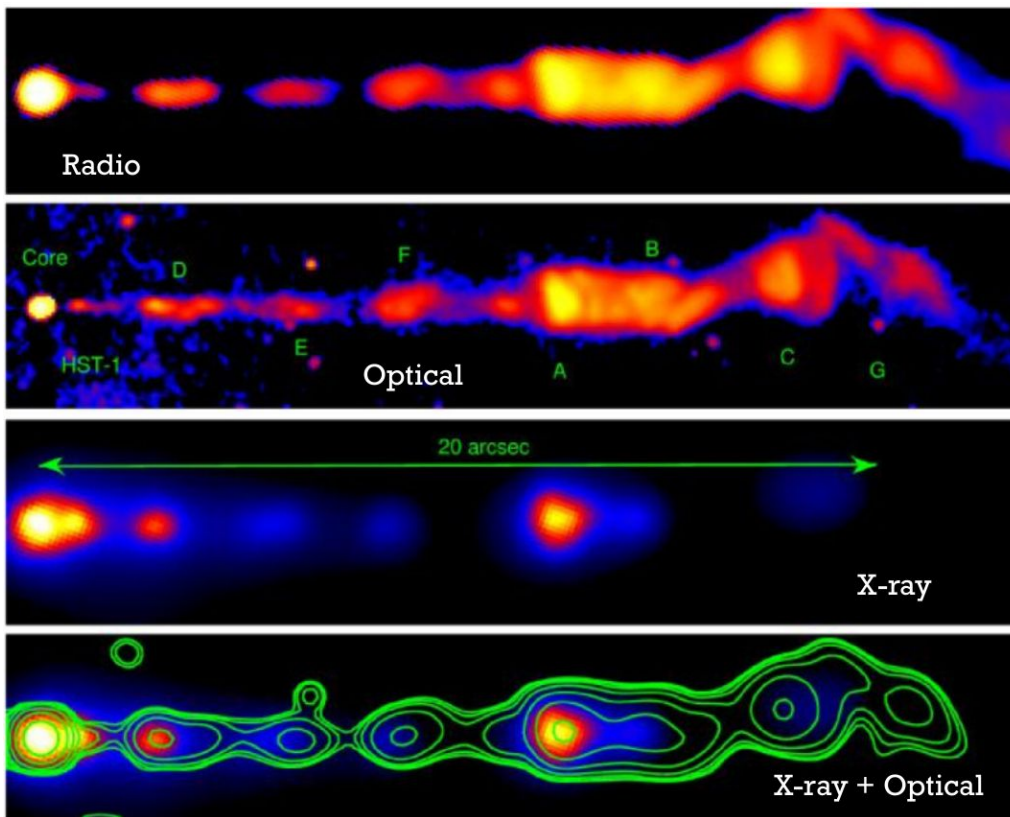
- We know the torus must lie between the BLR and NLR, but we can be more specific.
- We can now directly measure the size of the torus using
 - Dust reverberation mapping between the V-band and K-band light curves.
 - Interferometry in the NIR and MIR mapping the hot inner wall and the cool dust.
- The size of the torus appears to scale as $L^{0.5}$ (consistent with constant ionization parameter).
- The inner edge of the torus is at about 3 times the BLR radius for H β as determined from reverberation mapping.

Jets



- Could be several Mpc (this one 3 Mpc)

Jets properties



- Jets often appear relativistic based on beaming, apparent superluminal motions on sub-pc scales, and variability.
- Thus, the apparent properties of a jet depend strongly upon orientation.
- At least in some cases, jets are launched on very small scales (making much of the “core” radio emission). And they can be collimated over a huge range of scales.
- Jets are often seen in the X-ray and also the optical.

Flat vs. Steep Spectrum Radio Sources

- Often observe radio power-law spectra: $L_\nu \sim \nu^{-\alpha}$
- Radio-loud AGNs with dominant radio cores usually show “flat” radio spectra with $\alpha < 0.5$
- Radio-loud AGNs with dominant lobes usually show “steep” radio spectra with $\alpha > 0.5$
- Much of the difference in measured value of α is due to inclination of radio jet to our line-of-sight

Table 1. The characteristic spectral indices and 1σ uncertainties for all SUMSS detected sources in the SPT region and a subset of these, which we denote as BCGs, that lie within $0.1 \times \theta_{200}$ of the MCXC cluster centers. Mean spectral indices are presented for pairs of frequencies constructed from 150 GHz, 95 GHz and 843 MHz. The SZE correction is applied at 95 and 150 GHz.

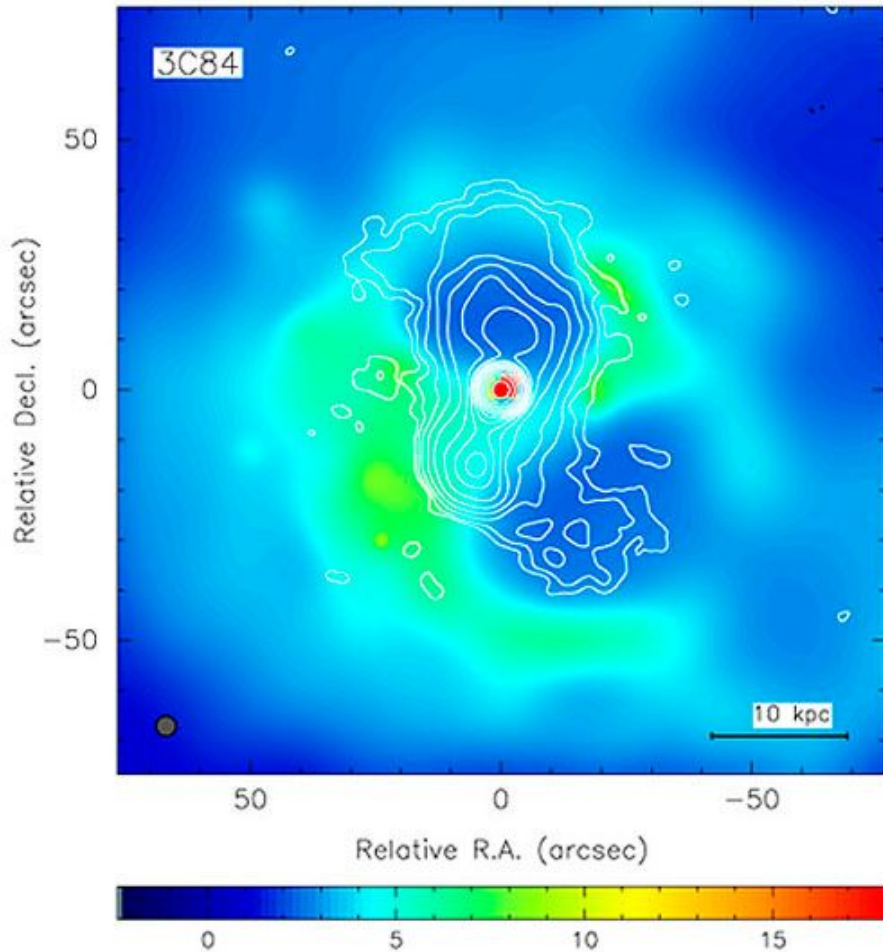
Dataset	$\alpha_{0.843}^{150}$	$\alpha_{0.843}^{95}$	α_{95}^{150}
SUMSS	$-0.38^{+0.28}_{-0.29}$	$-0.38^{+0.28}_{-0.31}$	$-0.50^{+0.24}_{-0.23}$
SUMSS BCGs	$-0.63^{+0.34}_{-0.29}$	$-0.64^{+0.33}_{-0.40}$	$-0.77^{+0.32}_{-0.31}$

How Are Jets Made?

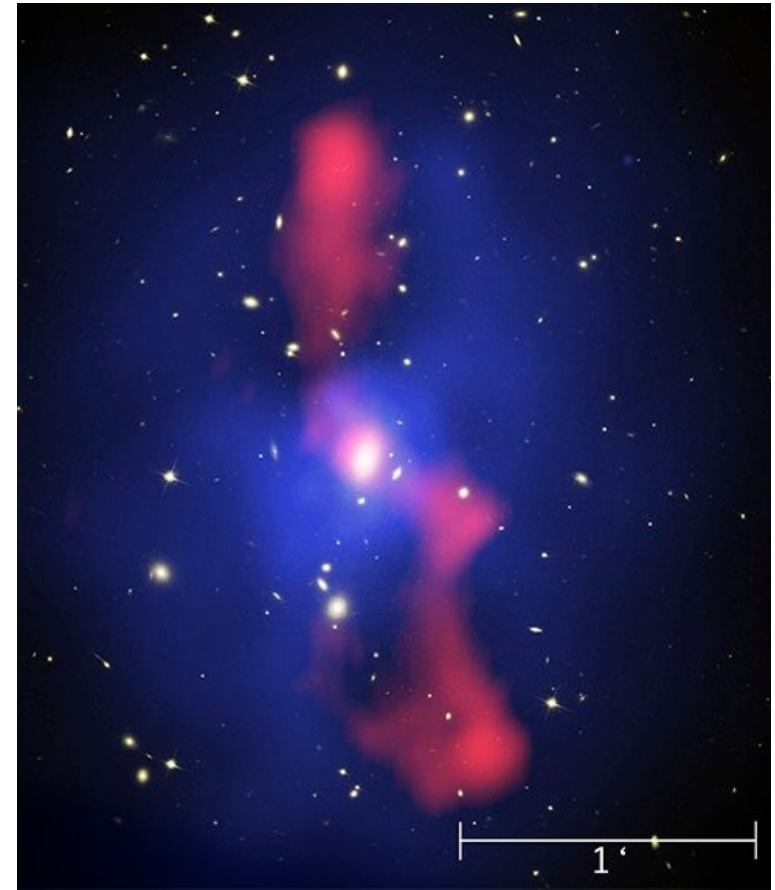
- Generally invoke MHD processes to divert some of the inflowing plasma outward and then keep it collimated.
- But exactly how to combine the “ingredients” remains poorly understood.
- What sets if a strong jet will be launched?
 - SMBH spin?
 - Magnetic geometry?
 - Environment?
 - Connection with Eddington Rate (ER)?
 - Lower ER → Radio Mode
 - Higher ER → Quasar Mode



Jet Feedback in Clusters



Fabian et al. (2003)



McNamara et al. (2005)

Jets can do substantial work against the hot gas in galaxy clusters

AGN Feedback in Clusters

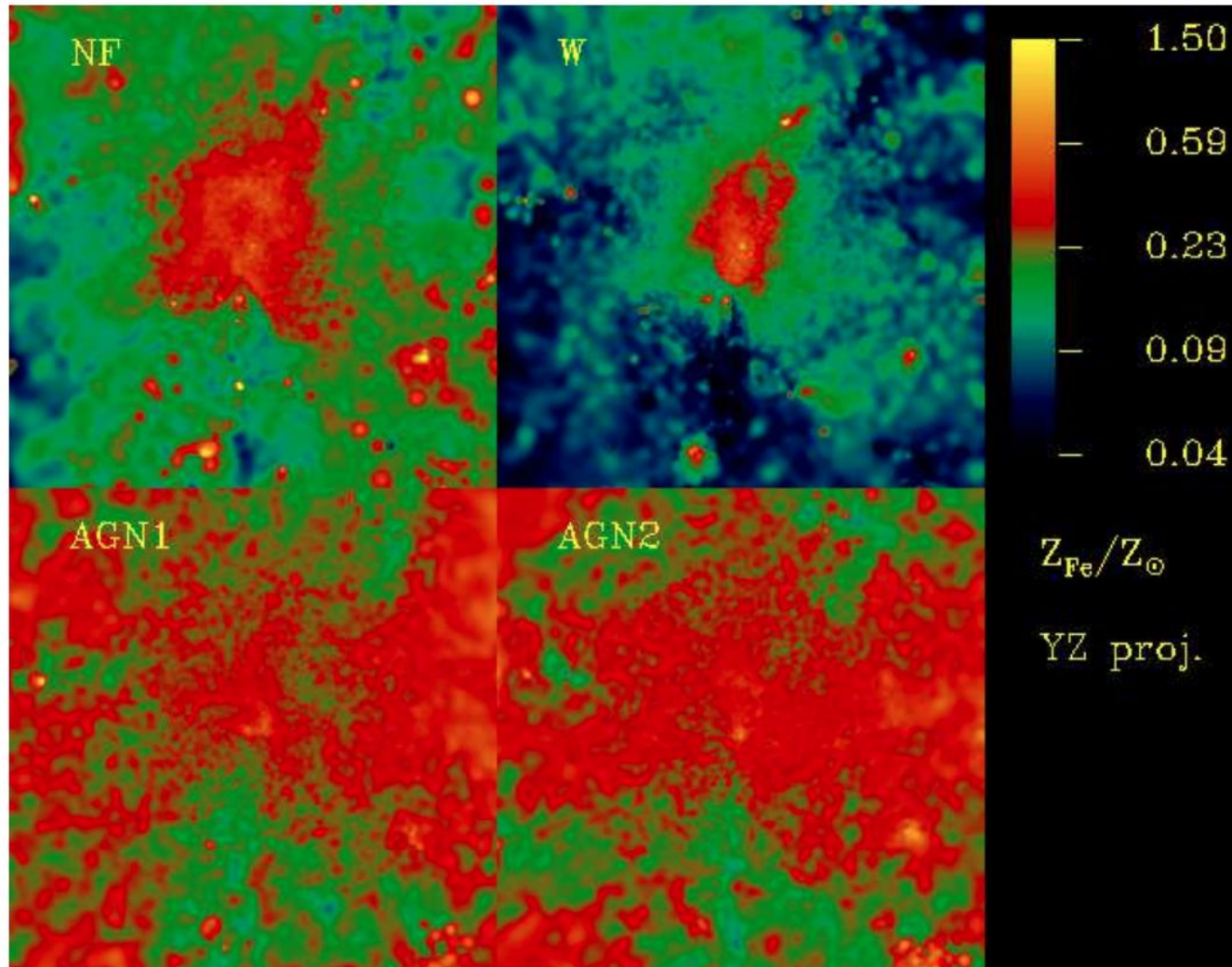


Figure 7. Maps of emission weighted Fe abundance in the g51 cluster for the runs without feedback (NF, top left), with winds (W, top right) and with AGNs (AGN1 and AGN2, bottom left and bottom right, respectively). Each map has a side of $2R_{vir}$. Abundance values are expressed in units of the solar value, as reported by Grevesse & Sauval (1998), with color coding specified in the right bar.